# IOWA STATE UNIVERSITY
**Digital Repository**

2018

# Sand and silty-sand soil stabilization using bacterial enzyme induced carbonate precipitation (BEICP)

Tung P. Hoang
*Iowa State University*

Follow this and additional works at: https://lib.dr.iastate.edu/etd

Part of the Geotechnical Engineering Commons

**Sand and silty-sand soil stabilization using bacterial enzyme induced carbonate precipitation (BEICP)**

by

**Tung Phuong Hoang**

A dissertation submitted to the graduate faculty

in partial fulfillment of the requirements for the degree of

DOCTOR OF PHILOSOPHY

Major: Civil Engineering (Geotechnical Engineering)

Program of Study Committee:
James Alleman, Co-major Professor
Bora Cetin, Co-major Professor
Jeramy Ashlock
Kaoru Ikuma
Zhiyou Wen

The student author, whose presentation of the scholarship herein was approved by the program of study committee, is solely responsible for the content of this dissertation. The Graduate College will ensure this dissertation is globally accessible and will not permit alterations after a degree is conferred.

Iowa State University

Ames, Iowa

2018

# DEDICATION

I dedicate this to my family for their love and overwhelming support!

# TABLE OF CONTENTS

# LIST OF FIGURES

# LIST OF TABLES

## ACKNOWLEDGMENTS

Completing my PhD program has been an unexpected and exciting journey on both professional and personal levels. I was sincerely blessed to be given an opportunity to pursue graduate doctoral studies, which have helped me to discover my true passion for academia. I would, therefore, like to take this opportunity to express my thanks to those who helped me complete this journey, and who have all encouraged me to enjoy this entire adventure.

First and foremost, I am very grateful to have worked with my co-advisors, Dr. James Alleman and Dr. Bora Cetin, for their invaluable guidance and support throughout the progress of my research at Iowa State University. Regular discussions with them drove me to successfully discover research problems and to identify appropriate solutions. Their enthusiasm, creativity, endless support, encouragement, guidance, and friendship truly inspired me to complete my doctoral research and dissertation. I hope to carry forward the lessons I have learned from my advisors throughout my future professional career, and to hopefully pass them on to my own future students.

My sincere appreciation also extends to my committee members for their efforts and contributions to this works: Dr. Jeramy Ashlock, Dr. Kaoru Ikuma, and Dr. Zhiyou Wen. Their constructive comments, instructional support with laboratory skills, and sharing experimental facilities played a significant role with building research skills and to establish critically necessary knowledge for my studies. Additionally, without their revision of my proposal and dissertation documents, I could not possibly have reached this point in my evolving academic career.

Moreover, I wish to thank Dr. Chu Jian, Dr. Shifan Wu from NTU, Singapore, Dr. Sun-Gyu Choi from KAIST, Korea, and Mr. Arash Maghsoudloo from TU Delft, Netherlands for their sharing of wonderful experience, insightful ideas, and valuable suggestions during my research work. I would also like to thank Mr. Warren Straszheim from MARL, Iowa State University and other laboratory technicians for their careful support of my laboratory experiments. I am further thankful to have had the support and encouragement from all of my colleagues, group members, undergraduate students, faculty, staff, and friends at Iowa State University, USA and Danang University of Science and Technology, Vietnam. Notably, I would like to specifically acknowledge the financial support provided by the Vietnam International Education Cooperation Department, the Hoover Chair and Cerwick Professor endowments, and Iowa State University CCEE.

Lastly, my biggest thanks go to my family. To my lovely wife, Huyen Do, I am extremely thankful for her endless love, patience, strength, support, and encouragement during this entire journey years. To my sweetheart daughters, Annie and Alice, I am so very thankful for the smiles and happiness they continually bring to our family. And to my parents plus my younger sister, their invaluable support has been a life-long blessing.

# ABSTRACT

The concept of bio-geotechnics represents an innovative, new technical merger between three traditional disciplines: geotechnical, material, and environmental engineering. As originally conceived decades ago, biogeotechnology mechanism uses live micro-organisms to improve and stabilize soils, by which their suitability for construction realizes engineering, environmental, and economical benefits. More recently, though, this concept has been broadened to include a suite of possible strategies, including: 1) using whole-cell microorganisms to secure 'Microbial Induced $CaCO_3$ Precipitation' (MICP), 2) using cell-free, free-'Enzyme Induced $CaCO_3$ Precipitation' (EICP), and 3) using 'Microbial Induced Desaturation and Precipitation' (MIDP). Although none of these biogeotechnical methods have yet reached a pragmatic level of commercial application, promising results have been achieved within laboratory, and in limited instances of large-scale and field-scale evaluation.

This dissertation documents the outcomes achieved during an investigation of a novel modification of the latter 'EICP' method which could be similarly employed to secure bio-mediated soil improvement. In this case, however, the operative catalytic enzyme (i.e., urease) was extracted from a bacterial source and then used in its free-enzyme form to secure a so-called 'Bacterial Enzyme Induced Carbonate Precipitation' (BEICP). A sonication method was applied to lyse living cells of *S. pasteurii* to obtain the desired urease solution. The urease activity rate of this bacterial extracted enzyme was higher, at an approximate 2X magnification, even though the volume of the sonicated solution had only been reduced one-fourth as compared to that of the original bacterial solution. Furthermore, extending beyond this benefit realized with producing an

even higher rate of enzymatic activity, the performance results obtained when using BEICP soil processing demonstrated several additional performance-based benefits.

This dissertation consequently documents the engineering properties achieved with BEICP-treated sand processing, as well as comparing these findings against that of traditional MICP treatment. These lab-level research results offer positive evidence for two possible benefits with the BEICP method: 1) mechanical stabilization of sands, and even including that of loose sandy soil materials, and 2) an ability to retain post-treatment permeability of the bio-cemented sands (i.e., as compared to MICP's typically higher reduction in treated soil permeability). The advantage of BEICP's free-enzyme processing approach stems from its nano-sized (water-soluble) catalyst dimension, where these nano-enzymes are far more easily able to penetrate the small pore space of a silty sand matrix. In turn, this BEICP method was successfully applicable to the solidification of silty-sand soil. The measurement of unconfined compression strength of BEICP-treated samples ranged from 0.4 to 1.1 MPa, and from 0.23 to 0.84 MPa with silt-sand mixtures at silt levels of 10 and 20 %, respectively. These results accordingly validated the biological treatment process BEICP as a prospectively applicable means of successfully solidifying natural sand and silty-sand soil systems.

As previous mentioned, BEICP treated is a new bio-based method, and this dissertation's accompanying research has further evaluated a variety of processing factors which might impact the resultant engineering properties of bio-cemented sand. Notably, a series of test-tube experiments was conducted to investigate the effects between the bacterial cell and urease in the chemical conversion ratio. The results showed that the precipitation ratio reduced when the concentration of chemical agents increased. These

experiments also characterized the urease activity of biological sources and chemical concentration for sand column tests. Two types of sand, including both coarse- and fine-grained sands, were examined in order to evaluate how these size factors impacts product strength and permeability with BIECP treatment. These findings correlated with previous studies on MICP and EICP, where the size of particle and the $CaCO_3$ content played a vital contributing factor relative to both strength increase and permeability reduction. However, more engineering factors, such as injection flow, temperature, chemical concentration, etc., needs to be studied in order to optimize the BEICP-treatment process.

Another significant aspect of BEICP-treated soil is that of the durability of the biocemented soil under the freeze-thaw cycling. Sandy soil and silty-sand soils which were originally packed in a loose condition were treated with BEICP processing as well as with commercial Portland cement and fly ash additions. The strength reduction following freeze-thaw cycling was examined on treated samples. This investigation revealed that the BEICP-treated samples retained higher strengths than that in Portland and fly ash cemented samples after freeze-thaw cycling. This approach suggests that this method may have beneficial use when applied to stabilize sub-grade and sub-base materials underlying pavement layers within cold regions.

This research effort subsequently started with the development of a sonication technique to lyse viable *S. pasteurii* bacteria cells in order to release their intracellular urease materials. A particular advantage of using this new method is that it produces distinctly higher levels of urease activity. The extracted enzyme was then used to treat a group of test columns bearing different percentages of coarse- and fine-grained soils by weight. The engineering properties of BEICP-treated soil were evaluated via a series of

lab tests. Another clear advantage for BEICP processing is that this method can form calcium-bearing crystals as bridges between fine (silt) and coarse (sand) soil grains, which then increases the overall strength of our silty-sand columns, while at the same time not unduly decreasing matrix permeability.

# CHAPTER 1.   INTRODUCTION

## 1.1 Overview

Natural soil properties vary significantly over time and region.  This variability and heterogeneity of the natural soils  makes it difficult to  develop engineering soil improvement mechanisms which are able to universally remediate all geotechnical soils (DeJong et al. 2011). Engineers have worked with a variety of methods to stabilize weak soils for different intended engineering purposes. The majority of these soil stabilization techniques include compaction of soils which is typically achieved via application of mechanical energy on soils. Thermal and electrical stabilization methods have also been applied in some civil engineering projects. Compaction of soils consumes substantial energy for operation and installation procedures, while chemical methods not only require energy for compaction but also injection process which may lead to environmental problems (DeJong et al. 2010a). The most popular chemical admixture used for soil stabilization is that of using Portland cement to enhance the mechanical properties with sands, as well as reducing hydraulic conductivity. However, this method has potentially major drawbacks: 1) a high carbon footprint in relation to cement manufacturing, 2) the expensive quarrying with large amounts of raw materials and associated land destruction, 3) a release of high pH residuals to the environment, 4) the necessity for many injection wells when treating a large land area, and 5) an overall high cost for its application and production methods (DeJong et al. 2011; Kirsch and Bell 2013).

Mitchell and Santamarina (2005) have reviewed the use of micro-organism processes in geotechnical applications. Since then many studies have been conducted to develop the suitable methodology for using micro-organism process in geotechnical engineering fields (from 2007 to 2018). The general field of microbial geotechnology has progressively shifted

into two different fields of application, including: (1) bio-clogging and (2) bio-cementation (Ivanov and Chu 2008). The main aim of these applications is to enhance soil shear strength and to reduce the permeability of natural soils in order to prepare these materials for construction and/or environmental remediation. Soil improvement via the microbial method promises an eco-friendly technique. Use of this technique results in significant reductions in embodied energy and carbon emissions, and less soil structure disturbance. However, research conducted on micro-organism process, i.e., which is called 'Microbial Induced Carbonate Precipitation' (MICP), over the last decade has shown that the MICP method still has some limitations. One distinct issue is that MICP treatment employs urease microbes who have an inherent constraint on the ability to physically migrate through soils unless their pore space voids are larger than that of medium to fine sands (Kavazanjian and Hamdan 2015). In turn, MICP is probably not suited for soil systems bearing finer-grained materials which would then impede bacterial migration. Another drawback for MICP technique involves the complex lifestyle of these microbial cells when they are transferred from their original growth culture media to a natural soil environment, where this transition might impose negative transitional impacts (e.g., lower metabolic rates during lag and adaptation phases).  In addition, the process of growing and preserving the microbe's viability under field-level conditions would have its own set of complications. After two decades of the first MICP lab-scale research, therefore, only few field-level case studies has yet been performed (Burbank et al. 2011; Gomez et al. 2015a; De Jong et al. 2009; Nassar et al. 2018; van Paassen 2011; van Paassen et al. 2009, 2010a; Phillips et al. 2016; van der Star et al. 2011).

A newer ureolysis method using nano-scale and water-soluble urease enzyme source also induces carbonate precipitation via ureolysis. The vast majority of these related prior

studies, urease sources are mainly extracted from agricultural sources for commercial purpose. The Enzyme Induced Carbonate Precipitation (EICP) method has been investigated for increasing strength, permeability reduction, and mitigation of fugitive dust by Nemati and Voordouw (2003), Nemati et al. (2005), Neupane et al. (2013); Hamdan et al. (2013); Park et al. (2014); Kavazanjian and Hamdan (2015); Hamdan and Kavazanjian (2016). The urease enzyme itself can overcome the disadvantages of microbes, such as size and water solubility. However, previous works have focused only on plant-derived enzyme and treatment of sandy soils. Most of this current research has used an agricultural urease which had been purchased from a commercial chemical company. Extraction of urease from plants requires time (plant rearing) and space, and it is produced in small amounts.

One significant goal of this dissertation project, therefore, was to develop a better method to produce the urease enzyme, where the approach is not only simpler but also able to generate higher urease activities than the ones observed within MICP method. A sonication technique was applied to break down viable cells of *S. pasteurii* bacteria to collect urease enzyme. This new method for urease enzyme extraction has been developed successfully which will provide a significant benefit in terms of avoiding the expensive purchase of urease from chemical suppliers as reported with previous EICP studies. Indeed, this 'do-it-yourself' approach with urease production also offers significant opportunities in terms of multi-scale research ICP projects. The goal of this research is to evaluate the performance of this new carbonate precipitation technique to improve the soil strength not only with sand but also with silty sand. This new method is called Bacterial-Enzyme Induced Carbonate Precipitation (BEICP). It was consequently used to treat a group of test columns with different percentages of fine-grained soils by weight. A particular advantage of using

this new method is that we are now able to generate far higher levels of urease enzyme activity, at levels roughly 2 times higher than those obtained with the conventional MICP method. Yet, another clear advantage for the BEICP method is that this process can form calcite crystals as bridges between fine- (silt) and coarse- (sand) grains soil which increases the overall strength of silty-sand columns.

Overall, this new BEICP method appears to offer the following advantages in regards to the employed free-enzyme catalyst: 1) the process of enzyme extraction is more expedient and less complex, 2) the resultant free self-extracted urease bears a significantly higher level of catalytic activity, which allows the BEICP technique having cost benefit compared to the EICP using purchased urease, and 3) this new enzyme is nano-scale in size and water soluble, which allows the BEICP treatment method to biostabilize finer soils, whereas the MICP method simply cannot be used with these more complex soils.

## 1.2 Scope of Research

The overall purpose of this research is to develop a novel nano-scale biostabilizer for silty-sand soil improvement using bio-chemical processing. The results of this study will create a new trend in the bio-geotechnical engineering research field, particularly in regard to fine-grained soil improvement. More specifically, this study addressed the following research questions:

- Which engineering method can extract urease enzyme from viable micro-organism cells?

- How can the extraction process be optimized to achieve high urease activity and produce enzymes in large quantities via shortest and simplest method?

- Can the use of a free-enzyme urease additional strategy produce successful bio-cementation with sand and silty-sand soils?

- What is the impact of fines content, grain size, calcium content, and freeze and thaw cycles on strength, deformation, and permeability of soils stabilized via the BEICP technique?

Possible outcomes of the study:

- Producing high activity enzymes, in large quantities, using an expedient, simplified enzyme extraction method,

- Forming the first intact silty-sand column samples in the published literature for bio-geotechnical processing where the applied method was based on a free-enzyme bio-stabilization process.

- Investigating the strength increase and permeability reduction in BEICP-treated soil samples.

- Understanding the factors influencing the strength and deformation of BEICP-treated soils which can be applied for field trials later on.

There are three main stages of this research project. Stage #1 included the sonication process to obtain the urease enzyme from viable bacterial cells. Stage #2 involved an investigation of the BEICP method in order to solidify the sandy soil and silty-sand soil columns. The microstructure of bio-cemented soil will be examined to confirm the calcite crystal cluster supporting the soil matrix and filling void spaces. Stage #3 involved an investigation of factors which impacted properties of BEICP-treated samples and a comparison with commercial treatment methods using Portland cement and fly ash admixtures. The concerned factors will be fine content, calcium content, moisture content,

porosity, freeze and thaw, and grain size. The scope of the research is summarized in Figure 1.1.
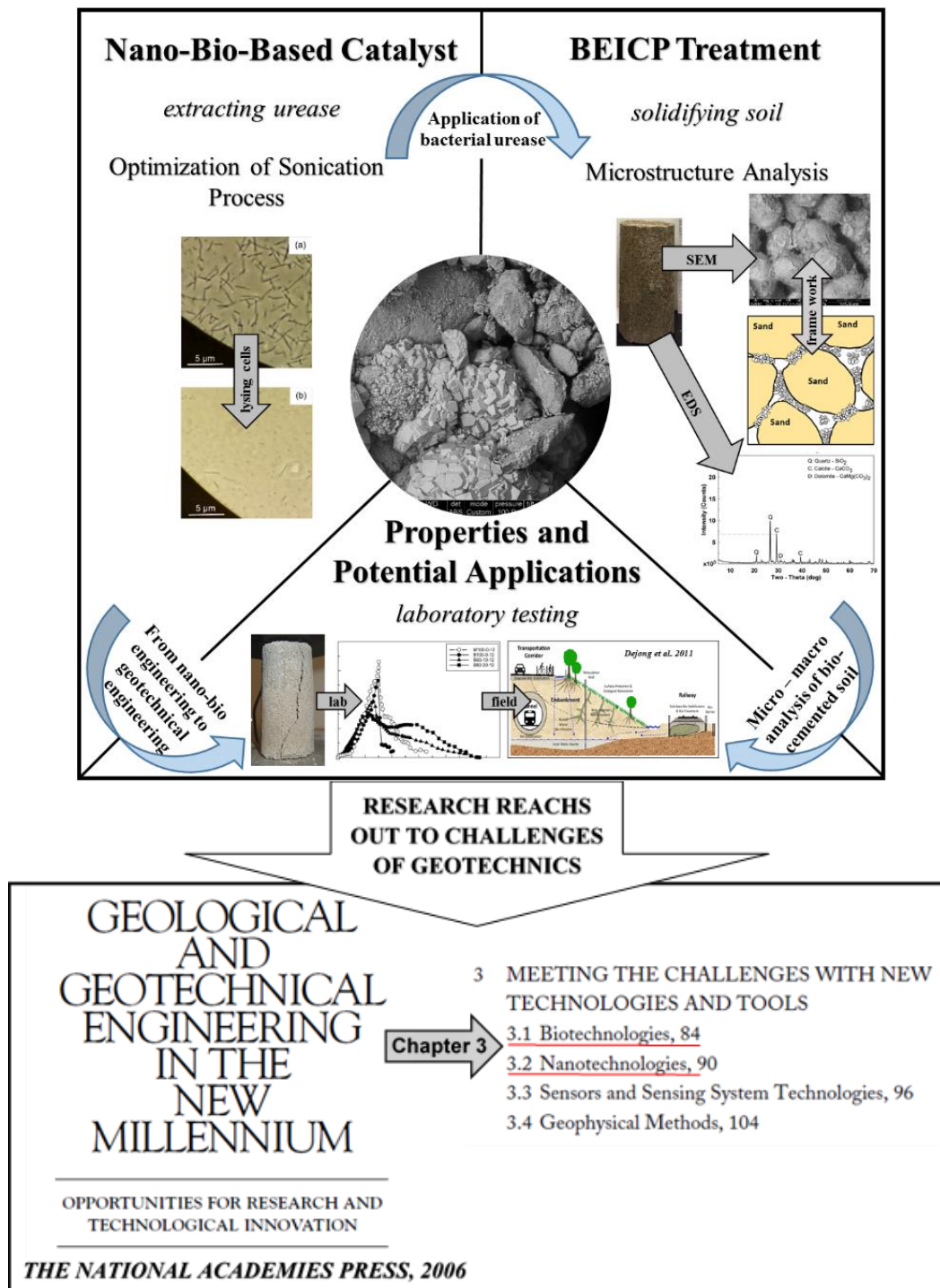


Figure 1.1 *Outline of research scope and reaching of research to challenges of geotechnical engineering in the new millennium (after Long et al. 2006)*

## 1.3 Dissertation Organization

The following table provides a summary breakdown of this dissertation's

organization:

Table 1.1 *Research organization*

| Section | Content |
|---|---|
| **Acknowledgements** | |
| **Abstract** | |
| **Chapter 1.** Introduction | |
| **Chapter 2.** Literature review | This chapter provides a summary review of literature relevant to this dissertation, including the following four sub-sections:<br>(1) General soil stabilization methods;<br>(2) Microbial induced carbonate precipitation (MICP);<br>(3) Enzyme induced carbonate precipitation (EICP); and<br>(4) Properties of urease. |
| **Chapter 3.** Sand and silty-sand soil stabilization using Bacterial Enzyme Induced Carbonate Precipitation (BEICP) | This chapter has been published as an online publication with the Canadian Geotechnical Journal.<br><br>This paper presents the process of enzyme extraction from viable bacterial cells and the properties of MICP-BEICP-treated soil samples |
| **Chapter 4.** Engineering properties of biocementation coarse- and fine-grained sand catalyzed by bacterial cells and bacterial enzyme | This chapter has been submitted paper to the ASCE - Journal of Materials in Civil Engineering.<br><br>The paper examines variations in chemical conversion efficiency in relation to bacterial cells and urease. The effects of grain size on strength and permeability of BEICP-treated sand are also investigated in this paper. |
| **Chapter 5.** Effect of freeze and thaw cycling on unconfined compression strength of BEICP-stabilized of sandy and silty-sand soils and a comparison to cement and fly ash stabilized soils | This chapter represents a 'paper in preparation' for upcoming journal submission.<br><br>This paper evaluates the engineering properties of BEICP-treated soil under freeze and thaw cycles and the comparison with soil stabilized by Portland cement and fly ash. |
| **Chapter 6.** Conclusions, research contributions, limitations and recommendations | |
| **References** | |

## CHAPTER 2.    LITERATURE REVIEW

### 2.1 Introduction

The selection of ground conditions at construction site areas is one of the most important considerations for civil engineering projects. From the point of view of geotechnical engineering, a good soil condition implies that sufficient strength and stiffness will be available for adequate load-bearing capacities without causing unacceptably large deformations or instabilities. For those instances and locations where poor soil conditions exist, civil engineers consequently need to apply stabilization methods to improve the foundational quality for subsequent construction. When modifying the properties of soil, therefore, geotechnical engineers have a number of possible strategies to achieve these improvements, such as replacement, compaction, piles, chemical admixture, and reinforcement methods. However, for many projects, none of these conventional techniques are technically, environmentally, and economically realistic. Advanced, alternative ground improvement technologies are, therefore, consequently being sought by geotechnical engineers and researchers in order to secure better (i.e., more efficient, less expensive, faster, etc.) soil improvement methods.

One such natural method is that of the biocementation which has occurred over geological time with the genesis of rock formations formed by layers of accretionary structuring of sedimentary grains which were initial bound by microbial mats of microorganisms and then subjected to further high pressuring by overlying geological strata. This natural cementation process occurs very slowly, over during millennia-level if not even billion-year time intervals. This sort of natural calcium carbonate precipitation has been found to be widely prevalent, though, with more than 4 % of the earth's crust and rocks (e.g.,

chalk, marble, travertine, tufa, and others) showing such formations (Krajewska 2018). For example, a type of common rock found near coastal areas (i.e., *Stromatolites,* from the Greek words, '*στρῶμα*' [layer] and '*λίθος*' [rock]) (Wikipedia 2018) which was formed by the layers of trapping, bridging, and cementation of soil grains via biofilms of cyanobacteria (Riding 2007). Figure 2.1 shows pieces of *Stromatolites* rock dating from 4.5 billion to 543 million years ago.

By mimicking these natural cementation processes, biogeotechnical engineers can accelerate soil stabilization mechanism under the laboratory conditions. These artificial bio-cementation technologies employ urease producing bacteria, or urease enzymes, in order to achieve urea hydrolysis, where a calcium source is also applied in order to induce $CaCO_3$ precipitation within a soil matrix. This technique has been investigated by geotechnical engineers since more than a decade. This dissertation consequently focuses on a new approach to artificial bio-cementation technology.



Figure 2.1 *Stromatolite was formed by the layers of trapping, bridging, and cementation of soil grains via biofilms of cyanobacteria in million years (Field Museum of Natural History, Chicago, Illinois, USA, by author)*

## 2.2 Soil Stabilization

Nowadays, we are facing the rapid growth of population, fast urbanization, and more development of infrastructure such as major highways, high speed railways, high-rise building and other structures which cause the reduction of availability of soils with desirable characteristics. Therefore, in many construction sites, civil engineers have to deal with soft and weak soils that possess high compressibility and low shear strength. Soil stabilization methods are a selection of civil engineers to improve ground mechanical properties.

According to the latest state-of-art report on ground improvement published by Chu et al. (2009), there are five primary categories and twenty-nine separate methods used for ground improvement. The first category mainly focuses on mechanical stabilization techniques without adding any admixtures in non-cohesive soils and fill materials. This category is divided into five methods of application: dynamic compaction, vibro-compaction, explosive compaction, electric pulse compaction, and surface compaction (including rapid compaction). The second category is ground improvement without adding admixtures in cohesive soils which is divided into seven methods such as replacement/displacement, preloading using fill, preloading using vacuum, dynamic consolidation with enhanced drainage, electro-osmosis consolidation, and thermal stabilization using heating or freezing, and hydro-blasting compaction. The principles of this category are based on soil excavation, dynamic load, drainage paths, electro-kinetic energy and energetic (i.e., explosive) soil extraction. The third category, which involves the supplemental use of substrate admixtures or inclusions, has seven sub-methods including: vibro-replacement, dynamic replacement, sand compaction piles, geotextile confined columns, rigid inclusions, geosynthetic reinforced columns, and microbial methods. Most of these sub-methods involve the use of piles, rigid or semi rigid columns, geotextile enhancement and natural products. The last, microbial sub-

method option involves bio-based induced calcium carbonate precipitation techniques. The fourth category involves ground improvement using grouting-type admixtures, including: particulate grouting, chemical grouting, mixing methods, jet grouting, compaction grouting, and compensation grouting. Most of these fourth-category options focus on chemical stabilization techniques. Lastly, earth reinforcement is the fifth category, with which there are three sub-methods. In this case, these methods rely of applications which take advantage of the tensile strength of steel, geosynthetic, and perhaps even plant-based materials in order mechanically stabilized earth, ground anchors and biological root-based methods using vegetation.

Berggren (2016) investigated the trends of soil improvement methods based on more than 4700 references from 1983 – 2016 document within the literature database of the Swedish Geotechnical Institute. Based on this review, the following trends for the available soil stabilization methods are being noticed:

- Piling, sheet piling and anchors represent the most commonly applied methods, and use of these methods are increasing,

- Grouting is the second most popular ground improvement method, but its popularity has decreased significantly in recent time,

- Both stone columns and vertical drain applications have been increased recently,

- Although bioengineering and environmental engineering methods did not exist in the literature of 1983 – 1997, application of these methods increased substantially in the second period of the search from 1997 to 2016.

Every soil stabilization technique still has its own disadvantages and advantages in terms of technical environmental and economic aspects. Limitations of technical methods

includes the availability of the equipment or soil conditions. These technical problems are the first major concerns of engineers which can be addressed relative to site-specific limitations (e.g., the constrained radius of mixing equipment, high viscosity of soil-stabilizer admixtures, quick hardening times when using chemical stabilizers, and difficult soil and rock conditions). A common potential solution to these challenges is that of using simply piling methods. However, ground improvement using piles is an uneconomical solution, requiring heavy machinery and longer times to complete (Kirsch and Bell 2013). Other methods using chemical products can have a significant impact on environment. Therefore, civil engineers are always trying to seek or develop new soil stabilization methods which have the least disadvantages on its own. More recently, bio-geotechnical ground improvement techniques have also been investigated for more than a decade. This potential method is expected provide multi-functional solutions with minimum cost and lower environmental impacts (DeJong et al. 2011).

### 2.3 Bio-cementation via Microbial Induced Calcium Carbonate Precipitation (MICP)

Microbial geotechnology has been an emerging branch of geotechnical engineering since 2004 (Chu et al. 2011). The main purpose of bio-cementation method is to enhance soil strength such that the bio-stabilized strata will be more suitable for construction and environmental objectives. This method has been proposed to improve the mechanical properties of soil by forming calcium carbonate precipitation through microbial activity or products. van Paassen 2009 provided the role of micro-organisms in calcium carbonate precipitation as follows:

13

1. producing carbonate (e.g. by hydrolysis, respiration, etc.).

2. producing alkalinity (increasing the pH locally, which causes the dissolved

   inorganic carbon which is mainly present as bicarbonate to dissociate causing an

   increase in carbonate concentration).

3. acting as nucleation sites in an already oversaturated solution.

An alkaliphilic of *Bacillus pasteurii* (American Type Culture Collection 6453) which

has been classified as *Sporosarcina pasteurii* (ATCC 11859), is the most widely used species

of hydrolyzing bacteria because of non-pathogenicity, high urease activity, and resistance to

high concentration of the ammonium by-product of urea hydrolysis (Whiffin 2004). *S.*

*pasteurii* bacteria use their urease to hydrolyze urea by following the reaction shown below:

$$(NH_2)_2CO + 3H_2O \rightarrow 2NH_4^+ + HCO_3^- + OH^- \tag{2.1}$$

An additional $Ca^{2+}$ source (i.e., typically $CaCl_2$) is then added to facilitate the desired

precipitation and crystallization of a calcium-rich (e.g., calcite) deposition mineral:

$$Ca^{2+} + HCO_3^- + OH^- \rightarrow CaCO_3 + H_2O \tag{2.2}$$

$$Ca^{2+} + 2HCO_3^- \leftrightarrow CaCO_3 + CO_2 + H_2O \tag{2.3}$$
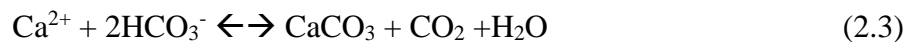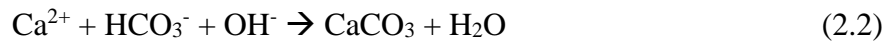
In most instances, an injected bacteria solution is then introduced to the soil matrix in

the presence of substrate urea and calcium source chemicals which then promotes $CaCO_3$

precipitation binding of soil grains, such that this overall reaction then results in increased

soil strength (Ivanov and Chu 2008; van Paassen 2009; DeJong et al. 2006; Al Qabany and

Soga 2013). Figure. 2.2 shows the role of the bacteria cell in this calcium precipitation

process.
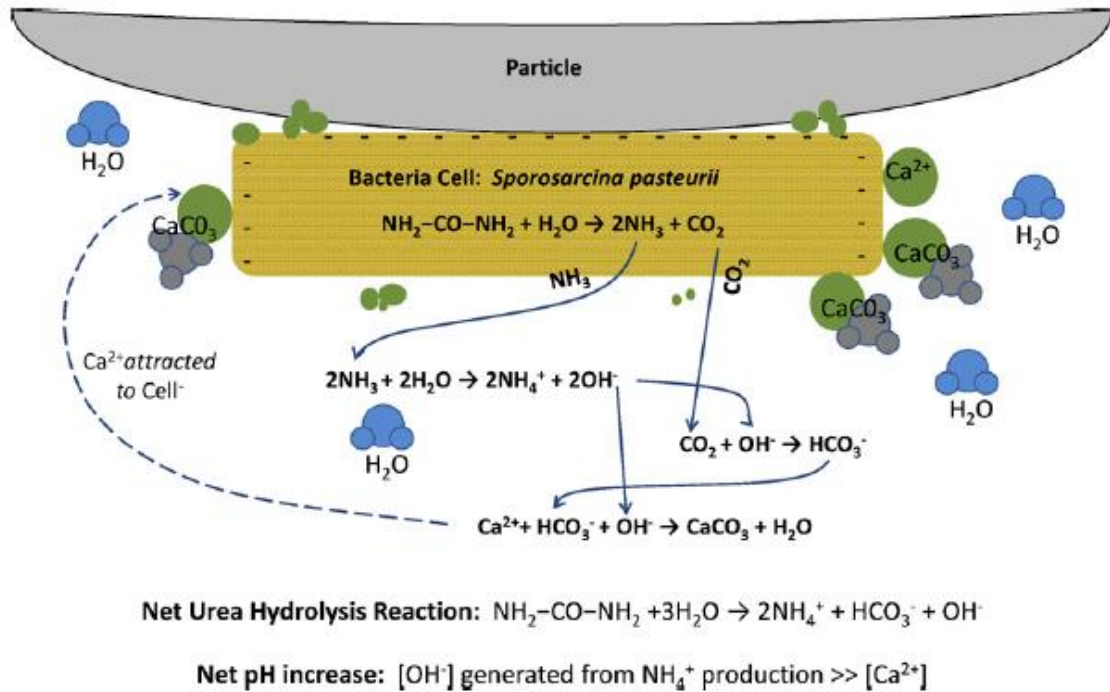
Figure 2.2 *Overview of bio-mediated carbonate precipitation using ureolysis (from Dejong et al. 2010)*

The process of MICP enhancing mechanical properties of sandy soil consequently

involves four main steps (van Paassen 2009):

1) growing suitable bacteria,

2) introducing and transporting micro-organisms in the porous media

3) injecting suitable substrates to generate bio-chemical process to precipitate $CaCO_3$

   crystals bridged gaps between the grains;

4) removing the remaining products

However, a major limitation of the MICP method is that of the pore space size within

the soil matrix. The cell diameter of the ureolytic cells is typically in the range of $0.5 - 3$ µm,

which can only be free to move in the pore spaces between large or medium soil grains. Silty

or clayey grains, though, have much narrower void spaces which then restrict the transport of

bacteria cells within the soil matrix (Mitchell and Santamarina 2005). In addition, the

introduction of exogenous microorganisms may cause major practical problems, such as obtaining approvals and licenses from government, microbial ecology safety (Ran and Kawasaki 2016), clogging nearby inlet points, and difficulties of in-situ producing and preservation of bacterial sources (Harkes et al. 2010; van Paassen et al. 2009). Therefore, an alternative, new method for using bacteria-free urease systems which are still able to induce $CaCO_3$ precipitation has been developed as an alternative method.

### 2.4 Bio-cementation via Enzyme Induced Calcium Carbonate Precipitation (EICP)

Urease enzyme–aided calcium carbonate precipitation is a process involving the catalytic action of urease to complete the hydrolysis of urea (Krajewska 2018). However, instead of using urease-producing bacteria within a conventional MICP approach, an innovative, new EICP method has been devised by which an applied, free-enzyme urease catalyst (as compared to using whole-cell ureolytic microbes) is typically synthesized from agricultural sources, bacteria, algae, and fungi. Recently, bio-geotechnical researchers mainly use commercial urease (Bang et al. 2009; Neupane et al. 2013; Hamdan et al. 2013; Park et al. 2014; Kavazanjian and Hamdan 2015; Hamdan et al. 2016; Hamdan and Kavazanjian 2016; and Oliveira et al. 2016). To date, only a few studies have been published where the researchers used with seed-extracted, plant-derived urease (Nam et al. 2014; Dilrukshi et al. 2018; Javadi et al. 2018).

The effectiveness of this newer EICP-based strategy is demonstrated by Yasuhara et al. (2012), who used urease purchased from Kishida Chemical to increase the mechanical properties of sandy soil, where this process produced a range of unconfined compression strengths between 0.4 and 1.6 MPa while the permeability of the samples was reduced 1.5 fold. A large-scale test was conducted to suggest that enzymatic calcium carbonate precipitation technique may be feasible for use in large-scale applications (Neupane et al.

2013). The plant-derived urease enzyme was applied to induce calcium carbonate cementation to modify the strength of sand samples (Ottawa #20/30 and F-60 silica sand) in laboratory column tests (Hamdan et al. 2013). The triaxial test result showed that substantial strength increase was observed for all 3 sand columns tested. Kavazanjian and Hamdan (2015) employed three methods including mixing & compacting and injecting methods to form cemented sand columns by EICP method. However, only mixing & compacting method was able to form intact within the sand columns which provided strength at the range of ~390 to ~530 kPa. The application of EICP method for fugitive dust control was studied by Meyer et al. (2011) and Hamdan and Kavazanjian (2016). Meyer et al. (2011) compared three treatment categories including EICP only; MICP only and EICP combined MICP for surficial stabilization of cohesionless fine sand. They concluded that the treatment using urease-only provided the highest increase in strength and resistance to erosion. Hamdan and Kavazanjian (2016) evaluated fugitive dust control on wind tunnel tests, which showed that EICP processing can be used to increase the resistance of soils to fugitive dust control emissions. Although chemical treatment of urea-calcium chloride (without urease) also had similar effect like EICP (i.e., additions of calcium chloride between 0.05 and 1.0 M were sufficient to control dust erosion), precipitation production from this sort of chemical-only treatment was solubilized when exposed to surface water runoff. Therefore, EICP treatment was a potential method of more durable, and also had a lower impact on the environment when applied for fugitive dust control. The previous studies reveal that EICP has a similar ability for increasing strength ad permeability reduction as MICP method. However, the EICP method relied on plant-derived enzyme still has several drawbacks. The commercially available urease (high level of purity) is very expensive for large-scale and filed-scale

experiments. The extracted-enzyme from jack beans (Nam et al. 2014) and watermelon seeds (Nam et al. 2014; Dilrukshi et al. 2018; Javadi et al. 2018) is limited of quantity. In addition, time and land consuming are also other major problems for agricultural enzyme sources.

## 2.5 Urease

### 2.5.1 Discovery and Structure of Urease

Urease is an important enzyme, with several important roles within our ecosystem at plant, animal, human, and even microbial levels (Mobley and Hausinger 1989). Furthermore, urease has been used as a diagnostic clinical agent, as in the case blood and urine analysis (Nakano et al. 1984). Our original knowledge regarding urease dates back more than a century; Takeuchi discovered the existence of urease within sub-surface bean products in 1909. Several subsequent researchers then determined that urease was also present in a wide range of higher plant forms, including castor beans, Indian seeds, sword beans, jack beans, and others. Sumner 1926 provided yet another critical research contribution, in terms of isolating and crystallizing solubilized enzyme urease extracted from jack beans (*Canavalia enxiformis*) in 1926, for which he was awarded Nobel Prize in chemistry in 1946. The first-ever extraction and purification of bacterial urease was then completed by Larson and Kallio (1953) at the University of Iowa using viable cells (*S. pastuerii*). Since those formative early years, a vast level of literature has continued to be published at academic, commercial, and even industrial levels relative to the isolation, purification, and application of urease enzymes.

Plant and bacterial ureases have different protein structures. Plant ureases are made up of single-chain polypeptide of identical subunits, typically of 90 kDa each (Krajewska 2009). The jack bean urease has an 'α'-subunit which has a molecular mass [i.e., without considering co-valent nickel (II) ions] amounting to 90.77 kDa. After considering the

presence of nickel, however, the mass of the hexameric enzyme form with 12 nickel ions should be 545.34 kDa. In contract, bacterial ureases are made up of three distinct subunits, one large (α) and two small (β and γ) sub-units, commonly forming (αβγ)$_3$ trimers. *S. pastuerii* urease (i.e., where these particular sub-unit segments have the following mass levels: 'α' = 61.4 kDa; 'β' = 14.0 kDa; 'γ' = 11.1 kDa). In turn, the resulting urease enzyme forms have an approximate molar mass range between 190 and 300 kDa.

### 2.5.2 Size and Kinetics of Urease

In order to determine the size of a protein molecule, engineers usually convert the mass of a protein molecule to an atomic-level structure or a nanometer-level length. Erickson 2009 offered the following perspectives for evaluating the approximate physical size of a protein. In this case, a protein can be assumed to have a simply, spherical, shape, such that the radius can be calculated. The minimal radius of a sphere would be calculated from the given mass of protein:

$$R_{min} = (3V/4\pi)^{1/3} = 0.066M^{1/3} \text{ (for M in Dalton, R}_{min} \text{ in nanometer)} \tag{2.4}$$

In turn, the urease enzyme size for urease could be approximated as follows:

- Bacterial urease has a mass of 190 – 300 kDa:  $R_{min} = 3.8 – 4.4$ nm

- Jack bean urease has a mass of 545.34 kDa: $R_{min} = 5.4$ nm

The kinetic properties of ureases can be mathematically presented with the use of a Michaelis-Menten equation, which involve a coefficient (i.e., $K_m$) which characterizes the maximal enzyme activity rate. Previous studies have determined that urease $K_m$ values for purified ureases are quite similar with the values measured for crude cell extracts (Mobley and Hausinger 1989). However, the Michaelis-Menten constant $K_m$ value is strongly depended on urease sources (types of plant and micro-organism), purity of enzyme, pH level,

buffers and temperature. Individual ureases present constant $K_m$ values ranging from 0.1 to >100 mM urea. For example, jack bean (*Canavalia ensiformis*) urease is from 2.9 – 3.6 mM (Krajewska 2009) while a range of $K_m$ values for *S. pastueurii* urease was published from 40 – 130 mM urea depended on pH level (Larson and Kallio 1953).

The specific activities of urease enzymes are strongly dependent on the level of purification and the conditions in which they are measured. Homogeneous jack bean urease has a specific activity of approximately 2700 – 3500 µmol urea/min/mg (Krajewska 2009). The purified micro-organism ureases also possess the similar magnitude as that of plant enzyme ranging from 1000 – 5500 µmol urea/min/mg (Mobley and Hausinger 1989). For instance, the urease isolated from *S. pastuerii* is around 2500 µmol urea/min/mg (Krajewska 2009).

### 2.5.3 Methods of Urease Activity Measurement

The urease was not only the first-ever enzyme to be isolated in crystalline form, but also has been applied widely in many industrial and research fields such as medical, waste water, treatment of uremia, treatment of waste water containing urea from fertilizer plants, (Qin 1994) and bio-cementation (Hamdan et al. 2013). Therefore, the determination of activities with urease-catalyzed hydrolysis is a very important aspect of urease enzyme studies and applications. Many previous researchers have investigated several urease activity measurement methods as follow (Qin 1994):

- Determination of the ammonia production rate, either by
    - Phenol-nitroprusside colorimetric method;
    - Nesslerization methods;
    - Enzymatic analytical methods;

- Ammonia or ammonium electrode; or

- The titration of ammonia;

- Determination of a carbon dioxide release rate;

- Evaluation of pH change;

- Colorimetric determination of urea concentration and reduction;

- Thermochemical methods; and

- Conductivity measurement.

Those methods measured substrate/products of the ureolytic reaction or byproducts of the reaction, for example ammonia, which then increase sample pH and conductivity. The most common assays employed to determine ammonia release from the ureolytic reaction are phenol-hypochlorite and Nessler's reagent, but those methods are time consuming, incompatible with common buffers, generate non-homogenous true color solutions, and have the disadvantage of using harmful chemicals (Ran and Kawasaki 2016). Although the titration and pH change methods are simple in operation, they do not provide good results and are strongly dependent on operator skills, let alone room temperature conditions. Recently, bio-geotechnical researchers have largely tended to use the conductivity method which essentially demonstrate the release of ionic products during the urea hydrolysis reaction. The rate of conductivity increase is proportional to the amount of active urease present in the solution. The conductivity method is simple, time saving and not using expensive and harmful chemicals. The recent study has applied the conductivity method for measure urease activity of *S. pastuerii* and extracted urease from themselves.

**2.5.4 Urease Stability and Extraction Methods**

The stability of urease enzyme vary within a large range when enzymes are exposed to different environmental conditions, and following perspectives regarding successful storage methods have been documented by Mobley and Hausinger (1989). Certain environmental conditions are known to inactivate urease, as for example would occur in the presence of heavy metals or strong oxidants (e.g., chlorine, hydrogen peroxide, etc.). Storage conditions are also important, including such factors as temperature, pH, time, chemical substrate presence, etc. Published results for ureases extracted from *Bacillus pastuerii, K. aerogenes*, *Proteus mirabilis*, and *Providencia stuartii* have demonstrated successful retention of full activity for more than a month when the enzyme was stored at 0 ℃ and in the presence of 50 mM HEPES, pH 7.5, buffer containing 1 mM EDTA and 1 mM 2– mercaptoethanol. Glycerol has also been used to stabilize stored urease. For example, nearby 70 % of *Brevibacterium ammoniagenes* urease activity was retained after 2 months at 20 ℃ in 50 % glycerol, 1 mM EDTA, 5 mM 2–mercaptoethanol, and 50 mM phosphate buffer at pH 7.5. Purified urease from *S. pastuerii* will significantly exhibit an irreversible loss of activity when exposed to pH values below 5.2. The range of stability of bacterial ureases was quite wide. The enzyme can stable from 5 – 24 h at pH value of 7 to 10 in temperature from 0 – 50 ℃ (*Providencia rettgeri* urease was stable at temperature up to 80 ℃ in the presence of urea).

As for methods used to disrupt cells and tissues in order to extract enzymes, there is a wide range of options depending on the biomass source, toughness, and what researchers intend to obtain. Several methods have been used to disrupt cells membranes, including the following options:

- French press use, where an applied hydraulic pressure is used within a special sample cell and pressure (20,000 psi),

- Sonication applied a continuous flow of shock waves to break down cell membrane,

- A so-called 'Polytron-tissumizer' technique can be used to apply shear forces from rotating blade to disrupt cells,

- Bead mill operation, where the mill provides shaking in the presence of inert beads

- Blender use, which is mostly applied for plant and animal tissues,

- Grinding with abrasive material, which might be applied when dealing with tough plant-type cellular material, and

- Gentle disruption methods were osmotic shock, chemical solubilization and homogenizer.

Once cells are disrupted, the enzyme will be collected by separation from larger residual cellular fragments using filtration or centrifugation techniques. Sumner (1926) was the first person to isolate urease enzyme using filtration and centrifuge methods to extract urease from fat-free jack bean meal powder. Bacterial urease was extracted from *S. pasteurii* by Larson and Kallio (1953) from University of Iowa in 1954 by using sonic vibration method during 30 mins processing periods. Christians and Heinrich (1986) also used sonication method to lyse *S. pastuerii* cells. A sonication bath Branson B12 with a maximum output of 60 W for 1 min/ml was used for the experiments completed by Christians and Heinrich (1986). During extraction process, temperature and pH values of buffer solution should be controlled.

# CHAPTER 3.  SAND AND SILTY-SAND SOIL STABILIZATION USING BACTERIAL ENZYME INDUCED CARBONATE PRECIPITATION (BEICP)

## 3.1 Abstract

This paper examines the bio-derived stabilization of sand-only or sand-plus-silt soils using an extracted bacterial enzyme application to achieve induced calcite precipitation (ICP). As compared to conventional microbial induced calcite precipitation (MICP) methods, which use intact bacterial cells, this strategy which uses free urease catalysts to secure bacterial enzyme induced calcite precipitation (BEICP) appears to offer an improved means of biostabilizing silty-sand soils as compared to that of MICP processing. Several benefits may possibly be achieved with this BEICP approach, including bio-safety, environmental, and geotechnical improvements. Notably, the BEICP biostabilization results presented by this paper demonstrate: 1) higher rates of catalytic urease activity, 2) a wider range of application with sand-plus-silt soil applications bearing low plasticity properties, and 3) the ability to retain higher levels of soil permeability after BEICP processing. Comparative BEICP versus MICP results for sand-only systems are presented, along with BEICP-based results for stabilized soil mixtures at 90-10 and 80-20 percentile sand-silt ratios. This BEICP method's ability to obtain unconfined compressive strength (UCS) results in excess of 1,000 kPa with sand-plus-silt soil mixtures is particularly noteworthy.

## 3.2 Introduction

This paper's coverage of a bacterial enzyme induced calcite precipitation (BEICP) procedure represents yet another iterative refinement of the overall concept of bio-inspired soil stabilization, which has evolved over the past several decades. The original, first-generation concept of using calcite precipitation by live, urease-active bacteria, albeit for improved oil recovery, dates back to the original work by Ferris and Stehmeier (1991), Ferris et al. (1991), and Kantzas et al. (1992). In turn, after shifting this concept's focus to soil biostabilization, several hundred papers have now been published in relation to application strategies and performance outcomes when using microbial induced calcite precipitation (MICP). The MICP mechanism is a calcium carbonate precipitation process derived from hydrolysis of urea following supplying calcium source as a result in a pH increase through the production of ammonia and an increase in $CaCO_3$ deposition and accumulation (van Paassen 2009; Whiffin 2004). The urea hydrolysis is carried out through urease enzyme generated from ureolytic bacteria. The bacterial cells are also nucleation sites on which calcite crystallization takes place to bind sand grains. These research findings, though, have revealed a couple of important application concerns. One notable issue raised by Kavazanjian and Hamdan (2015) involved the physical migration of MICP's urease-bearing microbes, which was thought to be limited to soils with pore spaces larger than that of medium to fine sands. In turn, at that point in time (circa 2015) MICP did not appear to be well suited to soil systems bearing finer-grained, higher plasticity soils which would then impede bacterial migration. The validity of this concern, though, is now unclear given that a limited number of more recently published papers have claimed successful MICP use with residual soil and silty sand soil (Lee et al. 2013; Soon et al. 2013, 2014; Oliveira et al. 2016; Jiang et al. 2017). A further complicating concern for MICP operations, though, involves the complex life cycle

of these microbial cells when they are transferred from their original, synthetic growth culture media to a natural soil environment. This transition may impose negative impacts (e.g., lower metabolic rates during lag and adaptation phases), which in turn could retard the desired calcite precipitation.  Even then, just growing and preserving the involved microorganisms under field-level conditions would have its own set of complications.  After two decades of active MICP research, therefore, it is noteworthy that relatively few large, meter-scale projects have yet been attempted within either lab or field studies using sand and natural soil systems (Burbank et al. 2011; Gomez et al. 2015a; De Jong et al. 2009; Nassar et al. 2018; van Paassen 2011; van Paassen et al. 2009, 2010a; Phillips et al. 2016; van der Star et al. 2011).

Prompted by these issues, the notion of using free enzyme induced calcite precipitation (EICP) was then launched in the early 2000's. Bang et al. (2001) triggered this new line of thinking, where a commercially-purchased urease was used to secure EICP-based metabolism for crack repair with concrete materials. The EICP treatment method employs purified urease enzyme instead of urease producing bacteria as the ureolytic agent. The purified enzyme is extracted from plant sources, mainly from jack bean (Canavalia ensiformis). As such, the advantages of free enzyme biostabilization processing was conceptually recognized at a point many years before the concept of using EICP for soil stabilization had even been conceived. For example, Nemati and Voordouw (2003) studied the direct application of urease to reduce the permeability of porous media, and Nemati et al. (2005) stated that the quantity of calcium carbonate produced by urease was almost three times higher than had been measured with MICP treatment.

At the present time, therefore, approximately twenty-five free-urease EICP-related papers have been published within civil and environmental engineering venues. Table 3.1 summarizes these publications relative to their native free urease agent, enzyme source options, and intended application goals per each publication.

Furthermore, two related patents have been recorded for this approach, filed by Park et al. (2011) and Kavazanjian and Hamdan (2013). Several enzyme sources could have been used for the extracted free-urease agents applied during these prior EICP studies, including that of plant, bacterial, and even commercial sources. To date, though, all of the aforementioned EICP-related research findings have used either plant or commercial urease applications, as opposed to this paper's focus on bacterial-derived urease.

The more recent EICP papers (using plant and commercial enzyme sources) have also largely focused on sand-based soil applications, with limited consideration of more complex soil mixtures with higher plasticity. Five of these papers, though, did study varying sand, silt, clay, and/or dust mixtures (Bang et al. 2009; Kavazanjian and Hamdan 2015; Oliveira et al. 2016; Hamdan and Kavazanjian 2016; Kavazanjian et al. 2017), although with varying degrees of success. For example, Oliveira et al. (2016) reported relatively low unconfined strength results (i.e., with a maximal 250 kPa UCS strength outcome) when treating a combined sand, silt, and clay soil using EICP processing.

This current paper consequently offers a set of new perspectives on the process and performance of EICP biostabilization, and uniquely that of the BEICP methodology, which were premised on the following two initial hypotheses:

(1) that the involved bacterial-derived urease enzymes could rapidly be grown and successfully extracted using sonication for subsequent BEICP use rather than relying on expensive commercial, or slower growing plant-based, enzymes sources, and

(2) that EICP-based biocementation of both sand and sand-silt soils could be achieved using a BEICP procedure which was uniquely different from the previously published MICP and EICP methods and outcomes.

This research effort subsequently started with the development of a sonication technique to lyse viable cells of *Sporosarcina pasteurii* bacteria in order to release their intracellular urease materials. This extracted enzyme was then used to treat a group of test columns bearing different percentages of natural fine-grained soil fractions by weight.

This paper investigated the applicability of BEICP processing, and notably that of using bacterial-derived urease enzymes, to stabilize both non-plastic, sand-only and low plasticity, silty-sand soil materials. Performance assessment included unconfined compressive strength measurements to quantify product soil stability, along with percentile calcium carbonate deposition levels plus product permeability. These results were correlated with three varied BEICP treatment regimes, including 8-, 12-, and 16-cycle sequential processing steps by which the operative free bacterial enzyme plus complementary urea and calcium chloride chemicals were applied. Triplicate testing was also conducted in each case to ensure valid performance outcomes.

Table 3.1 *Overview of Enzyme Induced Calcite Precipitation research publications*

| Urease source | Chemical supplier | Self-extracted | Application | References |
|---|---|---|---|---|
| Jack beans | x | | Permeability reduction | Nemati and Voordouw 2003; Nemati et al. 2005 |
| | x | | Permeability reduction | Larsen et al. 2008 |
| | x | | Dust suppression | Bang et al. 2009 |
| | x | | Permeability reduction & strength increasing | Yasuhara et al. 2011, 2012 |
| | x | | Permeability reduction | Handley-Sidhu et al. 2013 |
| | x | | Permeability reduction & strength increasing | Neupane et al. 2013, 2015a; b |
| | x | | Permeability reduction; strength increasing & dust suppression | Hamdan et al. 2013, 2016; Hamdan and Kavazanjian 2016; Kavazanjian and Hamdan 2015; Kavazanjian et al. 2017 |
| | x | x | Strength increasing | Nam et al. 2014; Park et al. 2014 |
| | x | | Strength increasing | Putra et al. 2016, 2017a; b |
| | x | | Ureolytic efficiency | Jiang et al. 2016 |
| | x | | Strength increasing | Oliveira et al. 2016 |
| | x | | Crack healing | Dakhane et al. 2018 |
| Water melon seeds | | x | Strength increasing | Dilrukshi et al. 2016 |
| Sword beans | x | | Strength increasing | Simatupang and Okamura 2017 |

## 3.3 Methods and Materials

### 3.3.1 Bio-preparation Procedures

**Biomass culturing**

This project's commercial bacterial isolate, *Sporosarcina pasteurii* ATCC-11859, was obtained from the American Type Culture Collection (Manassas, Virginia). A sterile pipet was used to transfer this seed into a culturing medium using a laminar flow hood to reduce the risk of culture contamination. This pre-sterilized culturing broth used an 'ammonium-trypticase soy broth' (NH4 -TSB) growth media which included: tryptic soy broth at 20 g/L, ammonium sulfate at 10 g/L, Tris buffer at 0.13 mol/L, and an overall solution pH of 9.0. The culture flask was then covered with a pre-sterilized sponge to filter out atmospheric bio-contaminants while still providing oxygen to the culture. A shaking incubator (Innova Model 4000, New Brunswick Scientific) was used to incubate this culture for 48 h with a continuous shaking speed of 160 rpm at 30 °C. After incubation, this stock microbial culture was then stored at 4 °C prior for subsequent use.

**Biomass sonication and enzyme extraction**

Urease extraction was completed using a repetitive series of cyclic 'run-cool' (i.e., 10 min 'on' followed by 10 min 'off') sonication steps. Six such cycles were applied over a two-hour period, with a 150 ml aliquot of the original stock microbial culture being placed directly into a sonication bath (Bransonic Model 220; 120 volt, 125W, and 50/60 kHz). Both continuous and cyclic 'run-cool' sonication modes were evaluated during preliminary scoping studies. Continuous sonication did produce a release of intracellular urease, albeit with a progressively escalating level of enzyme retardation likely caused by sample heating. Much the same outcome had been reported by Raymond et al. (2011), where a negative denaturing impact occurred with extracted enzymes subjected to prolonged sonication at

higher temperatures. Therefore, the cyclic processing mode was adopted given that it

provided the lowest temperature buildup (i.e., typically 32 – 34 ºC) and highest residual

enzyme activity.

The pH, temperature, and volume of each sample were measured during sonication

runs, and optical density (OD600) plus microscopic observation was used to qualitatively

confirm cell lysis. Figure 3.1 depicts the extent of cell lysis typically observed relative to pre-

and post-sonication. After completing these tests, the remaining lysed solution was then

subjected to a relative centrifugal force of 5500 RCF for 20 min to separate out residual

cellular debris solids from the extracted, soluble urease. This centrifuged free enzyme

solution was then diluted to achieve a desired final ureolytic activity as described below.
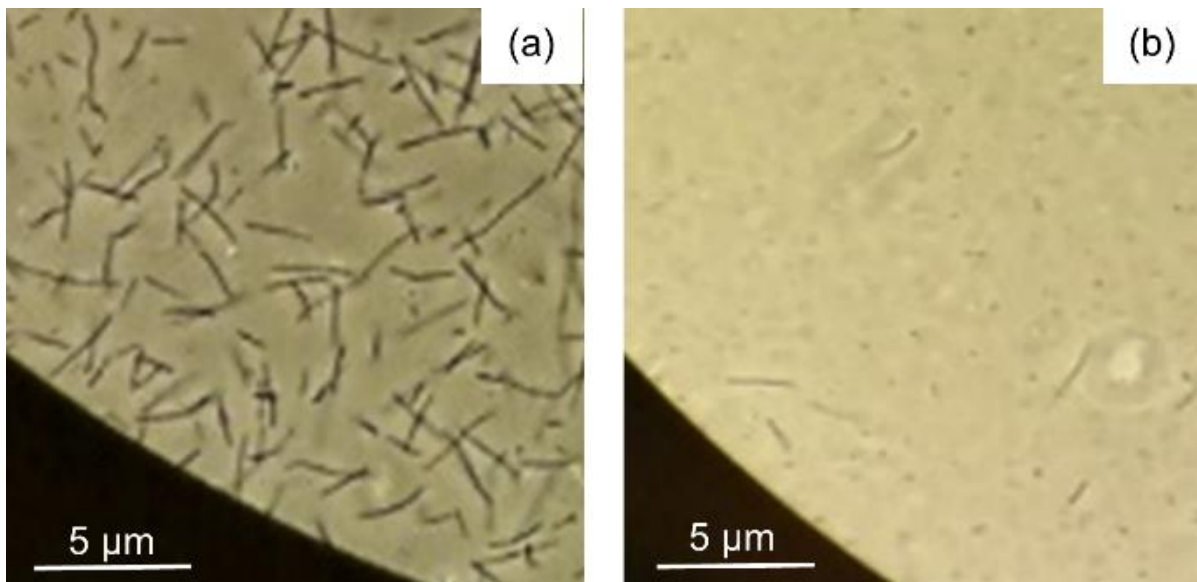


Figure 3.1 *Microscope images of culture: (a) before sonication (showing intact cells); (b) after sonication (showing cell lysis)*

### 3.3.2 Experimental Materials

#### Sand and silty-sand soil test materials

Ottawa #20/30 silica sand, as described in ASTM C778 (2014), was used as a coarser

soil fraction. This sandy soil material contained more than 98.7 % silica ($SiO_2$). The specific

gravity, maximum and minimum void ratios ($e_{max}$ and $e_{min}$) of the sand were 2.65, 0.74 and 0.51, respectively. The sand material was also initially washed with deionized water to remove any soluble chemicals, followed by oven drying at 105 °C for 24 h before being tested. A natural loess from Iowa was used in this study as a fine-grained soil. A sieve analysis test and a hydrometer analysis test were conducted to determine the particle sizes of the loess soil. Results showed that loess soil had 0.7 % of sand, 86.5 % of silt, and 12.8 % clay sized particles. The loess soil was sieved through a U.S. Sieve No. 200 (opening 0.074 mm) to collect only silt and clay particles. Three soil mixtures were prepared for packing the test soil columns. The test soils were prepared by mixing dry Ottawa sand #20/30 with oven-dried loess fines to achieve a desired fines content (FC). This percentage of fines content was calculated as the dry mass of silty soil to the sample's total dry soil mass. Three different soil blends were evaluated, including: 1) 100 % sand and 0 % fines, 2) 90 % sand and 10 % fines, and 3) 80 % sand and 20 % fines. These three options are subsequently referred to as: 1) 100-0, 2) 90-10, and 3) 80-20. The material properties and grain size distributions are summarized in Table 3.2 and Figure 3.2, respectively. The 100-0 mixture is classified as poorly graded sand (SP) according to the Unified Soil Classification System (USCS; ASTM 2010). The 90-10 and 80-20 mixtures are identified as poorly graded sand with silt (SP-SM) and silty sand (SM) and both of these mixtures are low plasticity soils based on the Atterberg limits presented in Table 3.2. The Atterberg limits of the 90-10 and 80-20 mixtures were similar. The liquid limit (LL) and plastic limit (PL) were conducted by following the ASTM D4318-17 standard which requires that the testing soil must be smaller than the sieve opening size of the No.40 sieve (0.42 mm). Therefore, all (99%) of the Ottawa sand # 20-30 (0.85 – 0.6 mm) was retained on the No.40 sieve, whereas fine-grained loess soil (smaller than 0.075

mm) was collected for LL and PL testing. As both the 90-10 and 80-20 mixtures used Loess

soil as the fines, the tests resulted in similar LL and PL for both mixtures.
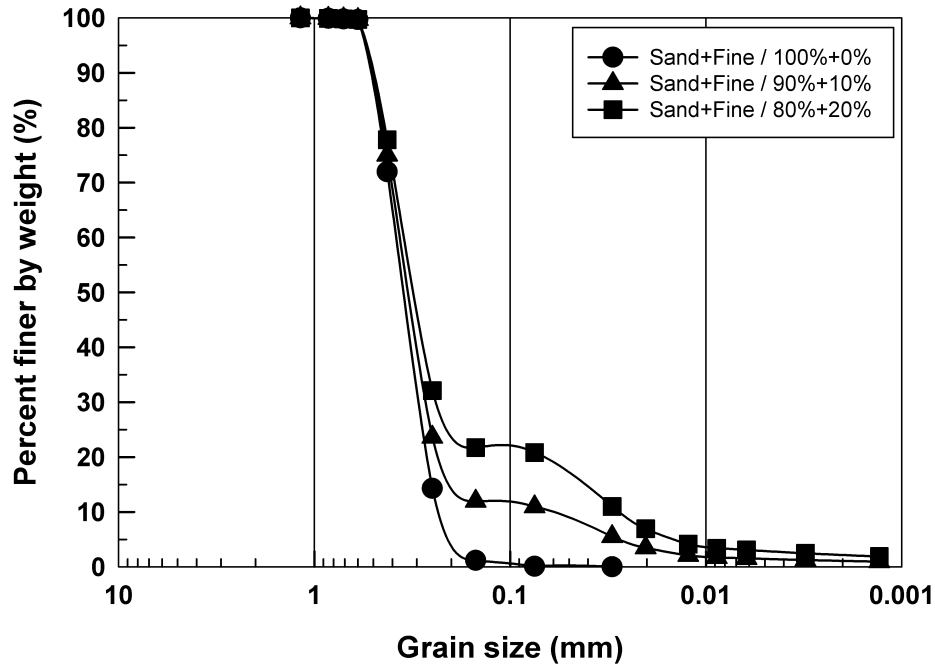


Figure 3.2 *Grain size distribution curve of tested soils*

Table 3.2 *Soil specimen properties*

| Material | USCS | Packing method | e | $D_{10}$ (mm) | $D_{50}$ (mm) | FC (%) | LL (%) | PL (%) | $CaCO_3$ (%) |
|----------|------|----------------|------|------|------|------|------|------|------|
| 100-0 | SP | Wet tamping | 0.58 | 0.58 | 0.72 | 0 | NP | NP | 0 |
| 90-10 | SP-SM | Wet tamping | – | 0.06 | 0.7 | 10 | 34.5 | 27.3 | 0.8 |
| 80-20 | SM | Wet tamping | 0.61 | 0.028 | 0.67 | 20 | 34.5 | 27.3 | 1.6 |

Note: NP = Nonplastic

### 3.3.3 Experimental Procedures

#### Soil stabilization column preparation

Soil stabilization columns were prepared for three different soil mixtures with both

sand-only and silty-sand soils. Each specimen was treated with MICP or BEICP to compare

the impact of both treatment methods on UCS and permeability. Soil specimens were treated

with either 8- 12-, or 16-cycles, given that Inagaki et al. (2011) and Choi et al. (2016) used

similar levels of ICP cycling. More detailed information regarding the treatment methodologies will be provided in the next section.

Prior to uploading soils into each test column, the dry soil mixtures were initially mixed with distilled water to achieve 5 % moisture. A moist-tamping method was then used to pack the specimens, where this pre-moistened soil was gently tamped in PVC columns with 50 mm diameter and 100 mm height dimensions. To achieve a similar specific density in each layer, pre-determined amounts of soil were added in ten successive layers of equal thickness (i.e., at 10 mm per layer) within each column. These column compaction steps were carefully conducted to achieve the similar void ratio (e) levels within all column samples shown previously within Table 3.2.

Both upper (inlet) and lower (outlet) ends of each column were then fitted with a pre-cut section of scouring pad material 3-M Scotch Brite Model 7447 to distribute flow streams and avoid clogging. The lower end of each column was also fitted with an additional plastic cap (i.e., glued below the scouring pad section) which had been pre-filled with gravel in order to prevent unwanted loss of the un-stabilized raw soil sample. The schematic diagram of the test set-up is shown in Figure 3.3.

**Batch column MICP and BEICP treatment procedures**

Two modes of soil stabilization were evaluated using the latter soil columns, including: 1) the BEICP method, and 2) a conventional microbial-based MICP method.  A circulated-percolation process was then applied to treat soil columns under partial-saturated condition. The sandy soil and silty-sand soil columns were processed using the following sequential procedure (Figure 3.3). First, the catalytic biological solution (either extracted urease for the BEICP method, or bacterial cells for the MICP method), was pumped and recycled into the top of a soil column and gravity drained out from the bottom. The urease

activity of the solutions was adjusted to approximately 4 – 5 mM urea/min by dilution with deionized water for MICP and BEICP treatment methods. A peristaltic pump (Masterflex Model 77202-50) with silicone tubing (Masterflex Model 96410-16) was used to recirculate this biological liquid for 3 h with the rate of 0.8 – 5 ml/min in order to achieve a 60% saturation level consistent with prior research by (Cheng et al. 2013), which allowed the bacterial cells or extracted enzyme to sorb onto or be trapped onto the soil particle surfaces.
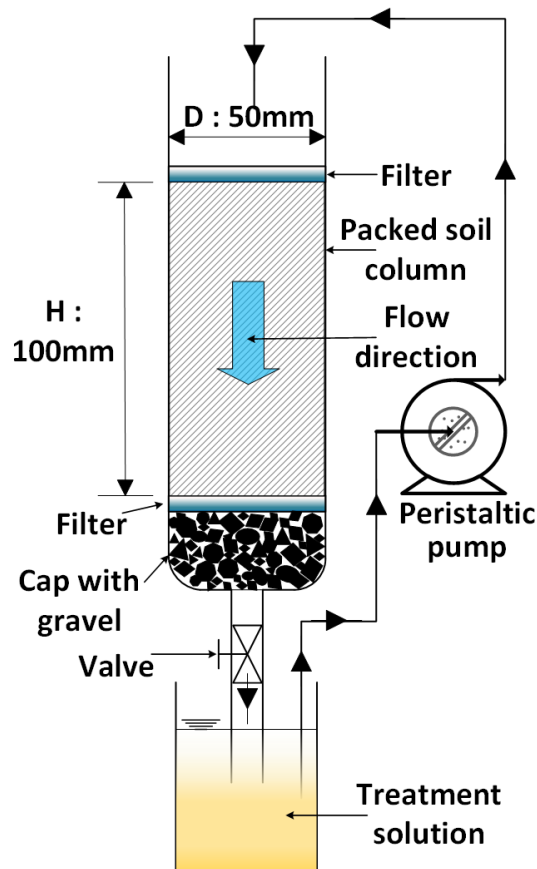


Figure 3.3 *Soil column circulating-percolation treatment (after Choi et al. 2016)*

Second, after the latter 3 h introduction of the catalytic agents (i.e., either MICP culture or BEICP enzymes), the pore volume biological liquid was drained off the soil column. Third, a mixed chemical solution of urea and calcium chloride (0.3 M by 1:1 ratio) was then introduced and circulated for 9 – 12 h. Fourth, the soil column was flushed with

cyclic deionized water pumping for 2 h to remove soluble byproducts and then the bottom cap was removed to drain off all liquid for approximately 10 h. After completing this treatment cycle, fresh biological solution and chemical were then introduced and recirculated through the soil column on each successive new cycle. This step-wise approach to introduce enzyme solution (or bacterial cells) and urea/calcium chloride solution was repeated on a 'one cycle per day' routine for either 8, 12, or 16 days total treatment phases. One clarification regarding the MICP testing regime is warranted, with which tests on the low plasticity, silty-sand soil was stopped after 12 cycles because this approach was unable to form fully intact bio-cementation columns. This behavior was attributed to $CaCO_3$ precipitation clogging of the upper portion (~ 30mm) of these specimens. In turn, the middle and bottom parts of these silty-sand MICP-treated samples remained un-solidified and physically unstable.

### 3.3.4 Analytical Procedures

#### Culture optical density

A qualitative assessment of viable biomass optical density (OD) was determined spectrophotometrically at 600 nm (i.e., OD600) using a visible light spectrophotometer (Hach Model #DR 3900).

#### Urease activity

Conductivity change was used to measure enzyme activity as ammonium ions were released during urea hydrolysis. The rate of conductivity increase is proportional to the amount of active urease present in the solution. This test was completed with initial 5 ml aliquots of either the bacteria cells or urease solution. After adding 50 ml of a 1-M urease solution, a conductivity meter was used to track the release of ammonium from urea, which

exhibited a linear correlation ($R^2$ = 0.9979) between the NH4+ (Y) concentration (in mM) and electric conductivity (X) in milli-Siemens (mS) (Chu et al. 2012):

$$Y = 9.3316X - 0.8198 \tag{3.1}$$

**Stabilized soil permeability**

The permeability of the bio-cemented soil samples was measured by using a constant head method (ASTM D2434-68) with a rigid side-wall device set-up while the samples were still held within the PVC test columns. Prior to the permeability tests, both filters (top and bottom) along with the gravel layer and bottom cap of the column were removed. Tap water (2 L) was pre-flushed through the bio-cemented soil samples under 15 kPa back pressure (hydraulic head of about 150 cm) to release trapped pore air and to saturate samples before measuring permeability (Cheng et al. 2013). Measurements of untreated sand soil and silty-sand soil permeabilities were also done to compare against the bio-treated specimens. After the initial saturation step, permeability tests were run until steady hydraulic conductivity values (k) (cm/sec) were reached. Tests were stopped after k of the specimen did not vary more than 20 % (data not shown here for brevity). This state would be reached only if the specimen was fully saturated.

**Stabilized soil unconfined compressive strength**

After measuring the hydraulic conductivity of bio-cemented samples, the columnar PVC molds were cut carefully with a band saw machine to separate the bio-cemented samples. The specimens could stand alone while in a wet condition, which meant that stabilization had occurred. Afterwards, samples were oven dried for 48 h at a moderate temperature (i.e., ~ 50 °C) to avoid baking clay minerals in silty-sand soil samples (Hawkins and Mcconnell 1992). The unconfined compressive strength (UCS) test was conducted in accordance with ASTM D4219-08. The tests were conducted on samples with a standard size

preset by the test column's dimensions (i.e., diameter D = 50 mm and height H = 100 mm). A Geotac constant-displacement mode UCS machine was used to shear the samples. The rate of loading was 2 mm/min. A plastic bag was used to cover each specimen during testing process to collect broken sample materials which were then used for further calcium content analysis (Al Qabany and Soga 2013).

### Stabilized soil calcium carbonate precipitation content

An acid-rinsed method was used to complete these calcium carbonate measurements, and these tests were completed immediately after the UCS tests (Feng and Montoya 2015). The calcium carbonate content of the stabilized soils was determined according to a percentile weight fraction. Deionized water was initially flushed through cemented specimens to dissolve and flush out any remaining soluble salts. After samples broken down by UCS test, approximately 5 g of biocemented soil was taken at the middle of soil column, and placed on a fiberglass filter pad. The small specimen and filter were then over-dried at 105 °C degree overnight. Then, the weights of the dry sample and filter were measured. Afterwards, 1 M HCl solution was added to dissolve the precipitated calcium carbonate until no bubbles were generated. Finally, that soil (and filter) was rinsed with deionized water and oven dried again to determine the dry weight of the acid-flushed residual soil (without $CaCO_3$). The amount of the precipitated $CaCO_3$ was calculated by the difference between the dry weight (W) of the specimens before (soil + $CaCO_3$) and after (soil only) washing in acid (% $CaCO_3$ = 100 % * ($W_{soil+CaCO3} − W_{soil}$)/$W_{soil}$).

It should also be noted that the fine-grained silty soil obtained from Iowa loess contained an original $CaCO_3$ content (i.e., ~8 %), and that it was subsequently necessary to adjust the final $CaCO_3$ content measured with the post-stabilized silty-sand soils relative to this initial amount of silt-based $CaCO_3$. When evaluating the plastic, sand-silt soils, therefore,

these pre-stabilization levels of calcium carbonate were 0.8 % (w/w) for the 90-10 sample

and 1.6 % (w/w) for the 80-20 sample. In turn, derivations with BEICP-treated soils had to

be adjusted to take into account these original, pre-treatment percentages.

**Scanning electron microscope and X-ray diffraction testing**

Scanning electron microscopy (SEM) was used to produce high resolution imagery of

the $CaCO_3$ precipitation deposited on tested soil particles with bio-cementation treatment.

These SEM analyses were conducted using an FEI Quanta-250 FE-SEM instrument managed

by the Iowa State University Materials Analysis and Research Laboratory. During additional

X-ray diffraction (XRD) testing, representative bio-cemented samples were pre-crushed and

ground before mounting on a glass filter. A Siemens Model D500 diffractometer was used to

identify crystal characteristics using comparative evaluation against International Center for

Diffraction Data records.

### 3.4 Results and Discussion

### 3.4.1 Urease Sonication Extraction

Table 3.3 presents the final sample temperature, sample volume reduction, optical

density, and urease activity results typically observed when using a cyclic 'run-cool'

sonication method, as compared to that of the original cultured biomass. These results

represent specific outcomes for the conditions of the previously identified sonication

hardware, sample size, and operating conditions.

Table 3.3 showed a slightly increase in temperature and a constant value for pH after

60 min of sonication. However, the OD600 values decreased significantly (by > 70 %) after

sonication compared to the control culture. This decrease was correlated to the lysing of

bacterial cells (Figure 3.1). In addition, the sonication method resulted in a 20 percent

volume reduction through evaporation. The 'cyclic run-cool' sonication method typically

produced an approximate two-fold increase in urease activity (see Table 3.3's value of 25.4 mM urea per min) as compared to the original whole cell solution. Even then, re-diluting the sample back to a full 150 ml volume would have still resulted in a 20.3 mM/min activity rate, which was ~75 % higher in urease activity compared to the original culture. This increase in enzyme activity may be due to the lack of transport constraints of the substrate (i.e., urea) through the cell wall in the free enzyme suspension. It should also be noted that these sonicated urease activity rates are either comparable to, or perhaps even higher than, that of the activities reported within many of the previously cited MICP and EICP publications.

Table 3.3 *Typical cyclic 'run-cool' sonication processing results for urease enzyme extraction*

| Test conditions and measurements | | Control (culture) | Cyclic run-cool sonication |
|---|---|---|---|
| Sonication total 'run' times (min) | | 0 | 60 |
| Optical density (600nm) | | 1.25 | 0.34 |
| pH | | 8 | 7.92 |
| Temperature ($^{o}$CP) | | 30 | 34 |
| Volume reduction (%) | | 0 | 20 |
| Urease activity (mM/min) | Measured | 12.1 | 25.4 |
| | Activity ratio (measured : control) | | 2.1 |

There was an also an element of uncertainty as to whether the obtained sonicated solution may have still contained viable ureolytic cells. However, as mentioned previously, microscopic observation showed only nominal levels of lingering intact cells following sonication. Furthermore, the sonicated solution was centrifuged to remove residual cellular material, and pre- and post-centrifuge activity testing showed less than 1 % difference. Furthermore, specific SEM observation of BEICP-stabilized sands showed no indication of

the surficial CaCO₃ buildup typically observed with viable cell activity during MICP processing (i.e., see upcoming Figure 3.7).

### 3.4.2 MICP *versus* BEICP Stabilization of Sandy Soil

The MICP and BEICP methods were comparatively evaluated with the treatment of sand-only test columns which received 8, 12 or 16 repetitive treatment cycles in order to achieve different levels of calcium carbonate content. A complete set of tabular testing results for all of the MICP and BEICP tests is provided in Table 3.4, covering both sand-only and silty-sand samples.

Figures 3.4 and 3.5 present the comparison of these MICP and BEICP methods on sandy soil in terms of strength and permeability. In both cases, these data are presented in relation to the associated levels of CaCO₃ precipitation measured according to treatment cycle numbers. In addition, Figure 3.6 shows the comparison of the efficiencies of increase in UCS and reduction in permeability between both methods. The following SEM photographs given in Figure 3.7 then provide a visual perspective of the stabilized sand products generated with these alternative methods.

**Unconfined compressive strength tests with MICP and BEICP treated sandy soil**

Figure 3.4 demonstrates that the MICP process consistently produced a higher unconfined compressive strength (UCS) for the same number of treatment cycles as compared to the BEICP treatment, while at the same time realizing a higher level of calcium carbonate precipitation. After 16 cycles, and as recorded in Table 3.4, the mean UCS values for MICP- and BEICP-treated samples were respectively 1,960 kPa and 1,691 kPa.

Table 3.4 *Geotechnical laboratory results for MICP- and BEICP-treated soils versus untreated soils*

| Sample ID | FC (%) | Cycle #'s | No. samples | UCS (kPa) AVG[a] | STD[b] | CaCO$_3$ (%) AVG[a] | STD[b] | Permeability (cm/s) AVG[a] | STD[b] | Relative error[c] | ICP options |
|---|---|---|---|---|---|---|---|---|---|---|---|
| B100-0-8 | 0 | | 3 | 600 | 119 | 2.23 | 0.45 | $3.60 \times 10^{-02}$ | $3.48 \times 10^{-02}$ | $4.20 \times 10^{-01}$ | |
| B90-10-8 | 10 | 8 | 3 | 394 | 79 | 4.10 | 0.56 | $1.28 \times 10^{-02}$ | $9.12 \times 10^{-03}$ | $3.10 \times 10^{-01}$ | |
| B80-20-8 | 20 | | 3 | 231 | 50 | 5.47 | 0.93 | $3.10 \times 10^{-03}$ | $1.57 \times 10^{-03}$ | $2.20 \times 10^{-01}$ | B |
| B100-0-12 | 0 | | 3 | 1340 | 105 | 5.23 | 0.91 | $2.34 \times 10^{-02}$ | $2.41 \times 10^{-02}$ | $4.47 \times 10^{-01}$ | E |
| B90-10-12 | 10 | 12 | 3 | 972 | 74 | 11.74 | 1.14 | $3.53 \times 10^{-03}$ | $2.20 \times 10^{-03}$ | $2.70 \times 10^{-01}$ | I |
| B80-20-12 | 20 | | 3 | 711 | 109 | 12.87 | 1.78 | $2.52 \times 10^{-03}$ | $2.62 \times 10^{-03}$ | $4.51 \times 10^{-01}$ | C |
| B100-0-16 | 0 | | 3 | 1691 | 634 | 7.12 | 1.51 | $6.52 \times 10^{-03}$ | $8.14 \times 10^{-04}$ | $5.42 \times 10^{-02}$ | P |
| B90-10-16 | 10 | 16 | 3 | 1118 | 45 | 12.59 | 1.52 | $9.62 \times 10^{-04}$ | $9.92 \times 10^{-04}$ | $4.47 \times 10^{-01}$ | |
| B80-20-16 | 20 | | 3 | 842 | 187 | 13.15 | 3.08 | $1.87 \times 10^{-04}$ | $1.52 \times 10^{-04}$ | $3.53 \times 10^{-01}$ | |
| M100-0-8 | 0 | 8 | 3 | 742 | 89 | 5.69 | 0.53 | $1.11 \times 10^{-02}$ | $6.40 \times 10^{-03}$ | $2.50 \times 10^{-01}$ | M |
| M100-0-12 | 0 | | 3 | 1662 | 191 | 11.04 | 1.75 | $2.40 \times 10^{-03}$ | $1.59 \times 10^{-03}$ | $2.88 \times 10^{-01}$ | I |
| M90-10-12 | 10 | 12 | 1 | | | | | Failure | | | C |
| M80-20-12 | 20 | | 1 | | | | | Failure | | | P |
| M100-0-16 | 0 | 16 | 3 | 1960 | 284 | 13.48 | 2.02 | $4.47 \times 10^{-04}$ | $3.96 \times 10^{-04}$ | $3.62 \times 10^{-01}$ | |
| U100 | 0 | | 1 | | | 0 | | $1.01 \times 10^{-01}$ | | | |
| U90 | 10 | 0 | 1 | N/A[d] | | 0.8 | | $6.41 \times 10^{-02}$ | | | Un-treated |
| U80 | 20 | | 1 | | | 1.6 | | $2.56 \times 10^{-02}$ | | | |

Note: [a] average; [b] standard deviation; [c] relative error necessary for log-based plots (Baird 1994); [d] not analyzed

These strength and CaCO₃ precipitation levels with MICP stabilization were similar to those reported during three preceding MICP studies (van Paassen et al. 2010; Al Qabany and Soga 2013; Cui et al. 2017). Yasuhara et al. (2012) also conducted four and eight-cycle EICP stabilization tests on sandy soil that provided a comparable range of unconfined strength from ~400 kPa to ~1,600 kPa.

These higher UCS and CaCO₃ precipitation levels achieved at each of the cycling levels with MICP versus BEICP suggest that viable MICP cells have a higher level of entrapment, binding, and sorption leading to subsequently higher levels of calcite formation than was the case with the smaller, soluble BEICP enzyme catalysts. A further characterization of the apparent stabilization 'efficiency', though, can also be derived by comparing UCS levels at roughly comparable CaCO₃ precipitation levels, where these data appear to suggest a higher UCS outcome with BEICP processing.
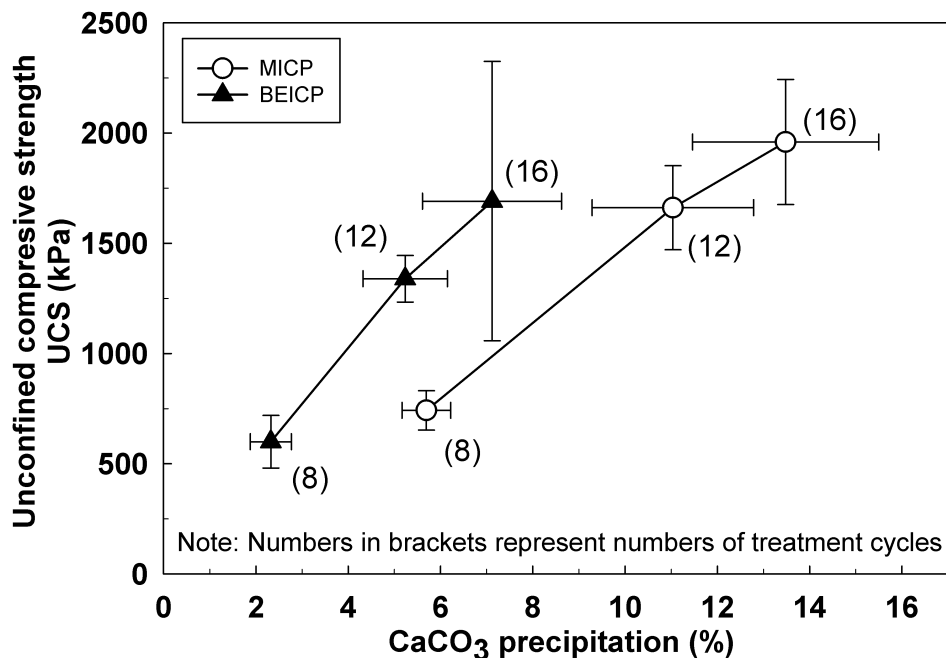


Figure 3.4 *Comparison between MICP and BEICP samples of sandy soil: unconfined compression strength versus CaCO₃ precipitation at different number of treatment cycles*

**Permeability tests with MICP and BEICP treated sandy soil**

The permeability results given in Figure 3.5 are again presented in relation to calcium carbonate precipitation results produced with samples being treated by either MICP or BEICP procedures. The original untreated sand had an initial permeability of ~10$^{-1}$ cm/s. In either case, a progressive reduction in permeability of sand treated by increased numbers of stepwise MICP and BEICP steps would be expected following the precipitation of calcium carbonate which had clogged previously open pore space (Nemati and Voordouw 2003; Whiffin et al. 2007). MICP treatment achieved nearly a three-log final decline after 16-cycle treatment. Note also that Figure 3.5 plots relative error values for permeability (see Table 3.4). As described by Baird 1994, relative error was calculated by the following equation: Relative error = (0.434) x (permeability standard deviation / average permeability).

For MICP-treated samples, these permeability data are similar to the results reported by Al Qabany and Soga (2013) and Choi et al. (2016) when using the same concentration of chemical solutions and when accumulating similar levels of calcium carbonate precipitation. For BEICP processing, though, the decline in permeability was distinctly different, with only an approximate one-log decrease even after the sixteenth cycle step. These BEICP permeability changes were also noticeably different (i.e., where BEICP produced a more permeable result) than had been previously reported by Yasuhara et al. (2012). However, Yasuhara et al. (2012) used a higher concentration of substrate urease and calcium source solutions than was the case with this research. Assumedly, the increased supply of urease and calcium chloride solutions used by these authors would have led to a higher degree of precipitate formation which then resulted in the greater reduction in permeability.

On the other hand, the progressively decreased permeability of MICP-based stabilization represents an inherent disadvantage for these cyclic, stepwise ICP methods given that increasing pore space clogging will then retard the desired transport of the operative urease-bearing bacterial cells. This sort of MICP limitation has been noted by Whiffin et al. (2007) and van Paassen (2009), where the migration of urease-bearing microbes away from the point of injection would be limited, and that in turn their ability to form uniformly cemented samples would be constrained. Conversely, BEICP's ability to stabilize sands without imposing nearly as much permeability reduction would be favorable, since it would allow further cycles of treatment if desired to achieve higher stabilization levels.
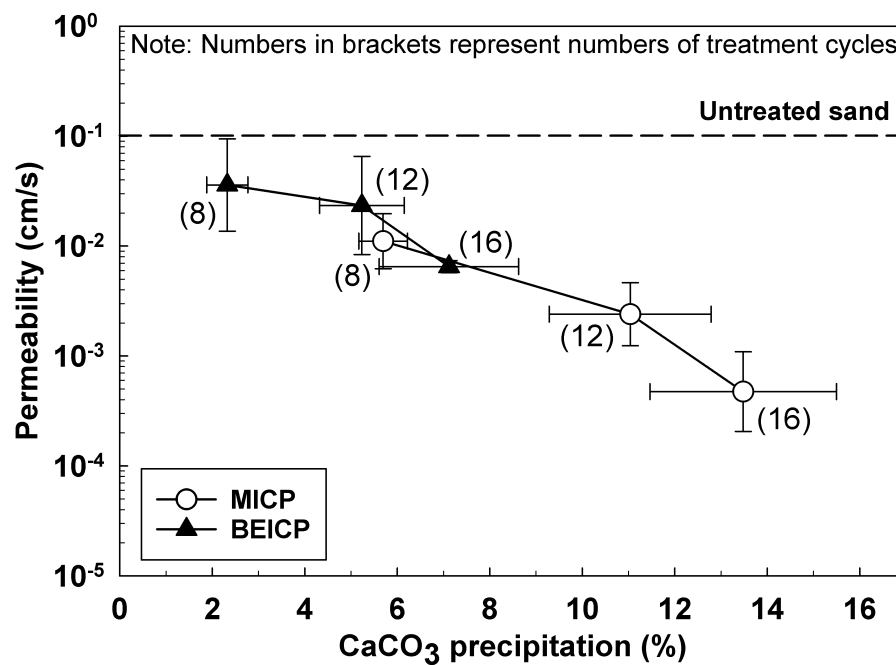


Figure 3.5 *Comparison between MICP and BEICP samples of sandy soil: Permeability versus CaCO₃ precipitation at different number of treatment cycles*

**Comparison of efficiency of increase in UCS and permeability reduction between MICP and BEICP methods**

Figure 3.6 compares the efficiency of MICP and BEICP methods in terms of strength gain and permeability reduction on sandy soils. The efficiency of UCS increase rate was determined using the ratio of the increment of mean increase of UCS to the increment of mean increase in $CaCO_3$ content (Figure 3.6a) while the efficiency of permeability reduction was calculated by ratio of the reduction in permeability to the increase in $CaCO_3$ content (Figure 3.6b). For example, the efficiency of increase in UCS of BEICP-treated sandy soil sample from 8 to 12 cycles was computed as $(UCS_{cycle12} - UCS_{cycle8})(kPa) / (CaCO_{3cycle12} - CaCO_{3cycle8})(\%)$. Similarly, the efficiency of permeability reduction of the sample from 8 to 12 cycles was determined as $|(permeability_{cycle12} - permeability_{cycle8})(cm/s)| / (CaCO_{3cycle12} - CaCO_{3cycle8})(\%)$.

In general, the increase rate of UCS in sandy soils obtained with BEICP method is higher than those observed with MICP method. It is apparent that the ratio of UCS to $CaCO_3$ content in BEICP-treated samples is approximately 1.5 to 2 times higher than those observed with MICP-treated samples. It is reasonable to suspect that the observed higher efficiency with BEICP-treated specimens is due to the precipitation of $CaCO_3$ mainly at contact points of sand grains, whereas the $CaCO_3$ was formed on particle-particle contacts and filled void space of the sand matrix during MICP treatment. This agrees with the findings of previous studies which stated that the calcite concentrated at interparticle connection points are the ones that mainly contribute to the strength improvement in soils (Cheng et al. 2012; DeJong et al. 2010b). Furthermore, it was observed that the strength gain efficiency of both systems were more similar at higher treatment cycles. The reduction in the UCS increase rate with higher treatment cycles is the result of saturation of sandy soils by $CaCO_3$. Although BEICP

method provided a higher UCS rate increase than MICP, it was clear that MICP treatment reduced the permeability of sandy soils to a greater degree than BEICP treatment, particularly with higher cycles of treatment (Figure 3.6b). The efficiency of permeability reduction of MICP-treated samples was slightly higher than BEICP-treated specimens at 8 and 12 cycles and was doubled at 16 cycles of treatment. The higher permeability reduction observed with MICP treated sandy soil was due to higher level of $CaCO_3$ precipitation which filled the void space of the sand matrix. This is described in detail in the following section.
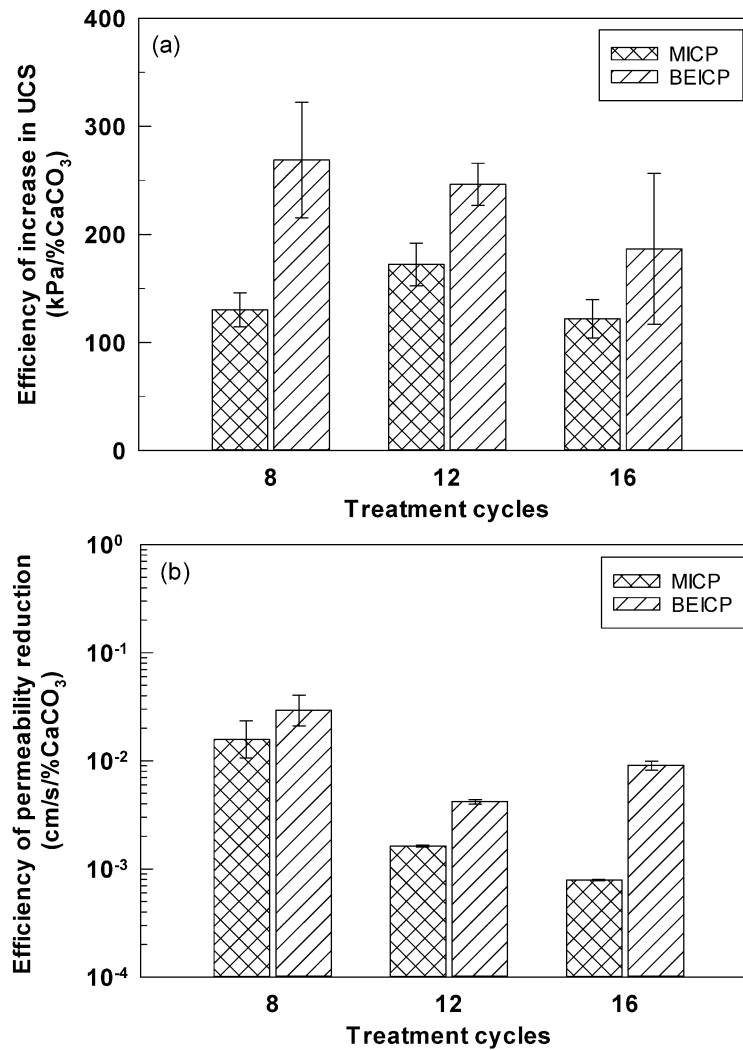


Figure 3.6 *Comparison of efficiency between MICP and BEICP methods: (a) efficiency of increase in UCS; (b) efficiency of permeability reduction*

**SEM and XRD analyses with MICP and BEICP treated sandy soil**

Figure 3.7 shows a series of SEM images for MICP- and BEICP-treated sands after eight and sixteen cycles of treatment, respectively. These images provide a visual perspective of the distribution, size, and packing density of the ICP-precipitated crystals which in turn led to the changes in strength and permeability of the stabilized sands discussed previously. Figures 3.7 a & b's MICP results show a considerably more highly populated and widely distributed extent of precipitate presence than is the case with Figures 3.7 c & d's BEICP-treated sands, which corresponds well with the preceding results for MICP's higher $CaCO_3$ content (i.e., see Table 3.4). The higher density of crystal precipitation with the MICP versus BEICP surfaces and void space also offers a qualitative correlation with the MICP-treated sand's higher UCS and reduced permeability. These results suggest that the microbial cells responsible for MICP treatment have a higher degree of surficial attachment than that of BEICP's enzyme catalysts, where there are likely physical, chemical, and even biochemical mechanisms that improve bacterial adhesion at a higher and more widely distributed extent than is the case with the smaller, soluble BEICP enzyme. One such mechanism for MICP treatment, where there is a higher cell affinity for sand surfaces, would be that of exocellular polysaccharide polymers surrounding microbes that might well increase surficial cell adhesion. A further observation with these MICP images is that their higher deposition of $CaCO_3$ crystals on exterior and internal void surfaces of the sand particles would then provide an even higher area for further successive attachment with each following treatment cycle.
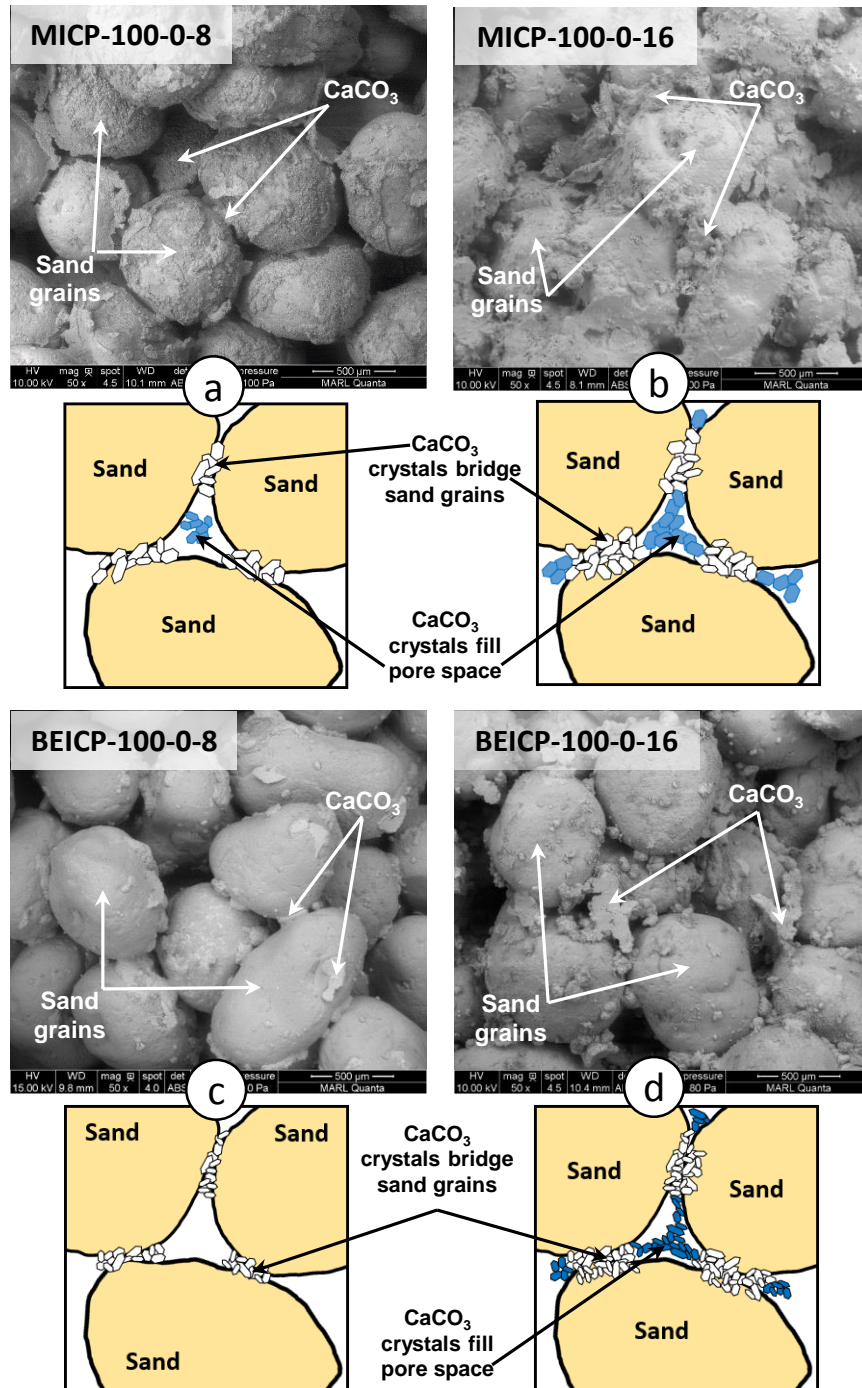
Figure 3.7 *SEM and schematic imagery of MICP- and BEICP-treated sandy soil samples (a) and (b) MICP at 8- and 16-cycle levels; (c) and (d) BEICP at 8- and 16-cycle levels*

For MICP, deposition initially takes place at three locations, including: 1) points of localized sand grain contact, 2) within the sand's internal pore space, and 3) on the surrounding sand surface area. Figure 3.7a's schematic location of these points of crystal deposition are stylized with white crystals which contribute to UC strengthening (i.e., located at the points of sand grain contact and binding). Figure 3.7a's darker (blue) crystals, depositing on the sand void space, would also contribute to reducing matrix permeability. It should be noted, though, that these schematics are simplified to the extent that they do not depict the additional $CaCO_3$, which further attaches to the sand surfaces, although this deposition is visually evident within the SEM photos. Further $CaCO_3$ deposition with higher treatment cycles (i.e., see Figure 3.7b for sixteen cycles) again happens at both surface and pore space locations, such that the overall $CaCO_3$ content continues to escalate and the pore space volume (and permeability) steadily reduces. As this phase of treatment is reached, though, there is likely more than a nominal fraction of the crystal deposition which is not necessarily helping to improve stability.

With BEICP, however, the initial deposition appears to happen almost exclusively at the points of sand grains contact (see Figure 3.7c). Conceivably, this behavior stems from physical trapping and crystal nucleation by the urease enzyme within this confined space. A similar calcium carbonate precipitation pattern was observed by Simatupang and Okamura (2017) in specimens treated by the EICP method. After eight cycles, the permeability of our BEICP-treated sample remained high, likely resulting in wash out of the solution from the sand's internal pore space. Therefore, there is no $CaCO_3$ precipitated at the sand grain gaps. As this deposition then continues through successive treatment cycles (i.e., see Figure 3.7d for sixteen cycles), continued accumulation occurs at both the contact points and internal

void space. In this case, therefore, further pore volume filling and resulting permeability reductions could be expected; however, the SEM images of BEICP-treated specimens (see Figures 3.7 c & d) indicated that this rate of buildup would be far lower than would happen during MICP cycling (see Figures 3.7 a & b).

Figure 3.8 displays the XRD spectrum of MICP- and BEICP-treated sandy soil samples. As is clearly shown in XRD analysis data, a distinct peak of calcite was observed in the treated specimens indicating that calcite was precipitated in biocemented sand through both MICP and BEICP treatment methods. The peak of calcite from XRD analysis was reported in previous MICP ( Li et al. 2015; Choi et al. 2017) and EICP (Yasuhara et al. 2012; Hamdan et al. 2013) studies. These results therefore confirm that the free bacterial urease is able to produce calcium carbonate for improving sandy soil strength via the ICP process.
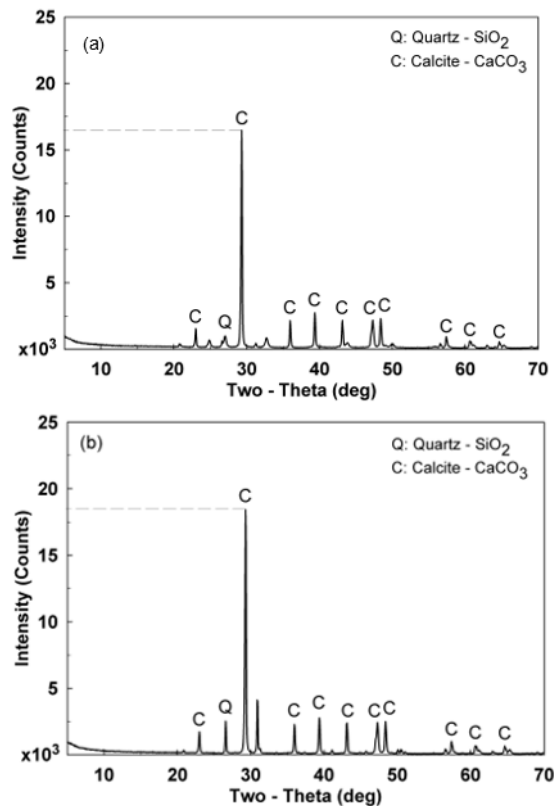


Figure 3.8 *XRD analysis of treated sand: (a) MICP-treated 100-0 sand and; (b) BEICP-treated 100-0 sand*

### 3.4.3 BEICP Stabilization of Silty-sand Soil

The following details and discussion for silty-sand treatment are limited to BEICP-only results since as shown previously in Table 3.3 the MICP treatment (at least using a twelve cycle method) proved to be not possible once a fine grain fraction had been added at either a 10 or 20 % level. Bio-clogging did occur during these MICP tests, but only at the column's inlet point where complete void plugging then stopped deeper penetration of the stabilization effect. The successful capability for BEICP processing to stabilize a full-depth sample column of silty-sand soils, though, is visually confirmed by the accompanying photograph given in Figure 3.9 (e.g., after an eight-cycle treatment).

As with the preceding tests completed on sand-only materials, these BEICP silty-sand tests were conducted with 8, 12, and 16 cycle step options, and the resultant UCS, stress-strain and permeability outcomes are presented in Table 3.4 and Figures 3.10, 3.11 and 3.12. A subsequent set of SEM images are also provided for these tests, as well as XRD results used to identify mineral compositions for both the original silt material plus the stabilized products.
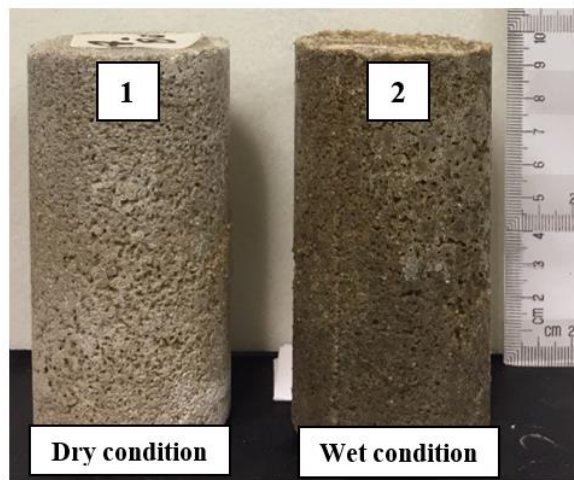


Figure 3.9 *Original BEICP-treated 80-20 samples after eight treatment cycles: sample 1 was oven-dried (~50 ºC, 48 h) before conducting UCS test; sample 2 was still in a wet condition after removal from its PVC mold*

### Unconfined compression strength with BEICP treated silty-sand soils

The observed pattern of UCS buildup relative to $CaCO_3$ precipitation with these BEICP silty-sand tests was similar to what was seen with the sand-only tests (Figure 3.10), where UCS increased with successive treatment cycle numbers. These results warrant multiple points of discussion. First, these silty-sand BEICP results for UCS were lower than the ones observed with the sand-only tests. Second, these BEICP silty-sand results for UCS at each of the cyclic step intervals declined as the fine grain fraction increased. Third, the latter decrease in UCS after 16 cycles was occurring even though the $CaCO_3$ deposition was increasing to levels higher than those observed during the sand-only tests (e.g., mean UCS = 1,118 kPa at 16 cycles for the 90-10 sand-silt mix, and mean UCS = 842 kPa at 16 cycles for the 80-20 sand-silt mix). This trend towards lower UCS values with higher silt fractions was similarly observed by Gomez and DeJong (2017), although in their case the measured calcite levels did not show the same tendency towards higher buildup. On the other hand, Kavazanjian and Hamdan (2015) observed a similarly increased level of $CaCO_3$ formation with EICP processing after adding bentonite to sand. Interestingly, though, their EICP tests were not able to form an intact, stabilized column. Oliveira et al. (2016) similarly reported elevated $CaCO_3$ precipitation levels (reaching 17 %) being developed during plant-based EICP tests on a heavily compacted sand-silt-clay soil mixture (i.e., at respective 73.4 %, 23.8 %, and 2.8 % silt levels), and here again their finished product UCS (i.e., ~250 kPa) was low. Soon et al. (2014) also reported similarly low UCS results for MICP treatment of silty-sand soils, ranging from 66 to 152 kPa. The results of the current study indicate that the BEICP is a promising method to treat silty sand soils.
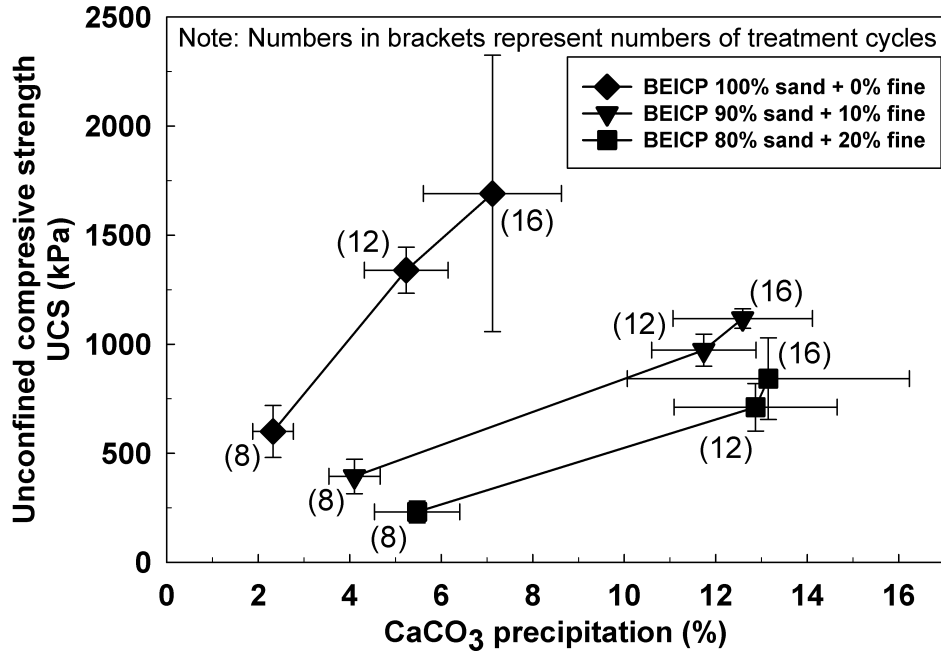
Figure 3.10 *Unconfined compression strength versus CaCO₃ precipitation of BEICP samples at different number of treatment cycles*

Figure 3.11 presents the typical stress-strain curves of the bio-stabilized specimens at 12 treatment cycles. For sandy soil, although the MICP-treated sample (M100-0-12) provided higher UCS than BEICP-treated sample (B100-0-12), their patterns of stress-strain are similar. Once the peak strength was reached, these stabilized sandy specimens experienced a sharp drop in stress within a small strain range (~ 0.6 %), indicating a typical mechanical behavior of brittle materials. However, BEICP-treated silty sand soil showed a different pattern of stress-strain behavior. After its initial linear increase, the stress of BEICP-treated silty sand samples continues to increase until the peak stress point, at which point the sample softening occurs before its final drop. The presence of fine grains in pore spaces decreases friction amongst the host sand particles, facilitating their subsequent displacement. While the strength of these stabilized sand-silt samples is reduced by increase the fines

percentage, the higher fines presence increases the treated sample's ductility. These findings are consistent with the results published by Oliveira et al. (2016).
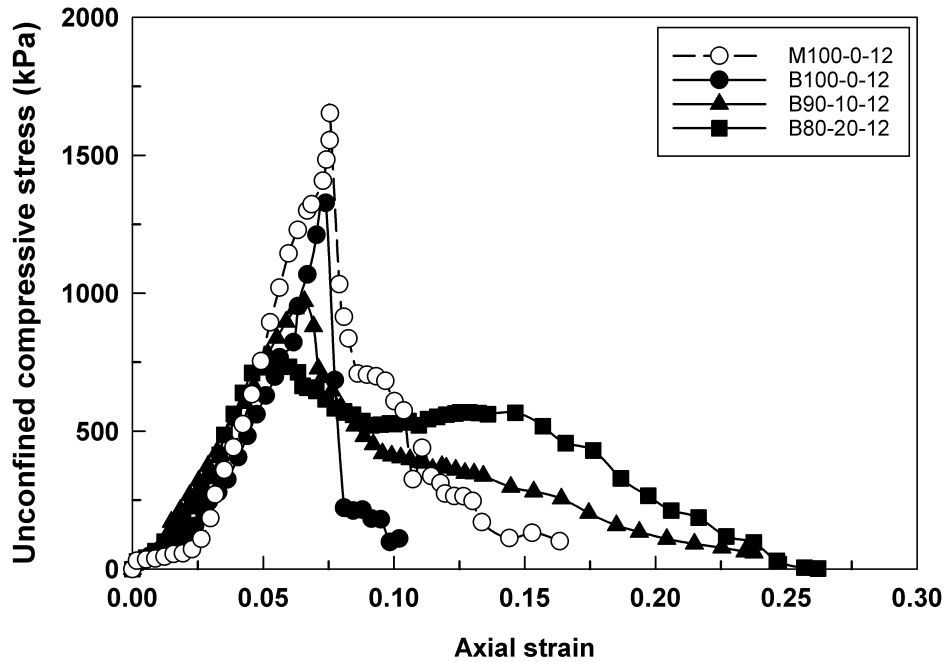


Figure 3.11 *Unconfined compression test, stress-strain curves of MICP- and BEICP-treated on sandy soil and silty-sand soil at 12 cycles of treatment*

### Permeability tests with BEICP treated silty-sand soils

The BEICP permeability results for silty-sand treatment given in Figure 3.12 include both values for raw, untreated materials and final, stabilized conditions. Here again, this Figure plots relative error values for permeability (see Table 3.4). As would be expected, the silty-sand findings generally exhibited an approximate one-log reduction in permeability than had been seen with the sand-only tests, where there was a combined effect of pore plugging due to silt presence plus $CaCO_3$ deposition. Of course, the further accumulation of calcite crystals which occur with repetitive treatment cycles for these stabilization procedures will further increase pore clogging and permeability reduction (Chu et al. 2012). BEICP treatment with the 90-10 soil mix showed an approximate two-log decline in permeability, and the 80-20 sample was somewhat higher at about a three-log difference. Again, these reductions are

occurring with far higher levels of CaCO₃ deposition, where the combined impacts of void

space plugging due to both silt presence and co-enmeshed CaCO₃ precipitation were

responsible for this higher hydraulic plugging.
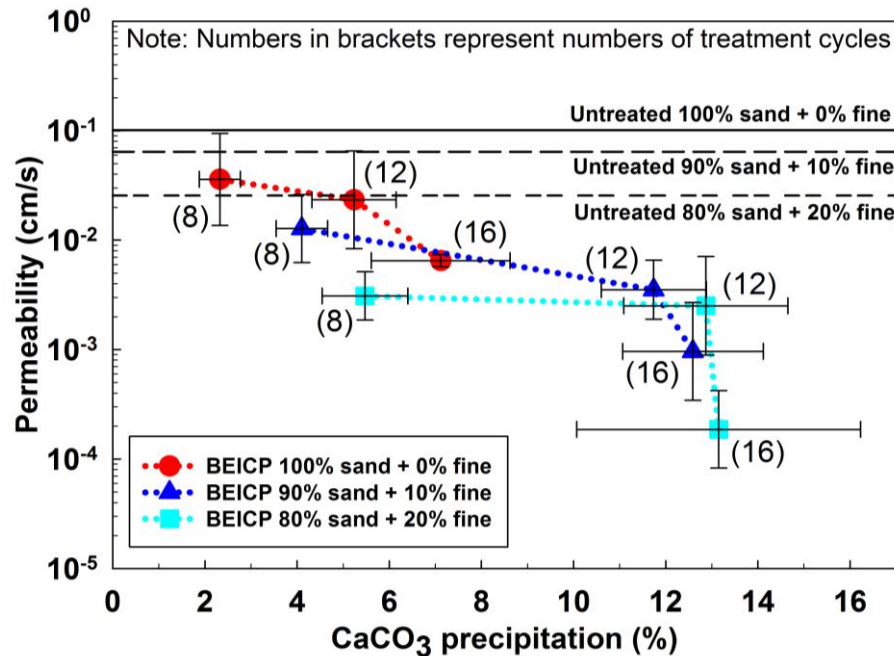


Figure 3.12 *Permeability versus CaCO₃ precipitation of BEICP-treated samples at different number of treatment cycles*

**SEM and XRD analyses with BEICP treated silty-sand soils**

Figure 3.13 presents two SEM images, plus accompanying schematics, which

collectively depict the high-level deposition of CaCO₃ crystals within both the 90-10 (Figure

3.13a) and 80-20 (Figure 3.13b) samples, after just eight BEICP cycles. The fact that the

sample used for these SEM observations was pulled from a mid-depth location on a test

column adds a further visual validation to Figure 3.9's perspective of full sample

solidification. In addition, these images show a widely distributed level of CaCO₃

precipitation. Figure 3.13 also indicates that sizable pore space deposition was taking place in

the presence of silts as compared to that of the BEICP-treated sand-only sample (Figures 3.7

c & d). This pore space filling was no doubt due to the combined presence of both silt fines

and the BEICP-formed $CaCO_3$ deposit. Collectively, the Figures 3.13 a & b images visually suggest that the BEICP process is binding together fine grain soils and precipitated calcite crystals into a cemented-bridge structure whose linkage then stabilizes the predominate sand grain matrix.
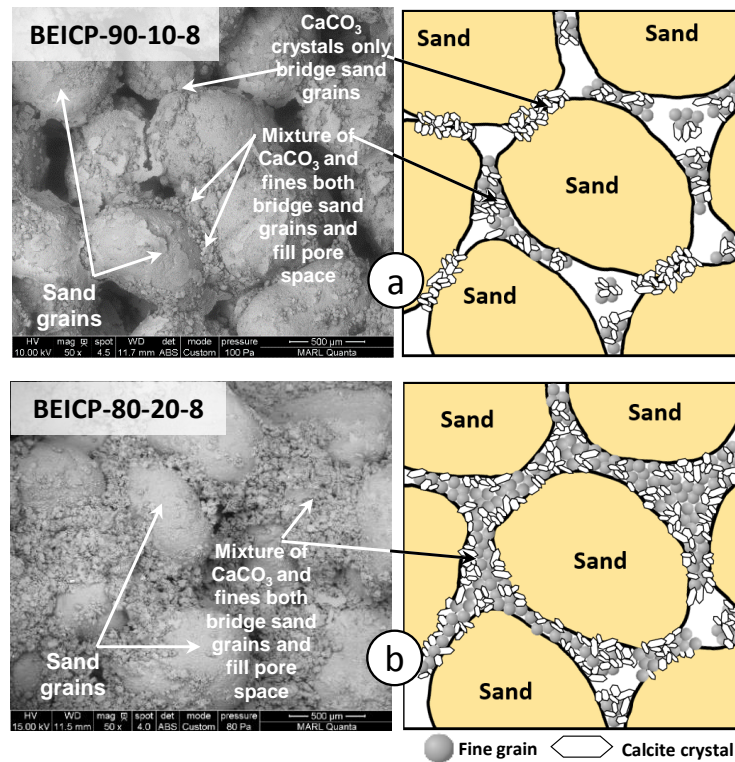


Figure 3.13 *SEM magnifications of eight-cycle BEICP silty-sand: (a) 90-10 treatment with both direct sand-sand bridging plus co-enmeshed silt and calcite; (b) 80-20 enmeshed sand-silt-calcite matrix with lower direct sand-sand calcite bridging*

With BEICP treatment of the 90-10 soils (Figure 3.13a), this stabilized product appears to involve a partial, and yet not complete, separation of the individual sand grains. In turn, this behavior implied that there was still some measure of $CaCO_3$ deposition at the remaining points of direct sand contact, as well as additional deposition taking place at both surficial and void space locations. However, once the fine soil addition reached the 80-20 level (Figure 3.13b), it appeared that the fine silt particles had produced a nearly full physical separation of the coarse sand grains. This observation is in general agreement with previous

studies on the intergranular soil mix classification and the influence of fines content on stress-strain behavior of silty sand (Lade and Yamamuro 1997; Yamamuro and Lade 1998; Thevanayagam et al. 2002). In turn, a considerable portion of the $CaCO_3$ deposition with the 80-20 samples would not have been in a position to directly strengthen the coarse sand soil skeleton. It is also noteworthy that these SEM images for silty-sand BEICP treatment, and their almost veneer-like thin surficial coating of $CaCO_3$ crystal deposition, were quite similar to the SEM imagery shown by Kavazanjian and Hamdan (2015) for EICP treatment of a sand-bentonite system.

The additional presence of the fine-grain particles within a sand-silt mixture will clearly impact the mechanisms and efficacy of these applied ICP processes. Notably, higher silt levels (i.e., 80-20 versus 90-10) led to a lower product UCS value (see Table 3.4), since it appeared that direct calcite bridging at sand-sand contact points was reduced (Figure 3.13b). Furthermore, the higher void deposition with calcite and silt further reduced permeability.

These impacts could be expected to involve a far more complex array of overlapping physical, chemical, and even biological factors versus that of much less complicated sand-only mixtures. The physical aspects will involve particle inter-mixing, orientation, spacing, void sizing and deposition, etc. Yet another group of chemical considerations will also come into play given the exceedingly more complex and reactive nature of the additional non-sand soil materials (i.e., involving redox, acid-base, chelation, sorption, buffering, etc. reactions which will occur in parallel with ICP's primary precipitation process). Adding in yet another likely set of biological issues which will escalate in importance along with these preceding factors (e.g., involving bio-transport, oxidation and reduction, surficial adhesion and

attachment, etc.), silty-sand soil processing will be far more complicated that had been previously considered with basic sand-only MICP treatment.

This respective presence of deposited calcium was confirmed using further XRD analysis as shown in Figure 3.14. In the XRD spectra, the peak of calcite in the BEICP-treated specimen (Figures 3.14 b & c) was significantly higher than the untreated fine-grained soils (Figure 3.14a). This is consistent with the XRD results obtained from BEICP-treated sandy soil. It is therefore evident that the BEICP technique resulted in calcium carbonate formation that bridged coarse and fine grain soil.
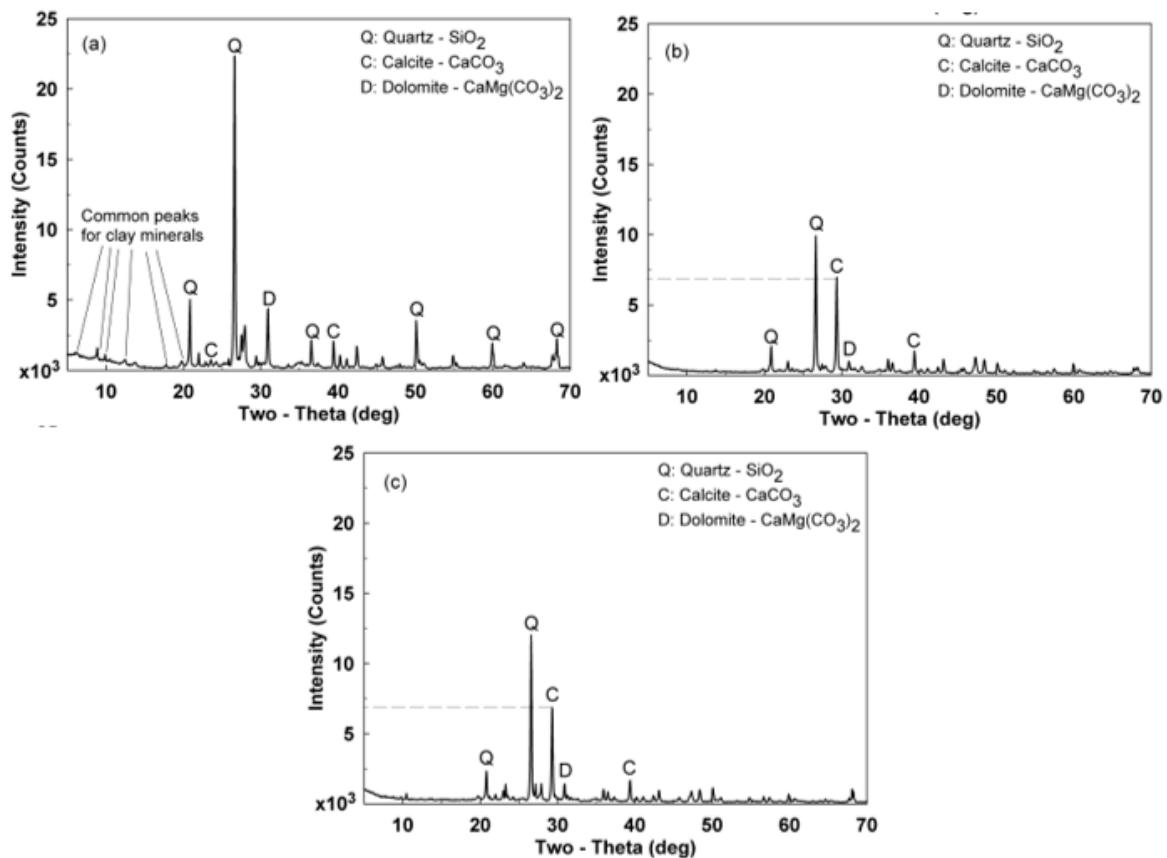


Figure 3.14 *XRD analysis of silty sand soil: (a) untreated loess fines; (b) BEICP-treated 90-10; (c) BEICP-treated 80-20*

### 3.4.4 SEM-based Perspectives on ICP Calcite Crystal Morphology

Three additional points about the size and morphology of the ICP calcite formation observed during these tests can be drawn from the following Figure 3.15 (SEM images and accompanying schematics). The most highly magnified Figure 3.15a image for eight-cycle MICP results shows crystal sizes which range between single-digit micron and ~8 to 10 µm levels, while the Figure 3.15b image for eight-cycle BECIP shows a noticeably smaller crystal size (i.e., typically ~1 – 4 µm). The size and morphology of calcium carbonate crystals precipitated via ureolytic bacteria were investigated in several previous studies (Mitchell and Ferris 2005, 2006a; b; Stocks-Fischer et al. 1999). In general, bio-induced calcite formation involves nascent seed nucleation within alkaline micro-environments surrounding ureolytic bacteria cells and/or free enzymes followed by progressive crystal expansion. In MICP, Mitchell and Ferris (2006b) reported the mean value of crystal diameter as 4.2 µm after a one-day reaction period, which then enlarged to 7.4 µm after a one-week duration. In contrast, nucleation of calcite on enzyme surfaces, such as in BEICP, results in much smaller nano-sized crystals. Sondi and Salopek-Sondi (2005) noted that vaterite and calcite precipitates initially formed by ureases purified from *S. pastuerii* were estimated to be approximately 20 nm in diameter. Tong et al. (2004) also reported a range of sizes for seed micro-crystals formed on amino acids as being 3 – 150 nm. A similar phenomenon likely occurred in the BEICP samples shown in Figure 3.15, resulting in smaller crystals formed compared to MICP treatment.
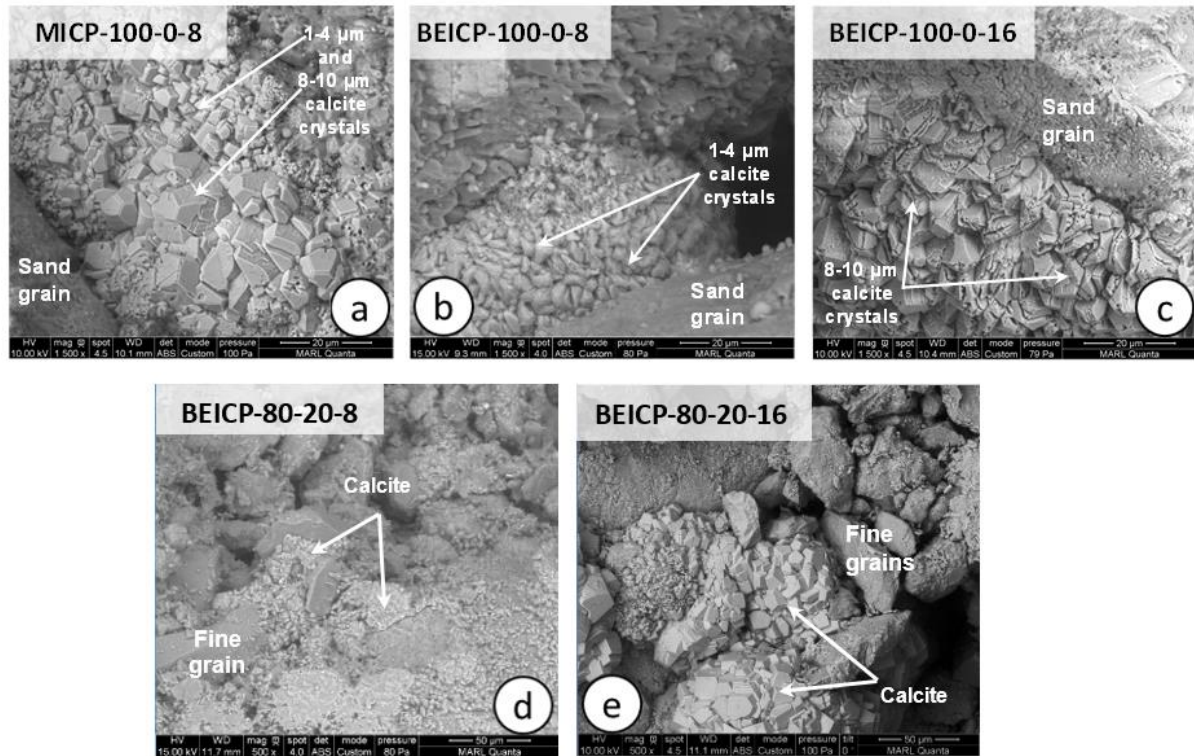
Figure 3.15 *Higher SEM magnifications of varied calcite crystal sizes relative to different MICP and BEICP treatments: (a) MICP-treated sand at 8-cycle levels; (b) and (c) BEICP-treated sand at 8- and 16-cycle levels; (d) and (e) BEICP-treated silty sand at 8- and 16-cycle levels*

Once BEICP processing has been continued for sixteen-cycles, though, the corresponding Figure 3.15c image shows that these crystals had escalated in size to an even larger scale comparable to that of MICP's level. The available evidence for an apparent difference in precipitate crystal sizes for MICP and BEICP is admittedly tentative at this point. However, the possibility for this sort of difference in crystal formation and size is consistent with findings reported by other MICP and EICP researchers (Whiffin et al. 2007; Al Qabany and Soga 2013; Cheng et al. 2013; Choi et al. 2016), where a number of inter-related factors may be responsible (e.g., substrate and calcium salt solution concentrations, cycling numbers, urease activity rates, upflow versus downflow cyclic flow patterns and related degree of void space saturation, etc.).

A second perspective revealed by these Figure 3.15 images for BEICP processing is that there appears to be a preferential pattern for BEICP's precipitating $CaCO_3$ formation at the contact points between sand particles. On the other hand, the 8- and 16-cycle MICP imagery (see Figures 3.7 a & b) shows an overlapping crystal buildup on sand surfaces where the $CaCO_3$ coverage produces even higher UCS. While the same impact of additional BEICP crystal deposition between 8- and 16-cycles also leads to a similar increase in higher UCS, the BEICP process notably has a lower net calcite accumulation. In turn, there is distinctly lower level of void volume deposition taking place with BEICP's reduced calcite deposition, such that the stabilized soil's permeability remains far higher than with MICP processing at similar treatment cycles.

The third point regarding BEICP calcite formation behavior which might be made on the basis of Figure 3.15e's silty-sand SEM image, relative to the location at which calcite appears to be preferentially forming. Notably, calcite deposition is taking place away from the silt particles, in a fashion which suggests that the enzyme passage had selectively followed a streamline through the sample's more permeable void space and not through the far less permeable silt-rich zones. Jenneman et al. (1982) mentioned much the same tendency of bacterial flow through porous sandstone to proceed through high-permeability zones versus low-permeability zones.

### 3.5 Conclusions

A core outcome with this research is that a bacterial enzyme induced calcite precipitation (BEICP) process can be applied using a relatively easily obtained cellular enzyme extract, and that this method is able to biostabilize both non-plastic sand as well as low plasticity silty-sand materials. In turn, the following set of bullet-listed conclusions are correspondingly offered:

- Intracellular urease enzymes can be effectively extracted for subsequent BEICP treatment using an expedient (approximately 2 h) cyclic run-cool sonication method,

- These extracted, soluble enzymes for BEICP processing achieved solidified, stabilized outcomes with non-plastic sand plus low plasticity 90-10 and 80-20 (i.e., respective sand and silt percentages) soil materials, and that the UC strength progressively increased with successive BEICP treatment cycles,

- Slightly lower UC strength levels were achieved with BEICP versus MICP processing of sand-only soils, although BEICP achieved this strength at lower level of $CaCO_3$ deposition,

- SEM observations showed that $CaCO_3$ deposition with BEICP treatment of sand-only soils predominantly occurred at the contact points for the sand grain skeleton, as compared to a far wider distribution of this precipitate during MICP treatment which spread across the sand surface as well as within the sand pore space,

- There was a distinct difference in the permeability outcome with BEICP processing as compared to MICP treatment, with less of a reduction in permeability with successive treatment cycles during both sand-only and silty-sand processing,

- The presence of additional fine silt soil particles could be successfully handled during BEICP stabilization, but that this did result in a corresponding UC strength reduction when compared to that of sand-only treatment at similar BEICP treatment cycles,

- SEM observations of BEICP treated silty-sand materials showed a far more widely spread deposition of $CaCO_3$ than had been seen with sand-only processing, both on exterior grain surfaces and internal void spaces, and

- The latter increase in BEICP-generated $CaCO_3$ deposition on silty-sand soils resulted in a further reduction of permeability than had been the case with sand-only treatment, but that the remaining permeability would likely have allowed for further cyclic treatment to secure even higher UCS outcomes.

### 3.6 Future Research Recommendations

- The following recommendations are constructively offered in terms of possible future research avenues intent on further elucidating this paper's BEICP concept:

- Further advancements with characterizing and optimizing the procurement, performance, and behavior of the urease catalyst used during BEICP are warranted. For example, an improved means should be developed to quantify sonicated urease activities based on specific activity relative to the extracted enzyme's relative protein mass, as a means of further understanding the enzyme activity beyond a mere substrate depletion rate. In addition, the sorption properties of these free enzymes should also be characterized.

- More detailed comparative assessment of the BEICP, MICP and EICP methods is warranted in terms of cost, application complexity and challenges, overall efficiency, etc.

- Shear strengths of BEICP and MICP treated specimens should be investigated under different saturation levels, including fully saturated conditions. Triaxial

testing would particularly beneficial in terms of allowable control over the degree of saturation with each specimen.

- Further optimization assessment for the BEICP concept is warranted. For example, tolerable and optimal environmental conditions need to be evaluated (e.g., for freeze-thaw, wet-dry, moisture, temperature, etc. parameters), field application methods need to be developed for urease production, handling, storage, application, etc.

### 3.7 References

Al Qabany, A., and Soga, K. (2013). "Effect of chemical treatment used in MICP on engineering properties of cemented soils." *Geotechnique*, 63(4), 331–339.

ASTM. (1996). "Standard test method for unconfined compressive strength index of chemical grouted soil." *ASTM D4219 - 08*, 1–6.

ASTM. (2006). "Standard test method for permeability of granular soils (constant head)." *ASTM D2434 – 68*, 68(Reapproved), 1–5.

ASTM. (2010). "Standard practice for classification of soils for engineering purposes (Unified Soil Classification System)." *ASTM D2487 – 10*, i, 1–12.

ASTM. (2014). "Standard specification for sand." *ASTM C778*, 1–3.

ASTM. (2017). "Standard test methods for liquid limit, plastic limit, and plasticity index of soils." *ASTM D4318 - 17*, 04(June 2017), 1–14.

Baird, D. C. (1994). Experimentation: An introduction to measurement theory and experiment design. (R. Henderson, ed.), Prentice-Hall, Inc., New Jersey.

Bang, S. S., Bang, S. S., Frutiger, S., Nehl, L. M., and Comes, B. L. (2009). "Application of novel biological technique in dust suppression." *Proc., Transportation Research Board 88th Annual Meeting, Transportation Research Board* (CD-ROM), Washington, DC, USA, DC, USA, 6–7.

Bang, S. S., William, A. E., and Ramakrishnan, V. (2001). "Application of an enzyme immobilization technique in calcite precipitation." *The 13th International Symposium on Microencapsulation*, Angers, France, France, Oral communication O-12.

Burbank, M. B., Weaver, T. J., Green, T. L., Williams, B. C., and Crawford, R. L. (2011). "Precipitation of calcite by indigenous microorganisms to strengthen liquefiable soils." *Geomicrobiology Journal*, 28(February), 301–312.

Cheng, L., Cord-Ruwisch, R., and Shahin, M. A. (2013). "Cementation of sand soil by microbially induced calcite precipitation at various degrees of saturation." *Canadian Geotechnical Journal*, 50(1), 81–90.

Choi, S.-G., Wang, K., and Chu, J. (2016). "Properties of biocemented, fiber reinforced sand." *Construction and Building Materials*, Elsevier Ltd, 120, 623–629.

Choi, S. G., Chu, J., Brown, R. C., Wang, K., and Wen, Z. (2017). "Sustainable biocement production via microbially induced calcium carbonate precipitation: use of limestone and acetic acid derived from pyrolysis of lignocellulosic biomass." *ACS Sustainable Chemistry and Engineering*, 5(6), 5183–5190.

Chu, J., Stabnikov, V., and Ivanov, V. (2012). "Microbially induced calcium carbonate precipitation on surface or in the bulk of soil." *Geomicrobiology Journal*, 29(March), 544–549.

Cui, M. J., Zheng, J. J., Zhang, R. J., Lai, H. J., and Zhang, J. (2017). "Influence of cementation level on the strength behaviour of bio-cemented sand." *Acta Geotechnica*, Springer Berlin Heidelberg, 12(5), 971–986.

Dakhane, A., Das, S., Hansen, H., O'Donnell, S., Hanoon, F., Rushton, A., Perla, C., and Neithalath, N. (2018). "Crack healing in cementitious mortars using enzyme-induced carbonate precipitation: Quantification based on fracture response." *Journal of Materials in Civil Engineering*, 30(4), 1–10.

DeJong, J. T., Mortensen, B. M., Martinez, B. C., and Nelson, D. C. (2010). "Bio-mediated soil improvement." *Ecological Engineering*, 36, 197–210.

Dilrukshi, R. A. N., Watanabe, J., and Kawasaki, S. (2016). "Strengthening of sand cemented with Calcium Phosphate Compounds using Plant-derived Urease." *International Journal of Geomate*, Japan, 11(25), 2461–2467.

Feng, K., and Montoya, B. M. (2015). "Influence of confinement and cementation level on the behavior of microbial-induced calcite precipitated sands under monotonic drained loading." *Journal of Geotechnical and Geoenvironmental Engineering*, 2, 1–9.

Ferris, F. G., and Stehmeier, L. G. (1991). "Bacteriogenic mineral plugging." Canada.

Ferris, F. G., Stehmeier, L. G., Kantzas, A., and Mourits, F. M. (1991). "Bacteriogenic mineral plugging." *Proc., 4th Petroleum Conference of the South Saskatchewan Section*, The Petroleum Society of CIM, Husky Oil Operation Ltd., Calagy, Regina, Sask, Canada, Canada, 11-1-11–12.

Gomez, M. G., and DeJong, J. T. (2017). "Engineering properties of bio-cementation improved sandy soils." *Grouting 2017 GSP*, 23–33.

Gomez, M. G., Martinez, B. C., DeJong, J. T., Hunt, C. E., deVlaming, L. A., Major, D. W., and Dworatzek, S. M. (2015). "Field-scale bio-cementation tests to improve sands." *Proceedings of the Institution of Civil Engineers - Ground Improvement*, 168(3), 206–216.

Hamdan, N., and Kavazanjian, E. (2016). "Enzyme-induced carbonate mineral precipitation for fugitive dust control." *Géotechnique*, 66(7), 546–555.

Hamdan, N., Kavazanjian, J. E., and S., O. (2013). "Carbonate cementation via plant derived urease." *Proceedings of the 18th International Conference on Soil Mechanics and Geotechnical Engineering*, Paris 2013, 2489–2492.

Hamdan, N., Zhao, Z., Mujica, M., Kavazanjian, E. J., and He, X. (2016). "Hydrogel-assisted enzyme-induced carbonate mineral precipitation." *Journal of Materials in Civil Engineering*, 25(October), 864–870.

Handley-Sidhu, S., Sham, E., Cuthbert, M. O., Nougarol, S., Mantle, M., Johns, M. L., Macaskie, L. E., and Renshaw, J. C. (2013). "Kinetics of urease mediated calcite precipitation and permeability reduction of porous media evidenced by magnetic resonance imaging." *International Journal of Environmental Science and Technology*, 10(5), 881–890.

Hawkins, A. B., and Mcconnell, B. J. (1992). "Sensitivity of sandstone strength and deformability to changes in moisture content." *Quarterly Journal of Engineering Geology and Hydrogeology*, 25, 115–130.

Inagaki, Y., Tsukamoto, M., Mori, H., Sasaki, T., Soga, K., Qabany, A. A., and Hata, T. (2011). "*The influence of injection conditions and soil types on soil improvement by microbial functions.*" ASCE Geo-Frontiers, 4021–4030.

Jenneman, G. E., Knapp, R. M., Menzie, D. E., McInerney, M. J., Revus, D. E., Clark, J. B., and Munnecke, D. M. (1982). "Transport phenomena and plugging in Berea sandstone using microorganisms." *Proc. Int. Conf. Microbial Enhanced Oil Recovery*, Afton, OK, US, 71–75.

Jiang, N. J., Yoshioka, H., Yamamoto, K., and Soga, K. (2016). "Ureolytic activities of a urease-producing bacterium and purified urease enzyme in the anoxic condition: Implication for subseafloor sand production control by microbially induced carbonate precipitation (MICP)." *Ecological Engineering*, 90, 96–104.

Jiang, N., Soga, K., and Kuo, M. (2017). "Microbially induced carbonate precipitation for seepage-induced internal erosion control in sand – clay mixtures." *Journal of Geotechnical and Geoenvironmental Engineering*, 143(3), 1–14.

De Jong, J. T., Martinez, B. C., Mortensen, B. M., Nelson, D. C., Waller, J. T., Weil, M. H., Ginn, T. R., Weathers, T., Barkouki, T., Fujita, Y., Redden, G., Hunt, C., Major, D., and Tanyu, B. (2009). "Upscaling of bio-mediated soil improvement." *Proceedings of the 17th International Conference on Soil Mechanics and Geotechnical Engineering: The Academia and Practice of Geotechnical Engineering*, 3, 2300–2303.

Kantzas, A., Stehmeier, L., Marentette, D. F., Ferris, F. G., Jha, K. N., and Mourits, F. M. (1992). "A novel nethod of sand consolidation through bacteriogenic mineral plugging." *Proc., 43rd Annual Technical Meeting, The Petroleum Society of CIM, CIM Journals*, Calgary, Canada, 46-1-46–15.

Kavazanjian, E., and Hamdan, N. (2013). "Mineral precipitation methods." *Arizona Board of Regents, A Body Corporate of The State of Arizona, Acting for and on Behalf of Arizona State University*, U. S. Patent 20160236943 A1, Filling date: October 28, 2013.

Kavazanjian, E., and Hamdan, N. (2015). "Enzyme induced carbonate precipitation (EICP) columns for ground improvement." *Proc., ASCE IFCEE 2015*, M. Iskander, M. T. Suleiman, J. B. Anderson, and Debra F. Laefer, eds., ASCE, San Antonio, Texas, 2252–2261.

Kavazanjian, E. J., Almajed, A., and Hamdan, N. (2017). "Bio-inspired soil improvement using EICP soil columns and soil nails." *Grouting 2017 GSP*, 13–22.

Lade, P. V, and Yamamuro, J. a. (1997). "Effects of nonplastic fines on static liquefaction of sands." Canadian Geotechnical Journal, 34(6), 918–928.

Larsen, J., Poulsen, M., Lundgaard, T., and Agerbaek, M. (2008). "Plugging of fractures in chalk reservoirs by enzymatic-induced calcium carbonate precipitation." *SPE Production & Operations*, 23(4), 4–7.

Lee, M. L., Ng, W. S., and Tanaka, Y. (2013). "Stress-deformation and compressibility responses of bio-mediated residual soils." *Ecological Engineering*, Elsevier B.V., 60, 142–149.

Li, M., Fu, Q. L., Zhang, Q., Achal, V., and Kawasaki, S. (2015). "Bio-grout based on microbially induced sand solidification by means of asparaginase activity." *Scientific Reports*, Nature Publishing Group, 5, 1–9.

Mitchell, A. C., and Ferris, F. G. (2005). "The coprecipitation of Sr into calcite precipitates induced by bacterial ureolysis in artificial groundwater: Temperature and kinetic dependence." *Geochimica et Cosmochimica Acta*, 69(17), 4199–4210.

Mitchell, A. C., and Ferris, F. G. (2006a). "Effect of strontium contaminants upon the size and solubility of calcite crystals precipitated by the bacterial hydrolysis of urea." *Environmental Science and Technology*, 40(3), 1008–1014.

Mitchell, A. C., and Ferris, F. G. (2006b). "The influence of bacillus pasteurii on the nucleation and growth of calcium carbonate." *Geomicrobiology Journal*, 23(3–4), 213–226.

Nam, I., Chon, C., Jung, K., and Choi, S. (2014). "Calcite precipitation by ureolytic plant ( Canavalia ensiformis ) extracts as effective biomaterials." *KSCE Journal of Civil Engineering*, 1–6.

Nassar, M. K., Gurung, D., Bastani, M., Ginn, T. R., Shafei, B., Gomez, M. G., Graddy, C. M. R., Nelson, D. C., and DeJong, J. T. (2018). "Large-scale experiments in microbially induced calcite precipitation (MICP): Reactive transport model development and prediction." *Water Resources Research*, 3, 1127–1145.

Nemati, M., Greene, E. A., and Voordouw, G. (2005). "Permeability profile modification using bacterially formed calcium carbonate: Comparison with enzymic option." *Process Biochemistry*, 40(2), 925–933.

Nemati, M., and Voordouw, G. (2003). "Modification of porous media permeability, using calcium carbonate produced enzymatically in situ." *Enzyme and Microbial Technology*, 33(5), 635–642.

Neupane, D., Yasuhara, H., Kinoshita, N., and Ando, Y. (2015a). "Distribution of mineralized carbonate and its quantification method in enzyme mediated calcite precipitation technique." *Soils and Foundations*, Elsevier, 55(2), 447–457.

Neupane, D., Yasuhara, H., Kinoshita, N., and Putra, H. (2015b). "Distribution of grout material within 1-m sand column in insitu calcite precipitation technique." *Soils and Foundations*, Elsevier, 55(6), 1512–1518.

Neupane, D., Yasuhara, H., Kinoshita, N., and Unno, T. (2013). "Applicability of enzymatic calcium carbonate precipitation as a soil-strengthening technique." *ASCE Journal of Geotechnical and Geoenvironmental Engineering*, 139(December), 2201–2211.

Oliveira, P. J. V., Freitas, L. D., and Carmona, J. P. S. F. (2016). "Effect of soil type on the enzymatic calcium carbonate precipitation process used for soil improvement." *Journal of Materials in Civil Engineering*, 29(4), 1–7.

van Paassen, L. A. (2009). "Biogrout: Ground improvement by microbially induced carbonate precipitation." *Ph.D. dissertation, Delft University of Technology*, Delft, Netherlands.

van Paassen, L. A. (2011). "Bio-mediated ground improvement: from laboratory experiment to pilot applications." *ASCE Geo-Frontiers*, 4099–4108.

van Paassen, L. A., Ghose, R., van der Linden, T. J. M., van der Star, W. R. L., and van Loosdrecht, M. C. M. (2010a). "Quantifying biomediated ground improvement by ureolysis: large-scale biogrout experiment." *Journal of Geotechnical and Geoenvironmental Engineering*, 136(12), 1721–1728.

van Paassen, L. A., Harkes, M. P., Van Zwieten, G. A., Van Der Zon, W. H., Van Der Star, W. R. L., and Van Loosdrecht, M. C. M. (2009). "Scale up of BioGrout: A biological ground reinforcement method." *Proceedings of the 17th International Conference on Soil Mechanics and Geotechnical Engineering: The Academia and Practice of Geotechnical Engineering*, 3, 2328–2333.

van Paassen, L. A., Van Loosdrecht, M. C. M., Pieron, M., Mulder, A., Ngan-Tillard, D. J. M., and Van Der Linden, T. J. M. (2010b). "Strength and deformation of biologically cemented sandstone." *Proc., Rock Engineering in Difficult Ground Conditions - Soft Rocks and Karst*, I. Vrkljan, ed., CRC Press, Cavtat, Croatia, 405–410.

Park, S.-S., Choi, S.-G., and Nam, I.-H. (2014). "Effect of microbially induced calcite precipitation on strength of cemented sand." *Journal of Materials in Civil Engineering*, 26(8), 47–56.

Park, S.-S., Nam, I.-H., and Choi, S.-G. (2011). "Natural soil-binder using natural bean and its use for soil cementation (콩을 이용한 지반의 천연고결제 및 이를 이용한 지반의 고결화 방법)." *Kyungpook National University Industry-Academic Cooperation Foundation, South Korea 1011522950000 (in Korean)*, South Korea 1011522950000 (in Korean).

Phillips, A. J., Cunningham, A. B., Gerlach, R., Hiebert, R., Hwang, C., Lomans, B. P., Westrich, J., Mantilla, C., Kirksey, J., Esposito, R., and Spangler, L. (2016). "Fracture sealing with microbially-induced calcium carbonate precipitation: A field study." *Environmental Science and Technology*, 50(7), 4111–4117.

Putra, H., Yasuhara, H., and Kinoshita, N. (2017a). "Applicability of natural zeolite for NH-Forms removal in enzyme-mediated calcite precipitation technique." *Geosciences*, (2).

Putra, H., Yasuhara, H., Kinoshita, N., and Hirata, A. (2017b). "Optimization of Enzyme-Mediated Calcite Precipitation as a Soil-Improvement Technique: The Effect of Aragonite and Gypsum on the Mechanical Properties of Treated Sand." *Crystals*, 7(2), 59.

Putra, H., Yasuhara, H., Kinoshita, N., Neupane, D., and Lu, C.-W. (2016). "Effect of Magnesium as Substitute Material in Enzyme-Mediated Calcite Precipitation for Soil-Improvement Technique." *Frontiers in Bioengineering and Biotechnology*, 4(May), 3–10.

Raymond, M., Gamage, M., Terefe, N. S., and Knoerzer, K. (2011). "Ultrasound in enzyme activation and inactivation." *Ultrasound Technologies for Food and Bioprocessing, Food Engineering Series*, H. Feng et al., ed., Springer Science+Business Media, LLC 2011, VIC, Australia, 369–404.

Simatupang, M., and Okamura, M. (2017). "Liquefaction resistance of sand remediated with carbonate precipitation at different degrees of saturation during curing." *Soils and Foundations*, The Japanese Geotechnical Society.

Sondi, I., and Salopek-Sondi, B. (2005). "Influence of the primary structure of enzymes on the formation of CaCO 3 polymorphs: A comparison of plant (Canavalia ensiformis) and bacterial (Bacillus pasteurii) ureases." Langmuir, 21(19), 8876–8882.

Soon, N. W., Lee, L. M., Khun, T. C., and Ling, H. S. (2013). "Improvements in engineering properties of soils through microbial-induced calcite precipitation." *KSCE Journal of Civil Engineering*, 17(4), 718–728.

Soon, N. W., Lee, L. M., Khun, T. C., and Ling, H. S. (2014). "Factors affecting improvement in engineering properties of residual soil through microbial-induced calcite precipitation." *Journal of Geotechnical and Geoenvironmental Engineering*, 04014006(11), 1–11.

van der Star, W. R. L., van Wijngaarden-van Rossum, W. K., van Paassen, L. A., and van Baalen, L. R. (2011). "Stabilization of gravel deposits using microorganisms." *Proceedings of the 15th European conference on Soil mechanics and Geotechnical engineering*, A. Anagnostopoulos, ed., IOS Press, 85–90.

Stocks-Fischer, S., Galinat, J. K., and Bang, S. S. (1999). "Microbiological precipitation of $CaCO_3$." *Soil Biology and Biochemistry*, 31(11), 1563–1571.

Thevanayagam, S., Shenthan, T., Mohan, S., and Liang, J. (2002). "Undrained fragility of clean sands, silty sands, and sandy silts." *Journal of Geotechnical and Geoenvironmental Engineering*, 128(10), 849–859.

Tong, H., Ma, W., Wang, L., Wan, P., Hu, J., and Cao, L. (2004). "Control over the crystal phase, shape, size and aggregation of calcium carbonate via a L-aspartic acid inducing process." *Biomaterials*, 25(17), 3923–3929.

Whiffin, V. S. (2004). "Microbial $CaCO_3$ precipitation for the production of biocement." *Ph.D. dissertation, Murdoch University*, Australia.

Whiffin, V. S., van Paassen, L. A., and Harkes, M. P. (2007). "Microbial carbonate precipitation as a soil improvement technique." *Geomicrobiology Journal*, 24(February), 417–423.

Yamamuro, J. a., and Lade, P. V. (1998). "Steady-state concepts and static liquefaction of silty sands." *Journal of Geotechnical and Geoenvironmental Engineering*, 124(September), 868–877.

Yasuhara, H., Hayashi, K., and Okamura, M. (2011). "Evolution in mechanical and hydraulic properties of calcite-cemented sand mediated mediated by biocatalyst." *Geo-Frontiers 2011 © ASCE 2011*, Dallas, Texas, 3984–3992.

Yasuhara, H., Neupane, D., Hayashi, K., and Okamura, M. (2012). "Experiments and predictions of physical properties of sand cemented by enzymatically-induced carbonate precipitation." *Soils and Foundations*, Elsevier, 52(3), 539–549.

# CHAPTER 4.   ENGINEERING PROPERTIES OF BIOCEMENTATION COARSE- AND FINE-GRAINED SAND CATALYZED BY BACTERIAL CELLS AND BACTERIAL ENZYME

*Tung Hoang, James Alleman, Bora Cetin, Sun-Gyu Choi (2018). "Engineering Properties of Bio-Cementation Coarse- and Fine-Grained Sand Catalyzed by Bacterial Cells and Bacterial Enzyme" ASCE - Journal of Materials in Civil Engineering (Submitted).*

## 4.1 Abstract

Biological induced calcite precipitation in one of the potential methods being investigated for improved soil stabilization. In terms of the associated urea hydrolysis concept, three main strategies have been developed over the past two decades, including: 1) using live urease producing bacteria, 2) using plant extracted urease, and 3) using bacterial-extracted urease.

This paper focuses on evaluating comparative benefits with two of these methods (i.e., either live bacterial cell or extracted bacterial urease methods for induced calcium precipitation) in terms of their biocementation performance. Cell-based ICP (i.e., MICP) testing was completed on standard Ottawa coarse-grained sand (#20/30), and bacterial-enzyme-based (i.e., BEICP) testing was conducted individually on both coarse-grained and fine-grained (#50/70) sands.  These comparative tests produced two notable observations. First, distinctly higher unconfined compression strength (UCS) strengths were achieved with the BEICP method when evaluated at similar levels of calcium precipitation. Second, residual permeability levels remained markedly higher after BEICP testing versus MICP. In terms of comparing performance relative to sand grain sizes, the UCS observed with BEICP coarse-grained treated sand is approximately 450 – 1500 kPa, whereas that of fine-grained treated sand had a notably lower range (i.e., 250 – 900 kPa) when evaluated at similar levels

of CaCO$_3$ production. These results subsequently indicated that calcium carbonate content is not the sole factor which impacts the strength of bio-cemented sand. Additional test-tube investigation of ICP-derived CaCO$_3$ precipitation was also used to evaluate the chemical conversion efficiency for each such optional method, either live cells (i.e., *Sporosarcina pasteurii*) or their extracted bacterial extracted urease. The results of the latter test-tube experiments revealed two findings. The calcite precipitation ratio declined at higher substrate chemical concentrations. However, this ratio increased with higher rates of enzymatic activity.

## 4.2 Introduction

Ground stabilization is a fast-growing discipline in geotechnical engineering. It includes more than thirty techniques classified within several categories, including: replacement, densification through dynamic energy, consolidation by dewatering, chemical grouting, admixture stabilization using cement, lime or fly ash, thermal stabilization, etc. (Mitchell 1981; Terashi and Juran 2000; Chu et al. 2009).

Within the past decade, though, a bio-based environmental grouting method has been investigated as an additional ground improvement via reduced hydraulic conductivity and enhanced strength and stiffness of cohesionless soil based on both: a) pore-filling (bio-clogging); and b) particle roughening plus inter-particle bridging (bio-cementation) (Ivanov and Chu 2008).

The majority of these bio-grouting methods rely on a biochemical reaction whose pH-elevating chemical products then induce calcium carbonate (CaCO$_3$) precipitation. Hamed Khodadadi et al. (2017) identified these strategies for microbial-induced CaCO$_3$ precipitation as either that of MICP (using intact, ureolytic microbial cells) and EICP (enzyme-induced CaCO$_3$ precipitation). These MICP and EICP processes both use a similar mechanism, i.e.,

urea hydrolysis. MICP employs live bacterial cells to achieve ureolysis. However, EICP treatment relies on free urease enzyme which was previously extracted from ureolytic cells using sonication.

MICP-based research has demonstrated multiple soil stabilization benefits (i.e., higher strength and stiffness, liquefaction resistance, and reduced permeability) of sandy soil. These outcomes have been established at varied experimental scales,  ranging from laboratory column tests (Cheng et al. 2012; DeJong et al. 2006; Whiffin et al. 2007) to several higher-level experiments (100 m$^3$ sand - van Paassen et al. 2010a ; 1000 m$^3$ gravel -  van der Star et al. 2011), and even field-scale evaluation (Burbank et al. 2011; Gomez et al. 2015b; van Paassen 2011).

Although the MICP method has been successful within these various scales of ground improvement testing, this method still holds several limitations in relation to non-uniform outcomes. Notably, problems have been experienced with both non-homogenous distribution of bacterial cells and cementation results (Whiffin 2004; Whiffin et al. 2007) as well as constraints on the pore-space transport of microorganism cells where they would be restrained by the presence of fine grained soil particles (Rebata-Landa and Santamarina 2006).

By comparison, the newer ureolysis methods using nano-scale and water-soluble urease enzyme biocatalysts (i.e where this enzyme is extracted from either plant or live cells sources) for in-situ calcium precipitation may offer beneficial processing benefits. Several researchers have subsequently published results for plant-derived free-enzyme biostabilization studies (e.g., Yasuhara et al. 2012; Hamdan et al. 2013). However, these researchers have commented on the high cost of purchasing commercially purified plant-

derived urease enzyme for their lab-scale experiments (Hamdan and Kavazanjian 2016a; Kavazanjian and Hamdan 2015; Larsen et al. 2008; Nam et al. 2014; Nemati and Voordouw 2003; Neupane et al. 2013, 2015a; Simatupang and Okamura 2017). Currently, only three research groups have subsequently reported on the innovative use of self-extracted urease obtained from agricultural sources. Both jack bean (Park et al. 2014) and watermelon seeds (Dilrukshi et al. 2016, 2018; Javadi et al. 2018) were used during these studies.

Unfortunately, this approach to extracting urease enzyme from plant sources appears to have a number of drawbacks, including: high time- and land-demand for plant growth, plus additional high processing costs for converting plant biomass into soluble extracted enzyme. To date, very few plant-based EICP publications have documented a comparison of biostabilization efficiency relative to that of conventional MICP processing. Similarly, only a few of these plant-based EICP researchers have addressed the effect of sand type and size (Hamdan et al. 2013; Hamdan and Kavazanjian 2016a; Kavazanjian et al. 2017; Neupane et al. 2015c; Simatupang and Okamura 2017)

Our own research team's recently published results subsequently documented a new biogeotechnical ground improvement method using bacterial enzyme calcium carbonate precipitation (BEICP) (Hoang et al. 2018). In turn, the paper at hand offers further demonstration as to the performance of BEICP versus standard MICP processing method relative to chemical conversion efficiency and coarse sand stabilization.

This current paper also provides valuable further insights regarding the impact of varying sand types (coarse- and fine-grained) in relation to this new BEICP strategy. These observations showed similar gains in chemical conversion efficiency when using either

whole-cell (MICP) or enzyme-only (BEICP) processing. However, distinct differences were recorded when using these alternative methods with varying sand sizes.

## 4.3 Materials and Experimental Procedures

### 4.3.1 Sand Materials and Sand Column Preparation

Two types of sand were used in the current study. First, silica/quartz sand was purchased from Gilson Company, Inc. USA. This coarse-grained sand was #20/30, HM-107 standard sand. Second, fine-grained sand (i.e., #50/70, HM-108) was also purchased from Gilson. These sand criteria are described in ASTM C778 (2014). These sands contained more than 98.7 % silica ($SiO_2$). The sand materials were also initially washed with deionized water to remove any soluble chemicals, followed by oven drying at 105 °C for 24 h before being tested. Further evaluation of the sand properties included: particle diameter at 10 % finer by mass ($D_{10}$), particle diameter at 50 % finer by mass ($D_{50}$), uniformity coefficient ($C_u$), coefficient of gradation ($C_c$), specific gravity ($G_s$), maximum and a minimum void ratio ($e_{max}$ and $e_{min}$), and Unified Soil Classification System (USCS; ASTM 2010). These properties are collectively summarized in Table 4.1. The grain size distribution curves of the coarse and fine sands are presented in Figure 4.1.

Sand columns were packed separately to include either coarse- and fine-grained sand soil. Prior to uploading sand into each test column, the dry sand was initially mixed with distilled water to achieve 5 % moisture. The following sequential preparation steps were then followed. First, an underlying gravel strata was layered into the bottom of the test chamber's plastic cap. Second, a pre-cut section of filter pad material (i.e., 3-M Scotch Brite Model 7447) was placed on top of the gravel layer. Third, a moist-tamping method was used to pack the specimens, where this pre-moistened sand was gently tamped within the PVC columns (i.e., 50 mm diameter and 100 mm height).
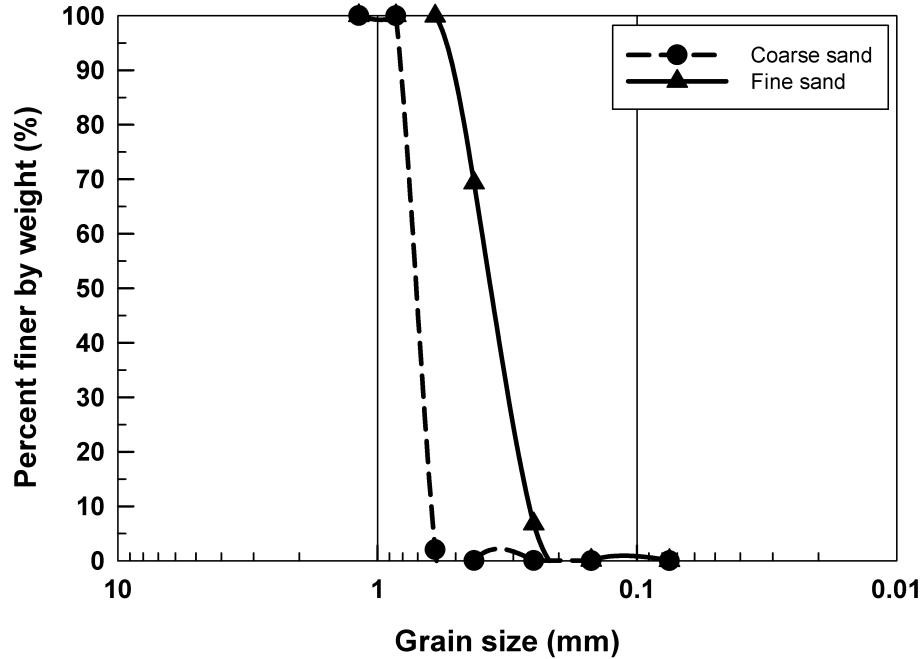
Figure 4.1 *Grain size distribution curve of tested sands*

Table 4.1 *Sand used properties*

| Sand type | Properties | | | | | | | | Column packing | | |
|---|---|---|---|---|---|---|---|---|---|---|---|
| | $D_{10}$ (mm) | $D_{50}$ (mm) | $C_u$ | $C_c$ | $G_s$ | $e_{max}$ | $e_{min}$ | USCS | Method | $D_r$ (%) | n (%) | k (cm/s) |
| Coarse | 0.61 | 0.72 | 1.21 | 1.02 | 2.65 | 0.74 | 0.51 | SP | Wet tamping | 64.6 ± 0.5 | ~ 37 | $1.01 \times 10^{-1}$ |
| Fine | 0.26 | 0.36 | 1.46 | 0.97 | 2.65 | 0.87 | 0.55 | SP | Wet tamping | 64.4 ± 0.5 | ~ 40 | $3.2 \times 10^{-1}$ |

To achieve a similar specific density in each layer, pre-determined amounts of soil were added in ten successive layers of equal thickness (i.e., at 10 mm per layer) within each column. These column compaction steps were carefully conducted to achieve similar relative density ($D_r$) levels within all column samples. The characteristics of sample columns for coarse and fine sands including $D_r$, porosity (n), and un-cementation permeability (k) were shown previously within Table 4.1. Finally, another filter pad was located on the top of the

sand layer for avoiding scouring and distributing flow streams. Figure 4.2 provides an overview schematic of one such filled column in operation, including its solution pump.
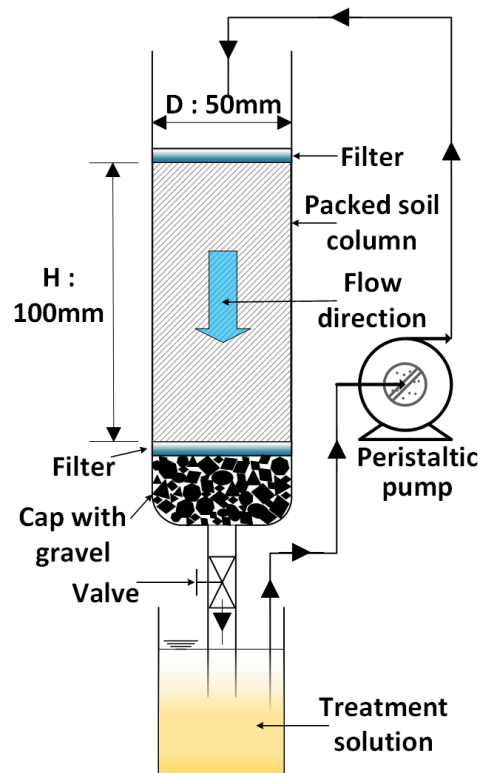


Figure 4.2 *Soil column circulating-percolation treatment (after Choi et al. 2016)*

### 4.3.2 Urease-producing Bacteria (UPB) Suspension and Chemical Solution

The urease active strain of *Sporosarcina pasteurii* (ATCC-11859 available now from the American Type Culture Collection, Manassas, Virginia, USA), which was obtained from the previous work ) (Hoang et al. 2018). The isolated strain was cultivated in a pre-sterilized culturing broth (i.e., an ammonium-trypticase soy broth [NH4 –TSB] growth media which included: trypticase soy broth at 20 g/L, ammonium sulfate at 10 g/L, Tris buffer at 0.13 mol/L, and an overall solution pH of 9.0. A shaking incubator (Innova Model 4000, New Brunswick Scientific) was used to incubate this culture for 48 h with a continuous shaking speed of 160 rpm at 30 °C.

This cultured biomass was measured the optical density (OD) at 600 nm using a visible light spectrophotometer (Hach Model #DR 3900). When the UPB solution had the OD range $0.9 - 1.3$, this stock microbial culture was harvested then stored at 4 °C prior for subsequent use. An electric conductivity meter was used to measure the urease activity of the UPB solution (Chu et al. 2012), resulting in a range from $8 - 13$ mM urea/min which is similar to those reported previously (Hoang et al. 2018). The concentrations of chemical solution used in the current study were 0.3 M at the same molar concentrations for soluble $CaCl_2$ and urea.

### 4.3.3 Biomass Sonication and Enzyme Extraction

Urease enzyme lysed directly from live bacteria of *Sporosarcina pasteurii* was used in the present study. The procedures of extraction and optimization method have been described previously (Hoang et al. 2018). Urease extraction was completed using a repetitive series of cyclic 'run-cool' (i.e., 10 min 'on' followed by 10 min 'off') sonication steps. Six such cycles were applied over a two-hour period, with a 150 ml aliquot of the original stock microbial culture being placed directly into a sonication bath (Bransonic Model 220; 120 volt, 125W, and 50/60 kHz). The cyclic processing mode was adopted given that it provided the lowest temperature buildup (i.e., typically at slightly below $32 - 34$ ºCP) and highest residual enzyme activity. After completing these tests, the remaining lysed solution was then subjected to a relative centrifugal force of 5500 RCF for 20 min to separate out residual cellular debris solids from the extracted, soluble urease. The sonication method typically produced an approximate urease activity rate of 25.4 mM urea per min.

### 4.3.4 Test-tube Experiments

Two different modes of test-tube experiments were used to examine and compare calcium consumption efficiency impacted by either bacterial cells (MICP) or extracted

bacterial urease (BEICP). These tests were performed within transparent 50 ml
polypropylene tubes. Neupane et al. (2013) and Yasuhara et al. (2012) also performed similar
test-tube experiments to evaluate the calcium carbonate precipitation ratio at different
concentration of commercial urease. A 15 mL equimolar solution of urea and $CaCl_2$ was
mixed with a 15 mL volume of either live bacteria cells or extracted bacterial urease. These
bio-reactive mixtures were then evaluated at various urease activity levels. The experimental
conditions are listed in Table 4.2. To ensure the repeatability of these reactions, three
replicates were tested. It should be noted that the activity rates for these tests were derived
(with a ~2 – 3 % accuracy) by proportionate dilutions from an initial free enzyme solution
with a known (and higher) enzyme activity. The diluted solutions (with either intact cells or
free enzyme) were adjusted to obtain three levels of urease activity, at either low (~2 mM
urea/min), moderate (~5 mM urea/min), and high (~10 mM urea/min) levels. In turn, in order
to conduct each of the test-tube experiments, 15 ml aliquots of these optional biological
solutions were then mixed with 15 ml volumes of the two chemical solutions (including 7.5
mls of urea and 7.5 mls of calcium chloride), by which the ureolytic activity of these
biological solutions was then reduced via dilution by a factor of two.

     The urease activity of these diluted solutions was then measured by the conductivity
method, which was previously explained in Section 3.3.4. The conductivity method required
the addition of a 5 ml biological solution with a 50 ml 1-M urea solution, such that this
mixture then had a net 0.91-M concentration of the urea substrate. However, the urea
concentration in these test-tube experiments was significantly lower than that in the
conductivity measurement process. Three levels of actual urea substrate concentration were
tested during these test-tube experiment, at 0.075, 0.125, and 0.25 M urea levels. Therefore,

given that these urea substrate levels were far lower than that of the reactive solution's

original level during conductivity-based activity testing (i.e., 0.91 M urea), the urease activity

expected with each test-tube experiment was then mathematically revised in order to take

into account the impact of Michaelis-Menten enzyme kinetics. Stocks-Fischer et al. (1999)

reported that the Michaelis-Menten model of urease from *S. pasteurii* showed a $K_m$ (half-

saturation coefficient) of 41.6 mM urea and a $V_{max}$ (maximum specific activity rate constant)

of 3.55 mM/min/mg. These values were then used as the reference data against which the

adjusted activity of the diluted solutions would be calculated. Figure 4.3 depicts the

Michaelis-Menten model relationship based on the latter $K_m$ and $V_{max}$ values cited by Stocks-

Fisher et al. (1999). In addition, this figure also provides a second y-axis correlation for the

expected impact of substrate presence on the diluted enzyme solutions used in this study.
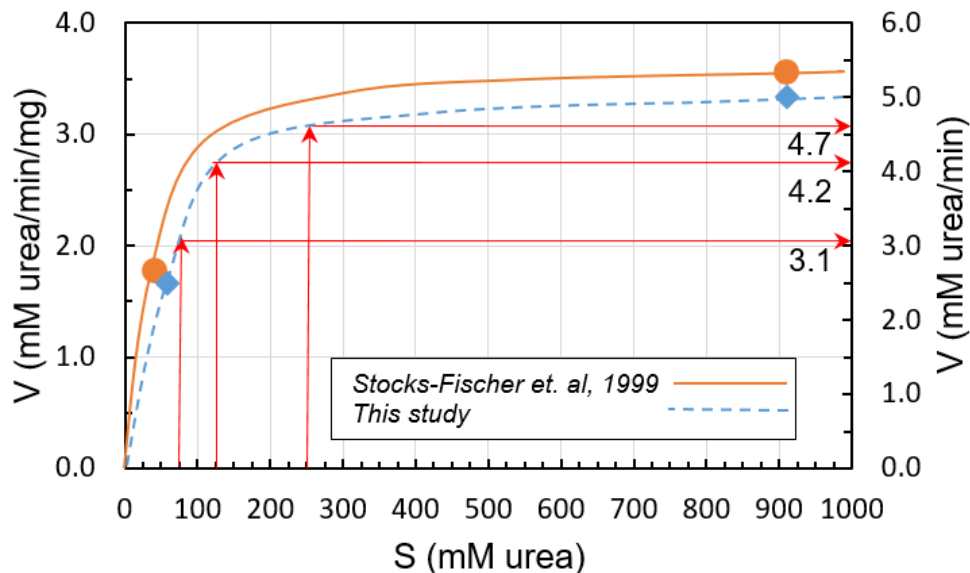


Figure 4.3 *Michaelis-Menton Enzyme Activity Modelling Correlation*

In both cases, it is clearly evident that the urea substrate level at which the original

enzyme activity measurements were made during this study (i.e., 0.91 M, or 910 mM, urea)

were vastly higher than that of the half-saturation constant (i.e., 41.6 mM). Furthermore, it is

similarly noteworthy that the test-tube experiments were also run at urea substrate levels which were also distinctly higher than that of the half-saturation level (i.e., 75 mM, 125 mM, and 250 mM), such that none of these conditions would have imposed a sizable substrate-limiting impact. After subsequently applying an approximated reduction in activity relative based on Michaelis-Menten modeling, relative to the latter three levels of urea presence, these results for adjusted urease levels, plus their associated standard deviation values, have been provided in Table 4.2.

These test tubes were shaken continuously for 24 h on a shake table at 25 $^{\circ}$C $\pm$ 1 to ensure complete mixing. At the completion of this shaking period, the product solutions were filtered through filter paper. These tubes, as well as the filter paper samples, were oven dried at 100 $^{\circ}$C $\pm$ 5 for 24 h. The weight for each calcium carbonate precipitation product (i.e., on either the filter paper and attached to the test tube wall) was then quantified on the basis of pre- and post-testing weights. The total levels of produced $CaCO_3$ content were then calculated by adding the $CaCO_3$ precipitated onto the test tube surface along with that remaining on the filter paper. The calcium consumed efficiency was then computed as the ratio of actual measured $CaCO_3$ mass in comparison to that of the theoretical $CaCO_3$ mass determined according to the input chemical concentration (Neupane et al. 2013; Al Qabany et al. 2012).

### 4.3.5 Testing Program and ICP Treatment Procedures

Each specimen was treated with either MICP or BEICP processing to compare the impact of these treatment methods on properties of coarse- and fine-grained bio-cemented sand. Sand columns were treated with either 4-, 8- 12-, or 16-cycles, given that Inagaki et al. (2011) and Choi et al. (2016) used similar levels of ICP cycling.

Table 4.2 *Test-tube experimental conditions*

| Substrate Urea (mM) (based on a Urea : CaCl$_2$ = 1:1 Mixture) | Urease activity (mM Urea/min) | | | | |
|---|---|---|---|---|---|
| | Range of Ureolytic Activity | *Conductivity measurement of diluted urea activity | Actual activity considering urea & CaCl$_2$ admixture dilution plus Michaelis-Menten impacts | | |
| | | | Calculation | Average | STD** |
| 75 | | | 0.89 | | |
| 125 | Low | 2 | 0.94 | 0.94 | 0.045 |
| 250 | | | 0.98 | | |
| 75 | | | 2.2 | | |
| 125 | Moderate | 5 | 2.3 | 2.30 | 0.100 |
| 250 | | | 2.4 | | |
| 75 | | | 3.1 | | |
| 125 | High | 10 | 4.2 | 4.00 | 0.819 |
| 250 | | | 4.7 | | |

NOTE: * These activity rates were mathematically derived, **Standard deviation

The experimental program is shown in Table 4.3, with three replicate samples at each testing condition in order to verify reproducibility. Two modes of soil stabilization were evaluated using the latter sand columns, including: 1) BEICP, and 2) MICP. A circulated-percolation down-flow process was then applied to treat these sand columns under partially-saturated conditions. The sandy soil columns were processed using the following sequential procedure (as shown in Figure 4.2). First, the catalytic biological solution (either extracted urease for the BEICP method, or bacterial cells for the MICP method, was pumped and recycled into the top of a sand column and gravity drained out from the bottom. A peristaltic pump (Masterflex Model 77202-50) with silicone tubing (Masterflex Model 96410-16) was used to recirculate this biological liquid for 3 h with the rate approximate 5 ml/min in order to achieve a 60 % saturation level consistent with prior research by Cheng et al. 2013, which allowed the bacterial cells or extracted enzyme to sorb onto or be trapped onto the sand particle surfaces. Second, after the latter 3 h introduction of the catalytic agents (i.e., either

MICP culture or BEICP enzymes), the pore volume biological liquid was drained off the soil column. Third, a mixed chemical solution of urea and calcium chloride (0.3 M by 1:1 ratio) was then introduced and circulated for $9 - 12$ h. Fourth, the sand column was flushed with cyclic deionized water pumping for 2 h to remove soluble byproducts and then the bottom cap was removed to drain off all liquid for approximately 10 h. After completing this treatment cycle (introducing urease or bacterial cells and then followed by urea/calcium chloride solution addition), fresh biological solution and chemical were then introduced and recirculated through the sand column on each successive new cycle. This step-wise approach to introducing enzyme solution (or bacterial cells) and urea/calcium chloride solution was repeated on a 'one cycle per day' routine for either 4, 8, 12, or 16 days total treatment phases.

### 4.3.6 Testing of Properties of Biocemented Sand Columns

After achieving the desired cycles of treatment, each column's bottom plastic cap and its internal filters were removed. The engineering properties of bio-treated columns were then evaluated with the following laboratory experiments: hydraulic conductivity, unconfined compression strength (UCS), calcium carbonate content, and microstructure imaging. The latter testing was completed using scanning electron microscope (SEM) and energy dispersive X-ray spectroscopy (EDS). The permeability test was conducted on untreated and treated sand columns. The untreated sandy soil was packed in a permeability testing device (ASTM D5856-15) at a similar relative density of packed sand columns in Table 1. The untreated sands were saturated and tested the permeability follow procedure of constant head test (ASTM D2434-68). The hydraulic conductivity of bio-treated specimens were conducted on the samples which were still held within the PVC test columns. The bio-cemented columns were saturated by applying 15 kPa back-pressure (Cheng et al. 2013). After the initial saturation step, permeability tests were run until steady hydraulic conductivity values

('k'; units = cm/s) were reached. Tests were stopped after k of the specimen did not vary more than 20 % (data not shown here for brevity). This state would be reached only if the specimen was fully saturated. (Hoang et al. 2018).

Table 4.3 *Experiment details*

| Test group | ICP options | Treatment cycles | Sand type | Number of specimens | | | |
|---|---|---|---|---|---|---|---|
| | | | | UCS test | Permeability test | CaCO$_3$ test | SEM/EDS |
| 1 | | 4 | | 3 | 3 | 3 | - |
| 2 | MICP | 8 | Coarse | 3 | 3 | 3 | 1 |
| 3 | | 12 | | 3 | 3 | 3 | 1 |
| 4 | | 16 | | 3 | 3 | 3 | 1 |
| 5 | | 4 | | 3 | 3 | 3 | - |
| 6 | BEICP | 8 | Coarse | 3 | 3 | 3 | 1 |
| 7 | | 12 | | 3 | 3 | 3 | 1 |
| 8 | | 16 | | 3 | 3 | 3 | 1 |
| 9 | | 4 | | 3 | 3 | 3 | - |
| 10 | BEICP | 8 | Fine | 3 | 3 | 3 | 1 |
| 11 | | 12 | | 3 | 3 | 3 | 1 |

After measuring the hydraulic conductivity, the columnar PVC molds were cut to separate the bio-cemented samples which were oven dried for 48 h at a moderate temperature (i.e., ~50 °C). The UCS test was then conducted in accordance with ASTM D4219-08. The elastic modulus ($E_{50}$) of bio-cementation sample was determined by slope of stress-strain curve at 50 % of peak stress (van Paassen et al. 2010a). After the samples were broken down during UCS testing, approximately 5 g of bio-cemented sand was withdrawn from the middle of sand column for calcium carbonate content measurement using an acid-rinsed method (Feng and Montoya 2015).

## 4.4 Results and Discussion

**4.4.1 Chemical Conversion Efficiency for Whole-cell *versus* Enzyme-only**

The chemical conversion ratios of various combinations of enzymatic solutions (i.e. either live cells or extracted enzyme) and substrate reagents were evaluated using a series of test-tube experiments. Figure 4.4 shows the efficiencies of chemical conversion in relation to the concentration of $CaCl_2$ for both biological sources. In general, the observed trend of chemical conversion was to decrease as substrate concentration levels were increased. The lowest level of precipitation efficiency was at 1 mol/L of reagent solution.

This result agrees with previous studies reported by Al Qabany et al. (2012) for MICP and Neupane et al. (2013), Putra et al. (2017) for EICP. The results published by all of these researchers suggested that the high substrate (i.e., urea and $CaCl_2$) concentrations appeared to restrain the urease activity of whole bacterial cells or free enzyme. A related hypothesis has been offered within this related literature as to a possibly negative impact caused by thicker calcium precipitation matrices which seemingly retarded ureolytic hydrolysis (Al Qabany et al. 2012; Al Qabany and Soga 2013). As can be seen within Figure 4.4, increased urease activity levels resulted in a higher efficiency of chemical conversion with both MICP and BEICP. This finding is again comparable to that reported in the literature data (Neupane et al. 2013; Putra et al. 2017a). This current paper actually offers two different relative perspectives as to this impact of substrate concentration. First, at lower substrate levels (i.e., 0.3 M), chemical conversion efficiency increases at higher urease activity levels. Second, the latter efficiency drops as substrate levels increase. Although the range of these latter chemical efficiencies at higher substrates levels is lower, they still retain a sequential correlation with enzymatic activity.

Another significant aspect of these test-tube studies was that of the observed correlation between enzyme form (i.e., whole-cell versus free enzyme) and chemical conversion efficiency. As shown in Figure 4.4, the chemical conversion efficiency for live cell testing was higher than that of free enzyme testing for the low and moderate levels of urease activity. This difference reverses, however, during tests conducted at the higher activity level. After reaching a 250 mM substrate concentration, though, both MICP and BEICP tests revealed a lower efficiency with calcium carbonate precipitation.

The highest efficiency of chemical conversion was observed at the high level of activity with a substrate level of 75 mM. However, the observed 10 – 20 % increase in the precipitation ratio corresponds to an approximate 50 % activity increase (i.e., changing from moderate to high activity levels). The approximate baseline urease activity of 5 mM urea/min (which after subsequent addition of urea and calcium chloride chemicals would then be reduced to 2.5 mM/min) was subsequently chosen for future tests given the pragmatic premise that a lower urease dosing level would be more economical when the original biological solution is to be diluted. In addition, Cheng et al. (2017) mentioned that a lower urease activity rate might be more effective with improving mechanical strength. In turn, a low level for the substrate reagent (0.3 M) was used during the column tests, based on this premise that higher strength and more uniform samples would be obtained for a given amount of calcium carbonate precipitation (Al Qabany and Soga 2013).
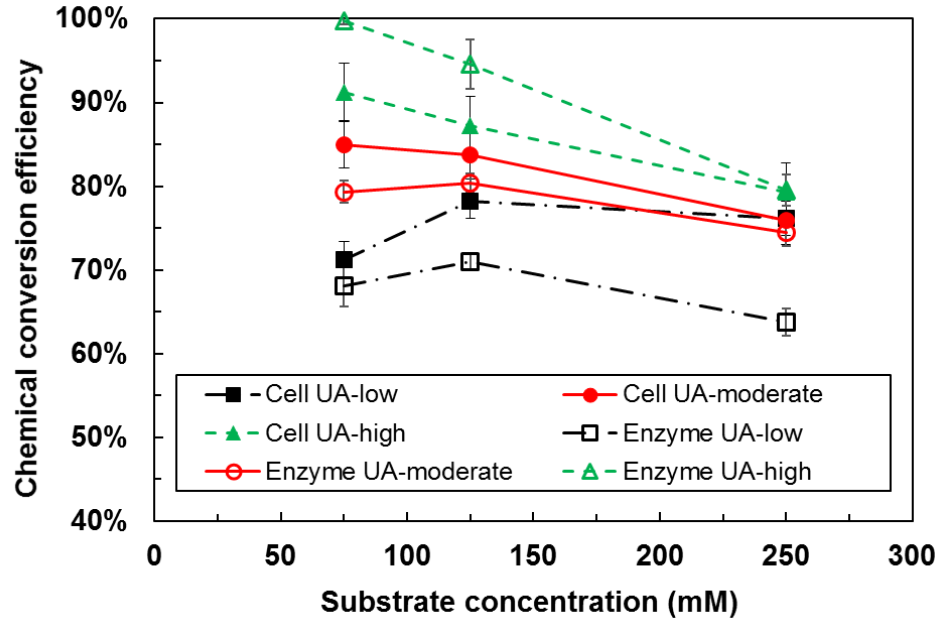
Figure 4.4 *Chemical conversion efficiency of biological sources: bacterial cells versus bacterial enzyme*

### 4.4.2 Whole-cell *versus* Enzyme-only Impact on Bio-stabilized Coarse Sand Properties

The coarse-grained sand columns were stabilized via intact bacteria and extracted enzyme ICP methods which received 4, 8, 12 or 16 repetitive treatment cycles in order to achieve different levels of $CaCO_3$ content. The properties of the bio-cemented samples were tested to comparatively evaluate the resulting variations with these alternative methods in terms of UCS, elastic modulus ($E_{50}$), permeability, and microstructure of bio-cemented coarse-grained sand.

### UCS and elastic modulus

Figure 4.5 identifies peak stress levels for MICP-treated samples, where these results varied considerably from 200 to 2300 kPa. However, the UCS estimates for BEICP-treated sands range from 400 to 1500 kPa and, in one sample, up to approximately 2400 kPa. Although the UCS range of treated sand was similar with both bio-treatment methods, the levels of $CaCO_3$ precipitation were substantially different between MICP- and BEICP-treated

samples. These precipitation values ranged from 2.5 to 16 % $CaCO_3$ for MICP-treated samples, and from 1.5 to 8 % for BEICP-treated specimens. The result demonstrated that MICP processing consistently produced a higher amount of $CaCO_3$ for the same number of treatment cycles as compared to BEICP treatment. The increased bio-cementation may be caused by whole-cell attachment to sand surfaces, let alone filtering and trapping of these intact cells within the sand pore matrix during down-flow percolation, where both would then induce $CaCO_3$ nucleation (Ginn et al. 2002). Furthermore, it is plausible that increased numbers of treatment cycles might have increased ionic particle charging which could then boost bacterial adhesion (Faibish et al. 1998; Foppen and Schijven 2006) on sand particles in relation to an elevated zeta potential (Dick et al. 2006). In contrast, the observed lower levels of $CaCO_3$ precipitation in BEICP-treated samples may have been caused by soluble urease enzyme flushing and loss due during cyclic drainage, as opposed to surficial binding or trapping retention. Back-calculated estimates of residual urease activity remaining in the column, versus that which was removed via flushing, were approximately 40 % of the original rate during BEICP processing at 1 – 4 treatment cycles (data not shown). However, this percentage of urease activity retention reached 60 – 70 % as the numbers of treatment cycles increased (data not shown), likely due to decreased permeability (and additional enzyme trapping) which developed at higher treatment cycles. While the $CaCO_3$ content of BEICP-treated sand did reach ~8 % after 16 cycles, this level was still far lower than that of MICP-treated sands.

In general, therefore, when considered on the basis of comparable levels of calcium carbonate precipitation, the strength range for BEICP-treated sand tended to be higher than MICP-treated. For example, at 2 – 4 % and 5 – 8 % levels of $CaCO_3$, the UCS of BEICP-

treated sand was approximately double that achieved with MICP processing. While Qian Zhao et al. (2014) also reported that EICP treatment had a lower range of $CaCO_3$ content, their tests showed lower UCS results as compared to MICP processing. However, these authors used a different treatment method, i.e., without adding fresh biological solution, such that on-going degradation of the originally added enzyme might have then decreased their EICP product outcome below that of MICP.

Although, the amount of $CaCO_3$ precipitation is undoubtedly an important factor impacting bio-cemented sands, the distribution patterns of the precipitated crystal clusters might have also played a vital role with product strength (Cheng et al. 2017; Cui et al. 2017; Hoang et al. 2018; Lin et al. 2016; Terzis and Laloui 2018). These distribution patterns involve three apparent factors, including: 1) location of the calcium crystals relative to sand inter-particle contact, 2) thickness of the crystal clusters, and 3) non-beneficial precipitation of $CaCO_3$ within sand surfaces. Microstructure analysis provided further insights regarding the influence of these latter three factors, and these details are covered in a further narrative section.

Figure 4.6 subsequently provides an informative comparison of current and previously reported findings for UCS results in relation to $CaCO_3$ precipitation, depicting current BEICP results in comparison to current and prior MICP results. The UCS strength levels recorded during this study are in exceptionally good agreement with previously published MICP findings Choi et al. (2016a, 2017), van Paassen et al. (2010a), Al Qabany and Soga (2013), where the prior researchers employed a similar substrate concentration (i.e., 0.3 M for both urea plus $CaCl_2$). However, the UCS trend line obtained from BEICP-treated

sand in this work was recorded at a noticeably higher range than that of MICP-treated data,

when compared according to comparable calcium deposition levels.
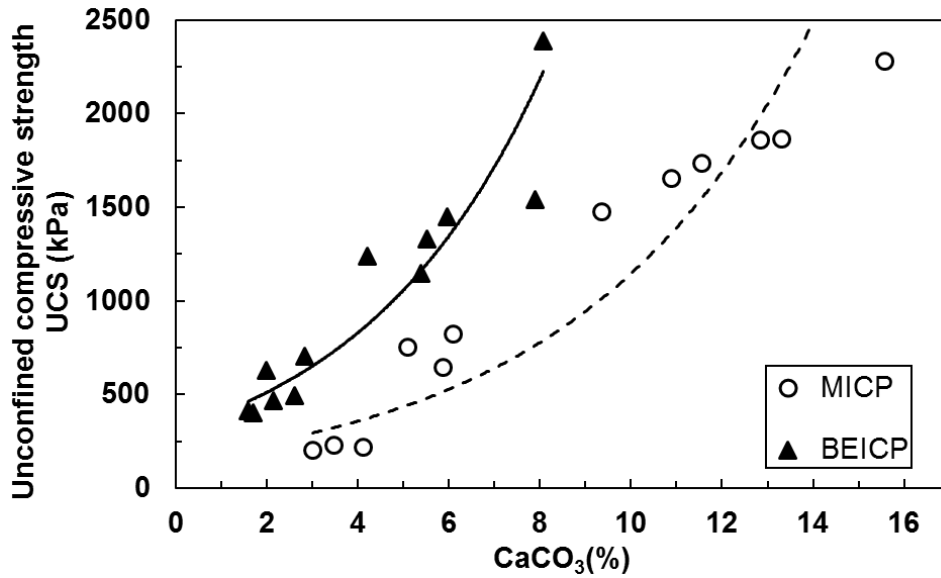


Figure 4.5 *UCS results for MICP- and BEICP-treated samples of coarse sand*
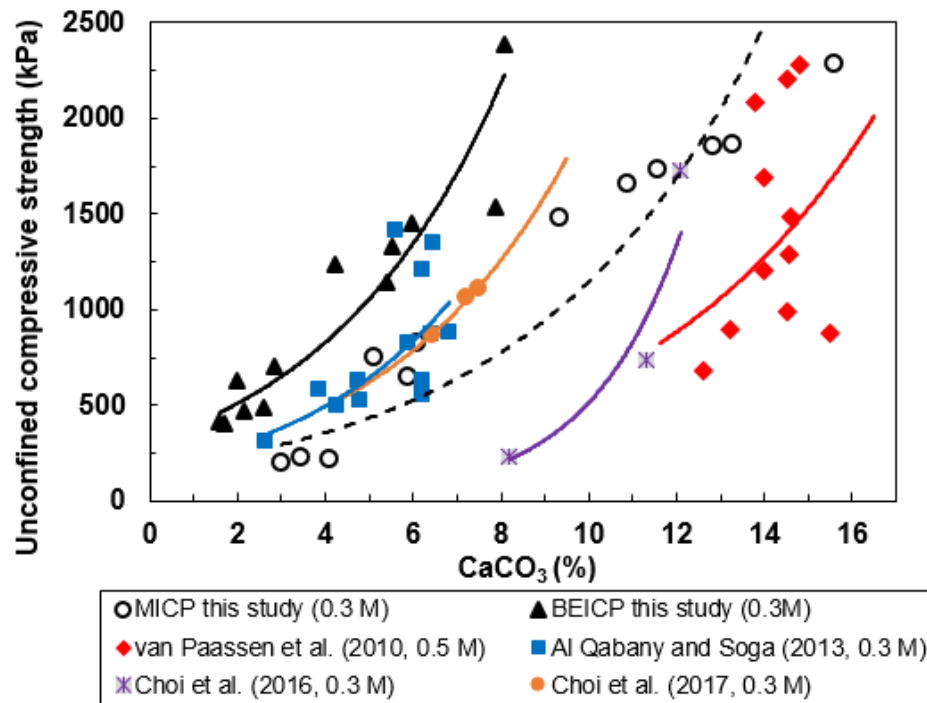


Figure 4.6 *UCS comparison of current BEICP and MICP results versus previous MICP data*

Typical stress-strain curves of bio-cemented sand obtained from unconfined compression testing at 4 and 8 cycles of treatment have also been presented in Figure 4.7. Both MICP- and BEICP-treated sand exhibited a brittle nature comparable to that which had been observed in other prior MICP testing (Bernardi et al. 2014; Choi et al. 2016b) and EICP (Kavazanjian and Hamdan 2015; Neupane et al. 2015a; Park et al. 2014). As can be seen from Figure 4.7, the peak stress of MICP-treated samples after 4-cycle treatment was clearly lower than similarly treated BEICP-treated sand. A lack of uniformity within MICP-treated sands resulted in lower UCS strengths. During these sample tests, failure did not occur within the whole core. Instead, sample failure occurred within the less solidified and weaker bottom section. Similar outcomes were reported both by Cheng et al. (2013); van Paassen et al. (2010b). Lower strengths within the MICP-treated samples could have been similarly caused by non-uniform biocementation conditions after low cycles of treatment (i.e., with lower calcium cementation at lower depths within treated columns).
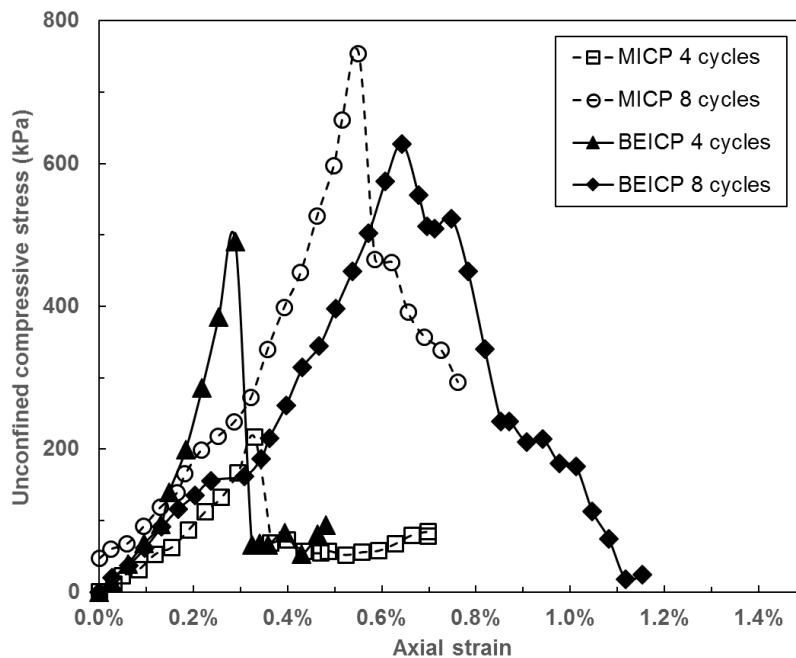


Figure 4.7 *Typical stress-strain relationship for MICP- and BEICP-treated samples of coarse sand*

The modulus was computed as a secant elastic modulus based on the strain required to mobilize 50 % of the peak stress, $E_{50}$ (Figure 4.8). The ranges of elastic modulus were from 20 to 250 MPa for the MICP-treated samples, whereas, the Young's modulus for BEICP-treated sand varied between 50 to 200 MPa. As can be seen, the increasing trend of $E_{50}$ correlated to $CaCO_3$ content provided by MICP-treated samples was comparable to that observed with BEICP treatment. Compared against previous $E_{50}$ testing results on MICP-treated sand, van Paassen et al. (2010a) found that $E_{50}$ results with ICP-treated sand ranged from 100 to 8500 MPa which were significant higher than the elastic modulus results in this study. However, BEICP processing produced an even higher elastic modulus than the EICP results reported by Yasuhara et al. (2012) (range 50 – 160 MPa) and Neupane et al. (2015a) (range 16 – 18 MPa). van Paassen et al. (2010a) reported his use of a high substrate concentration (1 M for $CaCl_2$ : urea) and high level of treatment (16 days), whereas a fewer number of treatment cycles were injected by Yasuhara et al. (2012) (4 and 8 times) and Neupane et al. (2015a) (2 times). These data, both past and current, strongly suggest that substrate strength and numbers of treatment cycles are the main factors for the finished strength of bio-cemented sand.
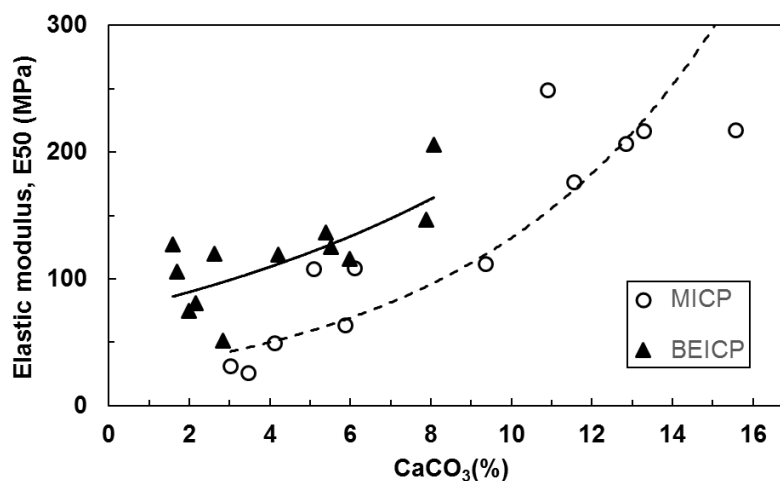


Figure 4.8 *Elastic modulus results for MICP- and BEICP-treated samples of coarse sand*

**Hydraulic conductivity**

The hydraulic conductivity results for bio-cemented sand, using both MICP and BEICP treatment, has been graphed within Figure 4.9. Here again, these findings are again depicted in relation to calcium precipitation levels. In general, these ICP-treated sand samples exhibited a reduction in hydraulic conductivity in relation to increases $CaCO_3$ content. The permeability levels for BEICP-treated sands was slightly lower at a range of 1.5 – 4 % $CaCO_3$ precipitation. For BEICP processing, the highest reduction of permeability at an 8 % $CaCO_3$ content. The impact of MICP processing, though, was more pronounced, with a 3- to 4-log decrease within a 13 – 16 % of $CaCO_3$ precipitation range. Although, MICP exhibited far lower permeability reductions than BEICP, both treatment options showed a similar pattern of reduction relative to $CaCO_3$ precipitation. This similarity may be attributable to multiple factors, as explained by the following logic. First, the sand columns were packed with the same type of sand (coarse grains sand, #20/30) and with the same porosity (see Table 4.2), which in turn, would then have been expected to produce similar initial permeabilities. Second, sample permeability would then have been reduced with progressive calcium-rich crystal formation within void spaces between sand grains. Third, escalating $CaCO_3$ precipitation within sand pore space would then have led to the lower permeability levels within the specimens. A consequent observation was that progressively increased calcium carbonate precipitation, induced by either whole-cells with MICP or extracted-enzymes by BEICP, plays a crucial role in reducing the permeability of bio-cemented sand.
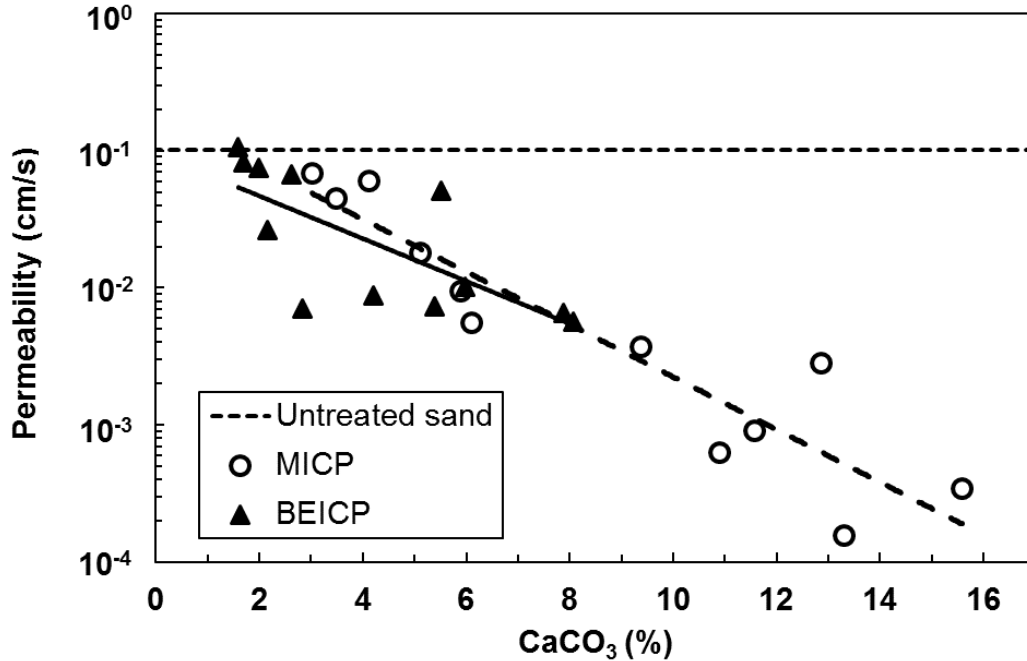
Figure 4.9 *Permeability results for MICP- and BEICP-treated samples of coarse sand*

### Microstructural analyses

The microscale morphology of precipitated calcite crystals within the coarse-grained

bio-cemented sand matrix was analyzed using scanning electron microscopy (SEM).

Photographs obtained with this SEM evaluation are provided in Figure 4.10. The initial

Figure 4.10 a – c photographs shows that calcium carbonate precipitated via bacterial cells

(i.e. MICP) were agglomerated and formed large crystal clusters with a substantial thickness

level from 50 to 100µm. One important feature in this regard was that of the large $CaCO_3$

clusters precipitated at the contact points between sand particles, which accumulated within

and progressively filled interstitial gaps between the adjacent sand particles and through

which agglomeration then clogged pore spaces within sand matrix. The crystal clusters

patterns observed during this current study agree with observation reported by previous

researchers (Cheng et al. 2012, 2017; Cui et al. 2017). In contrast, and as shown in in Figure

4.10 d – f the small crystal clusters produced via bacterial enzyme (i.e. BEICP) processing

were accumulated as noticeably smaller calcium-bearing crystals. The average size of these smaller BEICP-based cluster ranged from 5 to 20 µm. Interestingly, the distribution patterns for these smaller BEICP-derived crystal clusters is that they were observed primarily at the sand grain contact points and only intermittently on the sand particle surfaces. And given the smaller size of these crystals, there was less pore volume being filled within the BEICP-treated sands.

An explanation for these observed differences in the size of ICP-derived calcium formation between MICP and BEICP process has been offered within a previous publication by the our research team (Hoang et al. 2018). Figure 4.10c showed that most calcium crystal sizes ranged from 5 to 10 µm for MICP-treated sand, while BEICP crystals were noticeably smaller within a range of 1 to 4 µm (Figure 4.10f). The premise behind this change in crystal precipitation size is that of the nucleation sources, as derived either by whole-cell or enzyme-only mechanisms. Mitchell & Ferris, 2006 employed urea hydrolysis using whole-cell *B. pastuerii* bacteria for MICP processing, and observed calcium crystal diameters of 4.2 µm and 7.4 µm in 1 and 7 days, respectively. In contrast, nano-sized crystal formation (~20 nm) were reported by Sondi and Salopek-Sondi (2005), pursuant to their use of enzyme-only ureolytic treatment for ICP precipitation.

These findings suggest that the mode of urea hydrolysis is a key factor affect the size of calcite crystal in ICP process.  Perspectives regarding the distribution patterns of calcium crystal clusters have also been reported for MICP processing under various conditions. Al Qabany et al. (2012); Al Qabany and Soga (2013) reported on the impacts of substrate concentrations, retention times, and chemical addition flow rates. Cheng et al. (2013, 2017) investigated the effect of varying degrees of saturation, levels of urease activity, processing

temperatures, and other environmental factors. In order to further evaluate the distribution patterns of crystal clusters of MICP versus BEICP processing, therefore, EDS overlay imaging was conducted for both such sample specimens following 16 cycles of treatment. This imagery is given in Figure 4.11, and digital false-color rendering has been employed to visually highlight specific elemental content (i.e., 'blue' for calcium, 'yellow' for silica, and 'red' for chloride).

As can be seen, although the sand particles contact points were bridged by BEICP-deposited crystals, the pore space of the sand matrix was still fairly open (Figure 4.11a). However, MICP processing showed a noticeably higher level of calcium deposition (i.e., whose calcium-rich content is rendered with their blue color), as per Figure 4.11b. Indeed, these images reveal blue-colored calcite clusters deposited at three locations: 1) sand particle contact points, 2) sand grain surfaces, and 3) sand pore space volume.

These findings regarding differences in calcium precipitation via MICP and BEICP processing would appear to directly impact the finished mechanical properties, in terms of strength and stiffness of bio-cemented sand. One such apparent correlation would be that the strength of bio-cemented sands was moreso influenced by the location of calcium crystal deposition as compared to the total mass of $CaCO_3$ buildup. This premise agrees with previous studies reported by Cheng et al. (2013), Cui et al. (2017), Al Qabany and Soga (2013). For example, at the level 1500 kPa of UCS, BEICP-treated samples only need approximately 6 – 8 % of $CaCO_3$ precipitation, while MICP-treated sands required around 10 – 11 % of $CaCO_3$ content in order to achieve similar mechanical strength (Figure 4.5). Therefore, when quantified in relation to strength achieved per mass of deposited calcium, the efficacy of BEICP processing would appear to be higher than that of MICP treatment.

Furthermore, it would also appear that a more specific rationale for the high efficiency of increased UCS results with BEICP processing is that of calcium deposited at the contact points of sand particles governed the strength of sand, Similar perspectives have also been presented by Cheng et al. (2017), Martinez and DeJong (2009).

Yet another related aspect of this behavior is that the amount quantity of calcium deposition had a major impact on the reduction of permeability produced by MICP and BEICP. This correlation can be seen with the trends for permeability reduction depicted within Figure 4.9. The visual evidence given in Figure 4.11 confirmed that there were far higher levels of deposited calcium attached to sand grain surfaces and pore space volume during MICP processing (Figure 4.11b) versus BEICP processing (Figure 4.11e). Similar observations were made by previous researches (i.e., Cheng et al. (2013), Al Qabany and Soga (2013)). One further noteworthy observation shown within Figures 4.11 c & e was that of a significant difference between MICP (Figure 4.11c) and BEICP (Figure 4.11e) processing in terms of their relative chloride deposition levels. Although both modes of treatment had involved tap water flushing within 2 h after every treatment cycle in order to remove residual chemicals, Figure 4.11e clearly shows a substantial residual presence of chloride (i.e., false-colored as yellow). This chloride residual was, in turn, attributed to the far lower permeability of MICP treated samples after multiple treatment cycles. The reduced permeability then meant that chloride would not likely have been flushed from the sample during the post-processing tap water rinse step, and was then being 'baked' as it were into a solid, chloride-rich deposit inside the MICP cores during final oven drying. This covert chloride crystallization behavior could well have contributed to a falsely higher measurement of MICP mechanical strength levels as compared to what would have been expected had

long-term soaking and flushing of the chloride been achieved. This unexpected MICP finding suggests yet another benefit with BEICP processing, where no such chloride deposition occurred since tap water flushing was far more effective due to the higher residual permeability.

### 4.4.3 Effect of Sand Grain Size on BEICP-treated Samples

The following details and discussion address the influence of sand particle size on BEICP-treated columns. The type and size of sand grains subjected to ICP processing both represent key factors in terms of bio-cementation success. Previous researchers have addressed the effects of various sand grain size ranging from fine to coarse both using MICP processing (Bernardi et al. 2014; Cheng et al. 2013; Lin et al. 2016; Qian Zhao et al. 2014; Rebata-Landa and Santamarina 2006; Terzis and Laloui 2018) and EICP processing (Hamdan et al. 2013; Kavazanjian and Hamdan 2015). This current paper adds further insight to this prior understanding, in terms of BEICP's performance with coarse and fine sand. As with the preceding tests completed on coarse grained sand, these BEICP fine sand tests were conducted with 4, 8, and 12 cycle step option. Figures 4.12 and 4.13 show the resultant UCS, elastic modulus. Figure 4.14 offers a further comparison of UCS results for BEICP against other published EICP results. In addition, Figure 4.15 covers permeability outcomes and Figures 4.16 and 4.17 provides a set of SEM images.
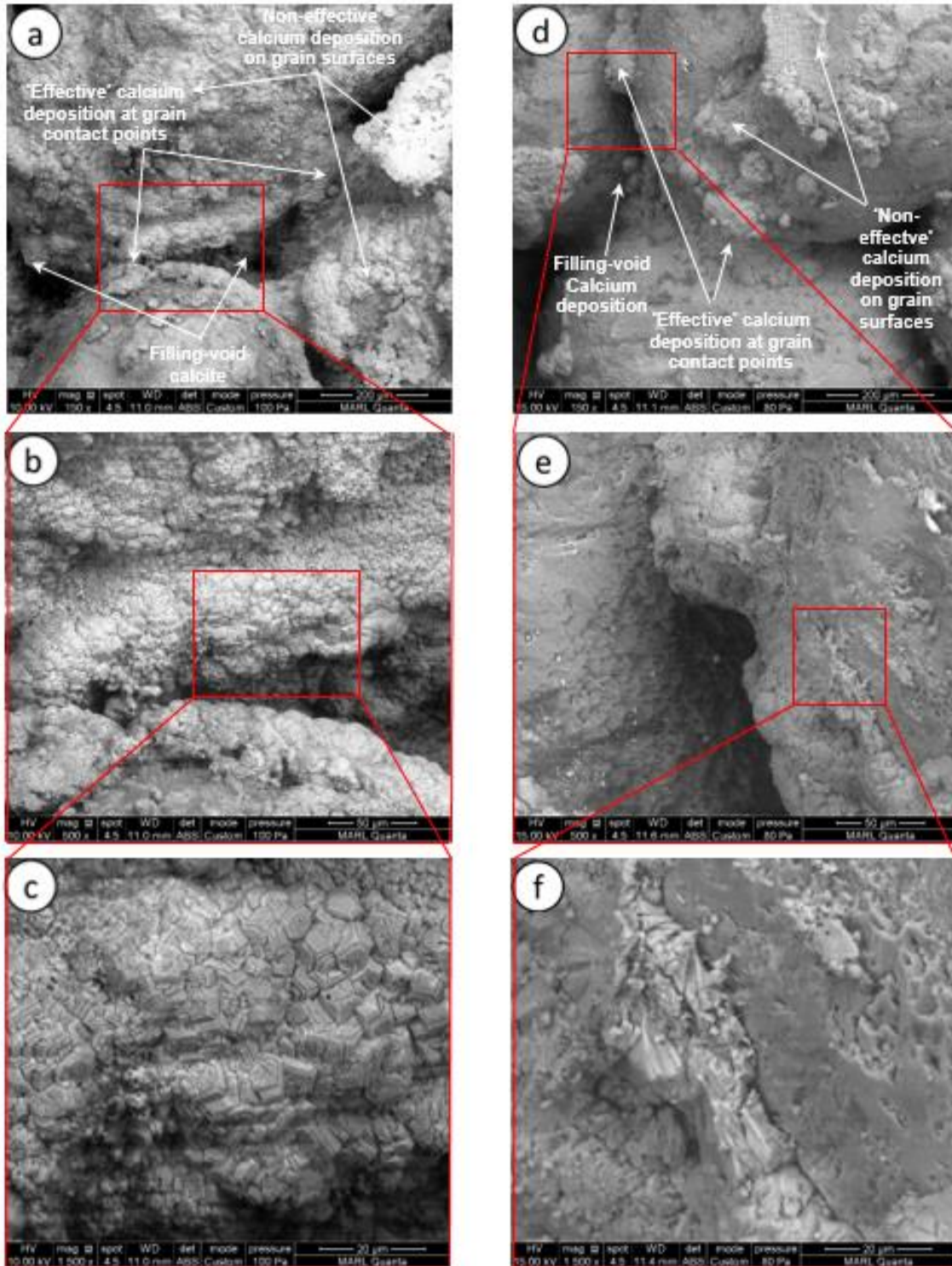
Figure 4.10 *SEM images of bio-treated samples for coarse sand: (a – c) MICP at 12-cycle levels; (d – f) BEICP at 12-cycle levels*
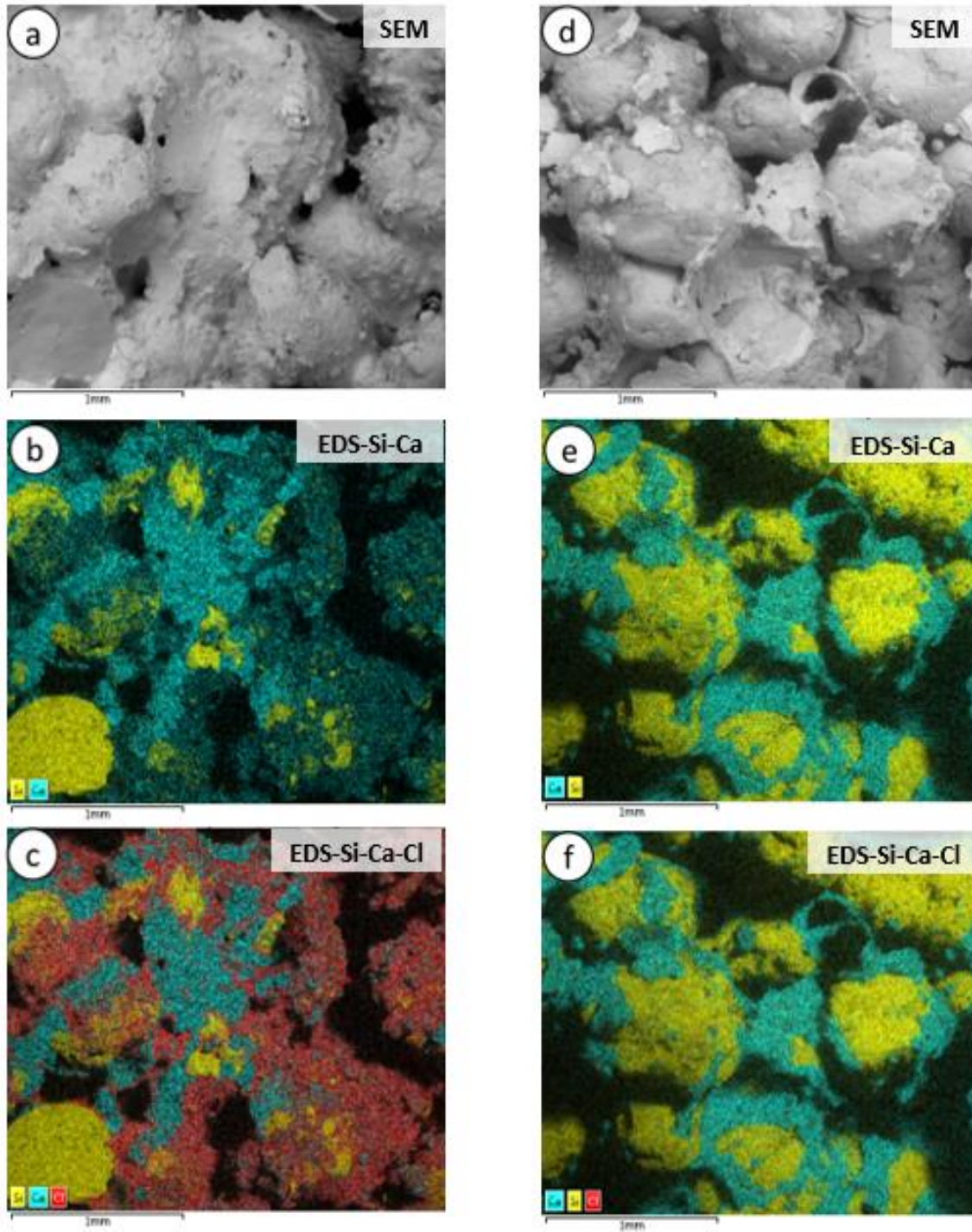
Figure 4.11 *SEM and EDS images of bio-treated samples for coarse sand: a – c) MICP at 16-cycle levels; (d – f) BEICP at 16-cycle levels*

**UCS and elastic modulus**

The results obtained with BEICP-based treatment revealed a more pronounced strength (Figure 4.12) and elastic modulus (Figure 4.13) stabilization when applied to cohesionless materials. The UCS of BEICP-treated coarse-grained sand fell between 450 and 1500 kPa for the level of calcium carbonate precipitation from 2 to 6 %. Meanwhile, BEICP processing of fine sand provided ranges of UCS from 200 to 900 kPa at similar $CaCO_3$ contents. Similar patterns of increased bio-cemented stiffness were observed in relation to increased calcium carbonate deposition for both sand types. The Young's modulus of coarse bio-cemented sand varied between 75 and 125 MPa, whereas that of fine bio-cemented sand varied from 25 to 75 MPa (i.e., when correlated with ranges of $CaCO_3$ varying from 2 to 6 % for both materials). The trend towards lower UCS and stiffness for BEICP-treated fine sand compared to coarse sand at the similar level of $CaCO_3$ content is consistent with results previously reported by Gomez et al. (2013), Lin et al. (2016), Qian Zhao et al. (2014), Terzis and Laloui (2018) for MICP process and by Hamdan et al. (2013), Kavazanjian and Hamdan (2015) for EICP processing. In contrast, Cheng et al. (2013) mentioned that at a similar $CaCO_3$ content, the fine MICP-treated sand achieved higher values of cohesion and friction angle as compared to that of MICP-treated coarse sand.

It should be noted that the overall bulk mass of calcium carbonate precipitation could not be considered as the sole factor governing the level of stabilization for bio-cemented sand Lin et al. (2016), Terzis and Laloui (2018). The 50/70 bio-treated sand had a higher $CaCO_3$ content compared with #20/30 bio-cemented sand when treated using similar numbers of treatment cycles, the peak shear stress values for BEICP-tread coarse sand was higher than that of BEICP-treated fine sand. For examples, at 8 cycles of treatment, the UCS values of coarse-grained bio-treated sand ranged from $450 - 700$ kPa at an average of 2.3 % of $CaCO_3$

content, whereas, those of fine-grained bio-treated sand ranged from 380 to 540 kPa at an average of 3.1 % of $CaCO_3$ content. The fact that finer sand had higher $CaCO_3$ content and lower strength matches observations made by previous studies on MICP and EICP processing (Kavazanjian and Hamdan 2015; Lin et al. 2016; Terzis and Laloui 2018).

Cheng et al. (2013) characterized the nature of this same behavior on the basis of a so-called 'hinge' mode of calcium deposition at the point of grain contact. Their corresponding assumption was that moisture retention is higher in this 'hinge' area under partially-saturated column conditions. Although their paper did not offer any further hypotheses about the extent of hinge development and corresponding calcium deposition, this paper's findings suggest that higher calcium deposition, higher hinge volume, and higher moisture retention were all more prominent when dealing with fine grain sand sizes. The group of researchers also indicated that for a partially saturated treatment, the calcium carbonate crystal cluster has precipitated mainly at the contact points of grains where had been formed solution menisci layers. Therefore, the $CaCO_3$ contents were higher value in the fine BEICP-tread sand which were treated by partially saturation method (percolation – circulation technique).

Terzis and Laloui (2018) investigated crucial microscopic characteristics of bio-cemented sand in relation to apparent biostabilization strength, covering such factors as the particle sizes of the crystalline bond lattice, bond-grain contacts, and particle orientations. Their study indicated that larger-sized bio-cemented sands had higher strength and stiffness than smaller-sized MICP-treated sand at the similar level of $CaCO_3$ content. According to Terzis and Laloui (2018), MICP-treated large sand had larger mean diameters of crystal clusters precipitated at sand grain contact points than that achieved with bio-cemented

smaller sand. Their conclusion was that this biocemented coarse sand grain behavior might lead to a higher resistance against particle shearing and increased particle inter-locking. In addition, the spatial orientation and population of calcium crystal clusters in large bio-cemented sands were found to be more homogenous in distribution as compared to calcium bonds precipitated with smaller grained sands. As a more homogenous distribution of calcium crystals developed within the spatial orientation space, a higher overall stress resistance developed due to inter-granular contact and cementation. Although the UCS and Young's modulus of coarse-grained BEICP-treated sand were higher than those of fine-grained bio-cemented sand at a similar level of $CaCO_3$, further studies of stress-strain behavior at various confining stress, friction angles, and cohesion should be investigated for both sand materials.
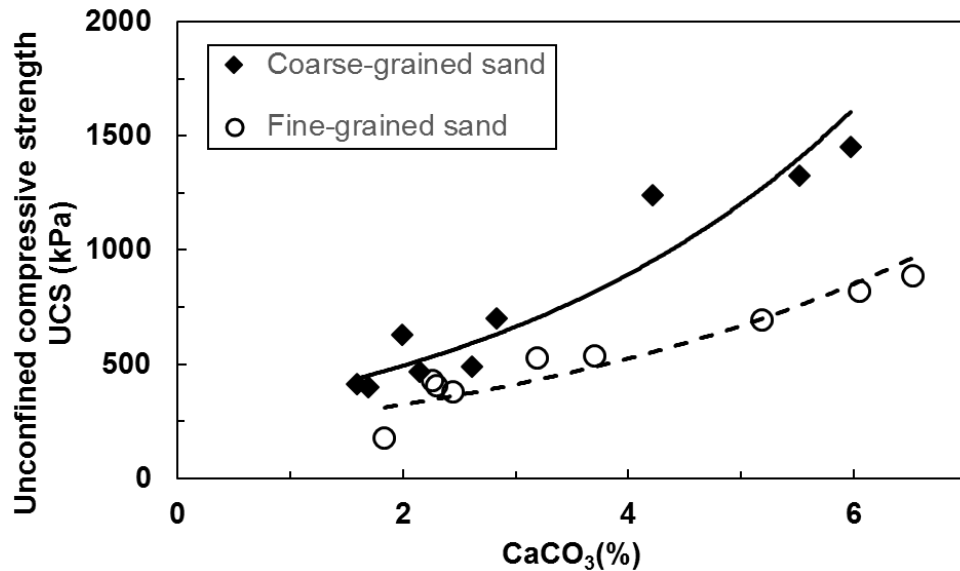


Figure 4.12 *UCS results of BEICP-treated samples for coarse- and fine-grained sands, compared to UCS data from previous studies*
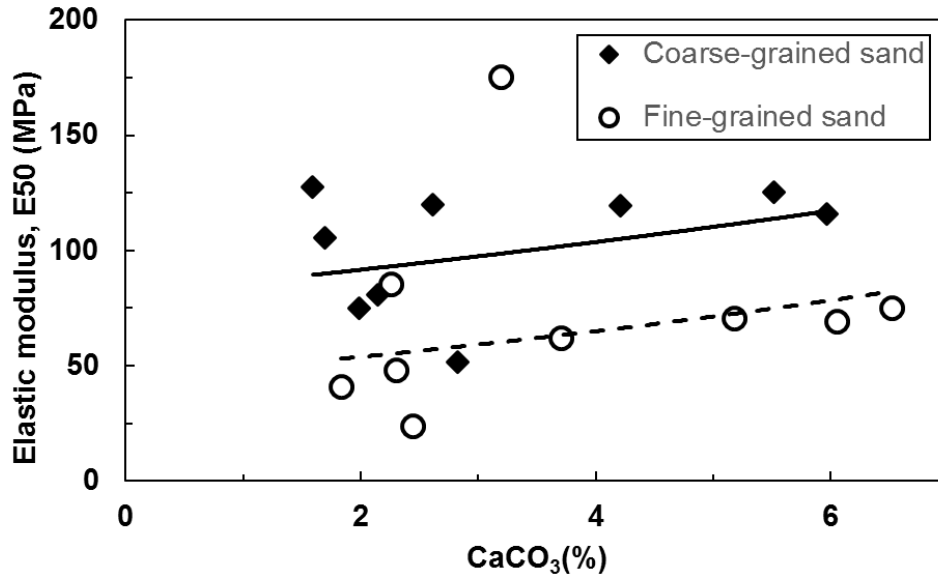
Figure 4.13 *UCS results of BEICP-treated samples for coarse- and fine-grained sands*

An additional visual comparison of this study's current BEICP testing showing UCS results versus those observed by other prior investigators using EICP biostabilization methods is within Figure 4.14 (Kavazanjian and Hamdan 2015; Neupane et al. 2015c; Oliveira et al. 2016; Park et al. 2014; Yasuhara et al. 2012). In this case, the current study's BEICP-derived UCS results are considerably higher when considered against the previously published EICP findings at comparable calcium deposition levels.
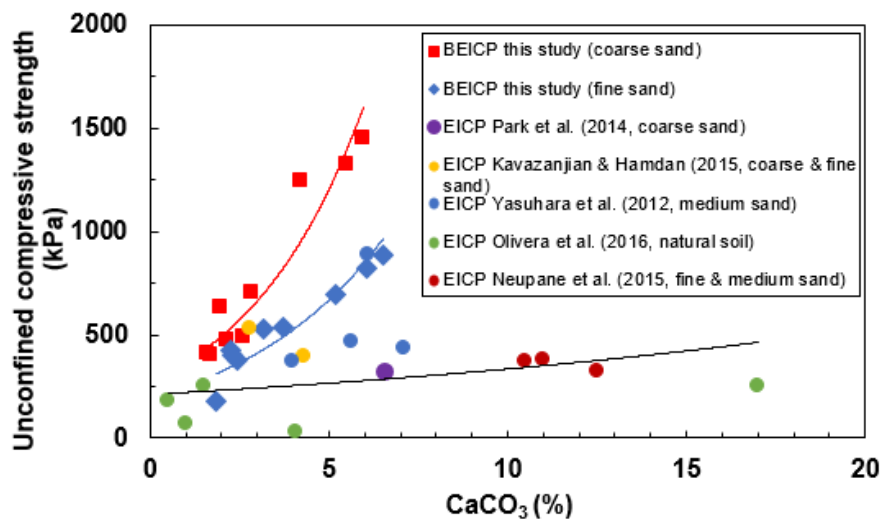


Figure 4.14 *UCS comparison of current BEICP results versus previous EICP data*

**Hydraulic conductivity**

The permeability results for coarse-grained and fine-grained BEICP-based sand treatment are given in Figure 4.15, including values for both untreated materials and biostabilized samples.  As expected, a permeability reduction realized during BEICP sand processing correlated with an increase in $CaCO_3$ content for both fine and coarse sand. However, the trend of reduced hydraulic conductivity observed with fine-grained bio-cemented sands showed a steady decline with higher calcium deposition levels, while the trend for coarse-grained sand showed sizably less reduction in permeability as calcium carbonate precipitation increased. This trend with lower permeability in fine-grained bio-treated sand compared to coarse-grained sand is similarly consistent with the data published by Cheng et al. (2013) when using MICP treatment. Interestingly, fine-grained BEICP-treated sand typically had lower permeability values when compared against the coarse-grained BEICP-treated sands at similar levels of $CaCO_3$ content. It should also be noted that both materials were packed at a similar relative density in the untreated state. This indicates that the permeability reduction of BEICP-treated coarse and fine sand might have been controlled by factors other than average or bulk $CaCO_3$ content (i.e., notably that of the distribution patterns with calcium carbonate precipitation). The following SEM analysis given in the next section will subsequently provide a visual perspective of calcite crystals distribution patterns observed with both coarse- and fine-grained BEICP-treated sand.
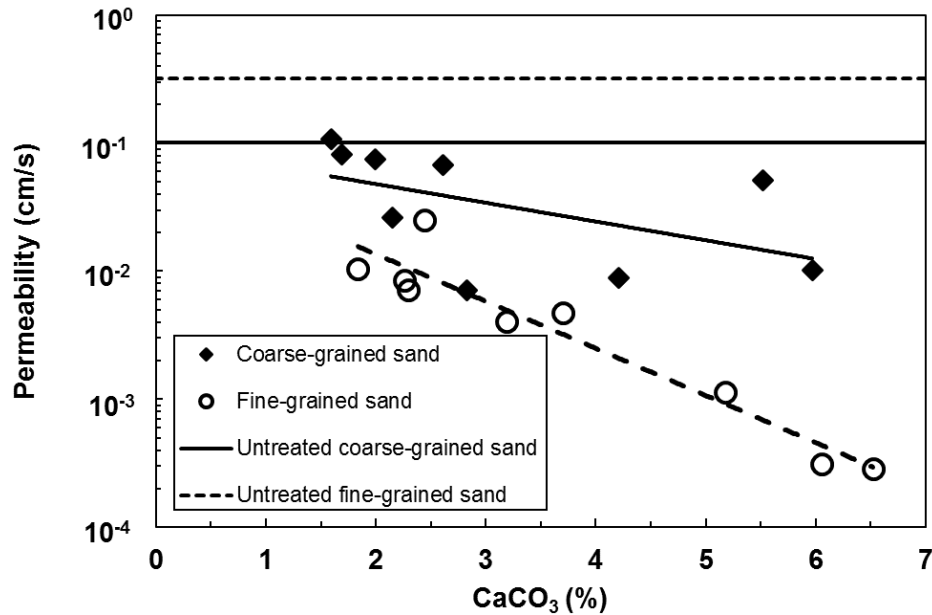
Figure 4.15 *Permeability results of BEICP-treated samples for coarse- and fine-grained sands*

### Microstructural analyses

Figures 4.16 and 4.17 provide a set of SEM images for BEICP-treated coarse-grained and fine-grained sands after 8 and 12 treatment cycles, respectively. These images depict calcium cluster deposition occurring at the contact points and surface of sand grains, but pore space deposition with these BEICP samples is noticeably less than had been observed with MCIP samples (see Figures 4.10a and 4.11a). A similar pattern of reduced pore-space volume deposition was also reported by Cheng et al. (2013), for MICP biostabilization applied with a partially-saturated state. During this sort of unsaturated processing conditions, and with pore space volume primarily filled with air, the down-flowing substrate solution would be retained as a moist film spread across the grain surfaces and in a retained menisci layer which formed due to surface tension at the point of sand grain contact. As shown in Figures 4.16 c & f, the size of a single calcium crystal initially formed by BEICP processing tended to be quite small, ranging from ~1 to 4 µm, for both bio-treated coarse- and fine-

sands. This is because the precipitation particle was built up from nano-sized crystals generated from BEICP's nano-scale free enzyme catalyst.

However, the amount and distribution pattern of calcium crystal precipitation differed widely between the coarse and fine materials. The $CaCO_3$ levels with 50/70 sand samples (Figure 4.16 d – f) were likely higher than those in 20/30 sand (Figure 4.16 a – c). However, as was discussed previously, the average mass of $CaCO_3$ was not a sole factor governing the strength of bio-cemented sand.

The calcium carbonate distribution pattern was another main factor with processed sample strength. Interestingly, the crystal clusters concentrated mainly at the contact points of sand grains for coarse-grained BEICP-treated sands, while these clusters predominantly coated the grain surfaces for fine-grained sands. Cheng et al. (2013), Cui et al. (2017), Hoang et al. (2018), Lin et al. (2016), Terzis and Laloui (2018) all mentioned that surface-coating calcium crystals tended to provide 'non-effective' grain bonding (i.e., as compared to 'effective' inter-particle bridging bonds, whose effectiveness likely governed stabilization strength). Therefore, the UCS and Young's modulus of the fine BEICP-improved sands were lower than that of coarse-grained sands (Figures 4.12 and 4.13).

The distribution pattern of calcium clusters likely impacted the reduction of permeability observed with BEICP-treated sands. Figure 4.16 showed the clusters deposited almost exclusively at the contact points of sand grains and sand surfaces after 8 cycles, whereas there was continued deposition both at the contact points and internal void space after 12 cycles (Figure 4.17). However, after 12 cycles of treatment, the amount of calcium crystal filling within void space during fine-sand BEICP-treatment (Figures 4.17 c & d) was likely higher than that taking place within coarse-grained sands (Figures 4.17 a & b). In this

case, therefore, more pore volume filling, and a resultant further reduction in hydraulic conductivity, could be expected.
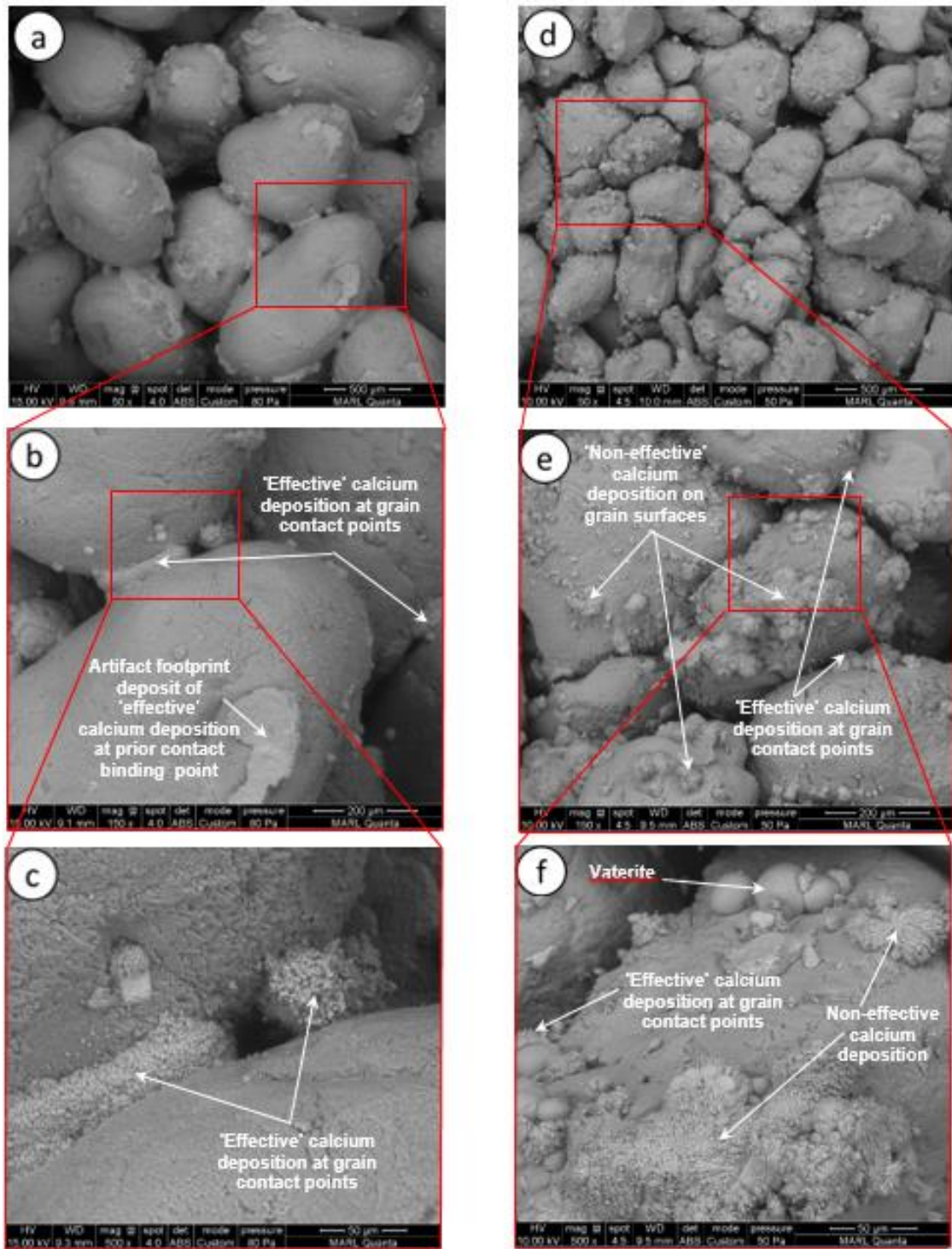


Figure 4.16 *SEM images of BEICP-treated samples: (a – c) coarse-grained sand at 8 cycle levels; (d – f) fine-grained sand at 8 cycle level*
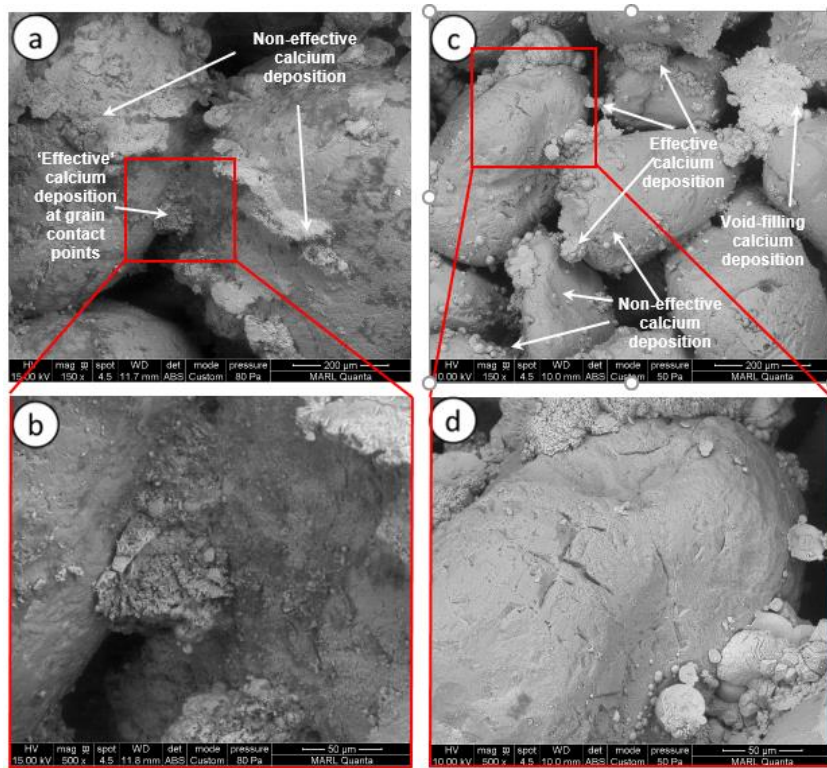
Figure 4.17 *SEM images of BEICP-treated samples: (a – b) coarse-grained sand at 12 cycle levels; (c – d) fine-grained sand at 12 cycle levels*

## 4.5 Conclusions and Recommendations

This paper provides a comparative investigation for whole-cell (i.e., MICP) and extracted bacterial enzyme (i.e., BEICP) methods focusing on two key factors: 1) chemical conversion efficiency, and 2) engineering properties. Both MICP and BEICP assessment was conducted using coarse sands, while only fine-sands were evaluated using BEICP. The following bullet-list points highlight the key conclusions identified with this research effort:

- Chemical conversation efficiency for both MICP and BEICP methods dropped as the concentration of applied substrate chemicals was increased.

- However, in both cases chemical conversion efficiency increased as the employed urease activity level increased.

- MICP processing (using whole-cell enzymes) produced higher levels of chemical conversion efficiency when evaluated between low and moderate levels of urease activity.

- However, the chemical conversion efficiency for BEICP (using bacterial-extracted free enzyme), was higher than that of MICP processing once at a high level of urease activity.

- BEICP processing demonstrated higher UCS strength levels than MICP with coarse sands, or even published EICP, results when considered at comparable calcium deposition levels.

- BEICP processing also generated smaller calcium crystal sizes when compared at comparable levels of treatment cycles. For example, BEICP completed at an 8-cycle treatment mode produced crystals at a 1 to 4 µm scale.

- MICP produced a noticeably higher level of calcium deposition within sand pore space volume relative to further formation at sand surface and meniscus areas, while BEICP tended to realize a higher proportion of calcium deposition at sand contact points and adjacent meniscus zones.

- MICP produced a higher reduction in permeability, given the latter tendency towards higher pore space calcium deposition.

- Conversely, BEICP processing tended to have a lower impact on reducing permeability. This particular behavior may be viewed as a distinct benefit, where multiple treatment cycle applications would not be as prone to column clogging.

- This paper's observed correlation between sand grain size, levels of $CaCO_3$ precipitation, and distribution patterns for calcium deposition clustering were prominent factors in relation to strength and permeability outcomes.

- BEICP processing of fine-grained sands showed lower strength levels versus coarse grain sands in relation to product UCS strength when compared at similar levels of $CaCO_3$ precipitation. This pattern for BEICP is consistent with prior EICP publications as well as prior MICP publications.

Two recommendations for future research are warranted to secure further knowledge regarding the mechanisms and performance of BEICP processing:

- To specifically quantify protein mass levels when using extracted free-enzyme removed from viable ureolytic cells, as an enhanced means of completing a specific characterization of enzymatic reactions relative to chemical conversion efficiency, and

- To investigate the use of BEICP processing within complex, natural soil systems.

### 4.6 References

ASTM. (1996). "Standard test method for unconfined compressive strength index of chemical grouted soil." *ASTM D4219 - 08*, 1–6.

ASTM. (2006). "Standard test method for permeability of granular soils (constant head)." *ASTM D2434 – 68*, 68(Reapproved), 1–5.

ASTM. (2010). "Standard practice for classification of soils for engineering purposes (Unified Soil Classification System)." *ASTM D2487 – 10*, i, 1–12.

ASTM. (2014). "Standard specification for sand." *ASTM C778*, 1–3.

ASTM. (2015). "Standard test method for measurement of hydraulic conductivity of porous material using a rigid-wall, compaction-mold permeameter." *ASTM D5856 − 15*, i, 1–9.

Bernardi, D., Dejong, J. T., Montoya, B. M., and Martinez, B. C. (2014). "Bio-bricks: Biologically cemented sandstone bricks." *Construction and Building Materials*, Elsevier Ltd, 55, 462–469.

Burbank, M. B., Weaver, T. J., Green, T. L., Williams, B. C., and Crawford, R. L. (2011). "Precipitation of calcite by indigenous microorganisms to strengthen liquefiable soils." *Geomicrobiology Journal*, 28(February), 301–312.

Cheng, L., Cord-Ruwisch, R., and Shahin, M. A. (2012). "Cementation of sand soil by microbially induced calcite precipitation at various degrees of saturation." *Can. Geotech. J.*, 50, 81.

Cheng, L., Shahin, M. A., and Mujah, D. (2017). "Influence of key environmental conditions on microbially induced cementation for soil stabilization." *Journal of Geotechnical and Geoenvironmental Engineering*, 143(1), 04016083.

Choi, S.-G., Wang, K., and Chu, J. (2016a). "Properties of biocemented, fiber reinforced sand." *Construction and Building Materials*, Elsevier Ltd, 120, 623–629.

Choi, S. G., Chu, J., Brown, R. C., Wang, K., and Wen, Z. (2017). "Sustainable biocement production via microbially induced calcium carbonate precipitation: use of limestone and acetic acid derived from pyrolysis of lignocellulosic biomass." *ACS Sustainable Chemistry and Engineering*, 5(6), 5183–5190.

Choi, S., Wu, S., and Chu, J. (2016b). "Biocementation for sand using an eggshell as calcium source." *Journal of Geotechnical and Geoenvironmental Engineering*, 142(10), 2–5.

Chu, J., Stabnikov, V., and Ivanov, V. (2012). "Microbially induced calcium carbonate precipitation on surface or in the bulk of soil." *Geomicrobiology Journal*, 29(March), 544–549.

Chu, J., Varaksin, S., Klotz, U., and Menge, P. (2009). Construction processes. *Proceedings of the 17th International Conference on Soil Mechanics and Geotechnical Engineering: The Academia and Practice of Geotechnical Engineering*.

Cui, M. J., Zheng, J. J., Zhang, R. J., Lai, H. J., and Zhang, J. (2017). "Influence of cementation level on the strength behaviour of bio-cemented sand." *Acta Geotechnica*, Springer Berlin Heidelberg, 12(5), 971–986.

DeJong, J. T., Fritzges, M. B., and Nüsslein, K. (2006). "Microbially induced cementation to control sand response to undrained shear." *Journal of Geotechnical and Geoenvironmental Engineering*, 132(11), 1381–1392.

Dick, J., De Windt, W., De Graef, B., Saveyn, H., Van Der Meeren, P., De Belie, N., and Verstraete, W. (2006). "Bio-deposition of a calcium carbonate layer on degraded limestone by Bacillus species." *Biodegradation*, 17(4), 357–367.

Dilrukshi, R. A. N., Nakashima, K., and Kawasaki, S. (2018). "Soil improvement using plant-derived urease-induced calcium carbonate precipitation." *Soils and Foundations*, The Japanese Geotechnical Society, 1–17.

Dilrukshi, R. A. N., Watanabe, J., and Kawasaki, S. (2016). "Strengthening of sand cemented with Calcium Phosphate Compounds using Plant-derived Urease." *International Journal of Geomate*, Japan, 11(25), 2461–2467.

Faibish, R. S., Elimelech, M., and Cohen, Y. (1998). "Effect of interparticle electrostatic double layer interactions on permeate flux decline in crossflow membrane filtration of colloidal suspensions: An experimental investigation." *Journal of Colloid and Interface Science*, 204(1), 77–86.

Feng, K., and Montoya, B. M. (2015). "Influence of confinement and cementation level on the behavior of microbial-induced calcite precipitated sands under monotonic drained loading." *Journal of Geotechnical and Geoenvironmental Engineering*, 2, 1–9.

Foppen, J. W. A., and Schijven, J. F. (2006). "Evaluation of data from the literature on the transport and survival of Escherichia coli and thermotolerant coliforms in aquifers under saturated conditions." *Water Research*, 40(3), 401–426.

Ginn, T. R., Wood, B. D., Nelson, K. E., Scheibe, T. D., Murphy, E. M., and Clement, T. P. (2002). "Processes in microbial transport in the natural subsurface." *Advances in Water Resources*, 25(8–12), 1017–1042.

Gomez, M. G., Martinez, B. C., and Dejong, J. T. (2013). "Bio-mediated soil improvement field study to stabilize mine sands bio-mediated soil improvement field study to." *Geo Montreal 2013*, 1–8.

Gomez, M. G., Martinez, B. C., DeJong, J. T., Hunt, C. E., deVlaming, L. A., Major, D. W., and Dworatzek, S. M. (2015). "Field-scale bio-cementation tests to improve sands." *Proceedings of the Institution of Civil Engineers - Ground Improvement*, 168(3), 206–216.

Hamdan, N., and Kavazanjian, E. (2016). "Enzyme-induced carbonate mineral precipitation for fugitive dust control." *Géotechnique*, 66(7), 546–555.

Hamdan, N., Kavazanjian, J. E., and S., O. (2013). "Carbonate cementation via plant derived urease." *Proceedings of the 18th International Conference on Soil Mechanics and Geotechnical Engineering*, Paris 2013, 2489–2492.

Hamed Khodadadi, T., Kavazanjian, E., Paassen, L. Van, and Dejong, J. (2017). "Bio-grout materials : A review." *Grouting 2017*, (January 2018), 1–12.

Hoang, T., Alleman, J., Cetin, B., Ikuma, K., and Choi, S.-G. (2018). "Sand and silty-sand soil stabilization using bacterial enzyme induced calcite precipitation (BEICP)." *Canadian Geotechnical Journal*, 1–66.

Inagaki, Y., Tsukamoto, M., Mori, H., Sasaki, T., Soga, K., Qabany, A. A., and Hata, T. (2011). "The influence of injection conditions and soil types on soil improvement by microbial functions." *ASCE Geo-Frontiers*, 4021–4030.

Ivanov, V., and Chu, J. (2008). "Applications of microorganisms to geotechnical engineering for bioclogging and biocementation of soil in situ." *Reviews in Environmental Science and Biotechnology*, 7(2), 139–153.

Javadi, N., Khodadadi, H., Hamdan, N., and Kavazanjian, E. J. (2018). "EICP treatment of soil by using urease enzyme extracted from watermelon seeds." *ASCE IFCEE 2018*, 115–124.

Kavazanjian, E., and Hamdan, N. (2015). "Enzyme induced carbonate precipitation (EICP) columns for ground improvement." *Proc., ASCE IFCEE 2015*, M. Iskander, M. T. Suleiman, J. B. Anderson, and Debra F. Laefer, eds., ASCE, San Antonio, Texas, 2252–2261.

Kavazanjian, E. J., Almajed, A., and Hamdan, N. (2017). "Bio-inspired soil improvement using EICP soil columns and soil nails." *Grouting 2017 GSP*, 13–22.

Larsen, J., Poulsen, M., Lundgaard, T., and Agerbaek, M. (2008). "Plugging of fractures in chalk reservoirs by enzymatic-induced calcium carbonate precipitation." *SPE Production & Operations*, 23(4), 4–7.

Lin, H., Suleiman, M. T., Brown, D. G., and Kavazanjian, E. (2016). "Mechanical behavior of sands treated by microbially induced carbonate precipitation." *Journal of Geotechnical and Geoenvironmental Engineering*, 142(2), 04015066-1–13.

Martinez, B., and DeJong, J. T. (2009). "Bio-mediated soil improvement: load transfer mechanisms at the micro- and macro- Scales." *ASCE 2009 US-China Workshop on Ground Improvement Technologies*, 242–251.

Mitchell, J. K. (1981). "Soil improvement state of the art report." *XICSMFE*, 4.

Nam, I., Chon, C., Jung, K., and Choi, S. (2014). "Calcite precipitation by ureolytic plant ( Canavalia ensiformis ) extracts as effective biomaterials." *KSCE Journal of Civil Engineering*, 1–6.

Nemati, M., and Voordouw, G. (2003). "Modification of porous media permeability, using calcium carbonate produced enzymatically in situ." *Enzyme and Microbial Technology*, 33(5), 635–642.

Neupane, D., Yasuhara, H., Kinoshita, N., and Ando, Y. (2015a). "Distribution of mineralized carbonate and its quantification method in enzyme mediated calcite precipitation technique." *Soils and Foundations*, Elsevier, 55(2), 447–457.

Neupane, D., Yasuhara, H., Kinoshita, N., and Putra, H. (2015b). "Distribution of grout material within 1-m sand column in insitu calcite precipitation technique." *Soils and Foundations*, Elsevier, 55(6), 1512–1518.

Neupane, D., Yasuhara, H., Kinoshita, N., and Unno, T. (2013). "Applicability of enzymatic calcium carbonate precipitation as a soil-strengthening technique." *ASCE Journal of Geotechnical and Geoenvironmental Engineering*, 139(December), 2201–2211.

Oliveira, P. J. V., Freitas, L. D., and Carmona, J. P. S. F. (2016). "Effect of soil type on the enzymatic calcium carbonate precipitation process used for soil improvement." *Journal of Materials in Civil Engineering*, 29(4), 1–7.

van Paassen, L. A. (2011). "Bio-mediated ground improvement: from laboratory experiment to pilot applications." *ASCE Geo-Frontiers*, 4099–4108.

van Paassen, L. A., Ghose, R., van der Linden, T. J. M., van der Star, W. R. L., and van Loosdrecht, M. C. M. (2010a). "Quantifying biomediated ground improvement by ureolysis: large-scale biogrout experiment." *Journal of Geotechnical and Geoenvironmental Engineering*, 136(12), 1721–1728.

van Paassen, L. A., Van Loosdrecht, M. C. M., Pieron, M., Mulder, A., Ngan-Tillard, D. J. M., and Van Der Linden, T. J. M. (2010b). "Strength and deformation of biologically cemented sandstone." *Proc., Rock Engineering in Difficult Ground Conditions - Soft Rocks and Karst*, I. Vrkljan, ed., CRC Press, Cavtat, Croatia, 405–410.

Park, S.-S., Choi, S.-G., and Nam, I.-H. (2014). "Effect of microbially induced calcite precipitation on strength of cemented sand." *Journal of Materials in Civil Engineering*, 26(8), 47–56.

Putra, H., Yasuhara, H., and Kinoshita, N. (2017). "Applicability of natural zeolite for NH-Forms removal in enzyme-mediated calcite precipitation technique." *Geosciences*, (2).

Al Qabany, A., and Soga, K. (2013). "Effect of chemical treatment used in MICP on engineering properties of cemented soils." *Geotechnique,* 63(4), 331–339.

Al Qabany, A., Soga, K., and Santamarina, C. (2012). "Factors affecting efficiency of microbially induced calcite precipitation." *Journal of Geotechnical and Geoenvironmental Engineering*, 138(8), 992–1001.

Qian Zhao, Li, L., Li, C., Li, M., Amini, F., and Zhang, H. (2014). "Factors affecting improvement of engineering properties of MICP-treated soil catalyzed by bacteria and urease." *Journal of Materials in Civil Engineering*, 26(January), 1–10.

Rebata-Landa, V., and Santamarina, J. C. (2006). "Mechanical limits to microbial activity in deep sediments." *Geochemistry, Geophysics, Geosystems*, 7(11), 1–12.

Simatupang, M., and Okamura, M. (2017). "Liquefaction resistance of sand remediated with carbonate precipitation at different degrees of saturation during curing." *Soils and Foundations*, The Japanese Geotechnical Society.

Sondi, I., and Salopek-Sondi, B. (2005). "Influence of the primary structure of enzymes on the formation of CaCO 3 polymorphs: A comparison of plant (Canavalia ensiformis) and bacterial (Bacillus pasteurii) ureases." *Langmuir*, 21(19), 8876–8882.

van der Star, W. R. L., van Wijngaarden-van Rossum, W. K., van Paassen, L. A., and van Baalen, L. R. (2011). "Stabilization of gravel deposits using microorganisms." *Proceedings of the 15th European conference on Soil mechanics and Geotechnical engineering*, A. Anagnostopoulos, ed., IOS Press, 85–90.

Terashi, M., and Juran, I. (2000). "Ground Improvement – State of the Art." *ISRM International Symposium*.

Terzis, D., and Laloui, L. (2018). "3-D micro-architecture and mechanical response of soil cemented via microbial-induced calcite precipitation." *Scientific Reports*, Springer US, 8(1), 1–11.

Whiffin, V. S. (2004). "Microbial CaCO3 precipitation for the production of biocement." *Ph.D. dissertation, Murdoch University*, Australia.

Whiffin, V. S., van Paassen, L. A., and Harkes, M. P. (2007). "Microbial carbonate precipitation as a soil improvement technique." *Geomicrobiology Journal*, 24(February), 417–423.

Yasuhara, H., Neupane, D., Hayashi, K., and Okamura, M. (2012). "Experiments and predictions of physical properties of sand cemented by enzymatically-induced carbonate precipitation." *Soils and Foundations*, Elsevier, 52(3), 539–549.

# CHAPTER 5. EFFECT OF FREEZE AND THAW CYCLING ON UNCONFINED COMPRESSION STRENGTH OF BEICP-STABILIZED OF SANDY AND SILTY-SAND SOILS AND A COMPARISON TO CEMENT AND FLY ASH STABILIZED SOILS

*Tung Hoang, James Alleman, Bora Cetin (2018). "Effect of Freeze and Thaw Cycling on Unconfined Compression Strength of BEICP-stabilized of Sandy and Silty-sand Soils and A Comparison to Cement and Fly Ash Stabilized" Géotechnique (In preparation).*

## 5.1 Abstract

This paper addresses a soil biostabilization technique using bacterial extracted urease induced calcium carbonate precipitation as an alternative to previous conventional methods included microbial induced carbonate precipitation and plant-derived enzyme induced carbonate precipitation. The extracted urease enzyme of viable *S. pastuerii* was used as a biological source along with calcium chloride and urea to solidify sandy soil and silty sand soil. The bio-treated soil columns were subjected to freeze and thaw (F-T) cycling to evaluate their durability. Engineering properties of biocemented soil including unconfined compression strength (UCS), calcium carbonate content, moisture content, porosity, permeability, and microstructure were examined before and after the F-T durations. The increase in cycles of F-T caused a strength reduction of bio-treated soil. However, the UCS reduction rates of treated sandy soil were level off after 5 F-T cycles while those of biocemented silty sand soil significant decreased after 3 F-T cycles. The strength reduction of samples resulted from micro-cracked formed in calcium clusters and between bondings of sand-calcite. The higher $CaCO_3$ content samples performed the better F-T durability. The results revealed that the porosity, permeability, and fine content impacted to the capillarity water content which correlated to the strength reduction. In addition, a comparison with

conventional stabilizers including Portland cement and F class fly ash materials showed that the bacterial urease-treatment and the cement shared a similar F-T resistance while the fly ash did not improve the frost durability of soil.

## 5.2 Introduction

Engineered applications of ureolytic biomineralization has become popular in recent years. Use of urease in calcite ($CaCO_3$) precipitation for improving the engineering properties of soil is one of the potential engineering applications of bio-stabilization process (DeJong et al. 2006, 2010b; Ivanov and Chu 2008; Krajewska 2018; Neupane et al. 2013; van Paassen et al. 2010a; Phillips et al. 2013; Al Qabany and Soga 2013; Ran and Kawasaki 2016; Terzis and Laloui 2018; Whiffin et al. 2007). More recently, though, the biostabilization method has been included a suite of possible strategies, including: 1) microbial induced $CaCO_3$ precipitation (MICP), 2) enzyme induced $CaCO_3$ precipitation (EICP), and 3) microbial-induced desaturation and precipitation (MIDP). Both methods of MICP and EICP produce $CaCO_3$ precipitation via hydrolysis of urea (ureolysis) while the MIDP processing employs denitrification processing to generate biogas (for desaturation purpose) and induce calcium carbonate precipitation (for binding purpose) (Hamed Khodadadi et al. 2017). The MICP is the most common technique of ureolysis processing, which employs the precipitation of urease produced from bacterial cells with added urea/calcium agents (van Paassen 2009). The EICP method is using free enzyme for the catalytic reaction during the hydrolysis process of urea (Krajewska 2018).  Currently, most of the urease enzyme are plant-derived enzymes that are commercially available (Bang et al. 2009; Hamdan and Kavazanjian 2016b; Yasuhara et al. 2012). In addition, there are self-extracted enzymes from agricultural sources (Dilrukshi et al. 2018; Javadi et al. 2018; Nam et al. 2014). A newer urease-aided $CaCO_3$ mineralization, bacterial enzyme induced $CaCO_3$

precipitation (BEICP), has been introduced by Hoang et al. (2018). This study used nano-scale urease extracted from viable *S. pastuerii* to solidify sand and silty-sand soil. The results showed that the unconfined compressive strength (UCS) of BEICP-treated Ottawa sand (#20/30) were approximately 0.6 – 1.7 MPa depending on the number of treatment cycle while the UCS of BEICP-treated silty-sand soil ranged from 0.2 to 0.8 MPa. The research mentioned that the MICP method was unable to solidify a whole silty sand soil column (Hoang et al. 2018). The UCS ranges of BEICP-treated sandy soil were in line with previous studies of MICP- and EICP- treated sands at a similar concentration of reagents. For example, Al Qabany and Soga (2013) presented the UCS range of MICP-treated sand from 0.45 to 1.5 MPa at 0.25 M of urea and $CaCl_2$. Choi et al. (2016, 2017) reported that the strength of biocemented sand was from 0.23 to 1.7 MPa at 0.3 M of chemical argent. Yasuhara et al. (2012) employed plant-enzyme improved strength of sand to approximately 0.4 – 0.9 MPa at the level of 0.5 M cementation. Therefore, Hoang et al. (2018)'s results indicate that the BEICP method has a great potential to be used for stabilization of natural soils.

The engineering properties of bio-treated soil have been investigated more than a decade (Chu et al. 2013; DeJong et al. 2006; Hamdan and Kavazanjian 2016a; Safavizadeh et al. 2018; Whiffin et al. 2007) . However, studies on the effect of F-T cycles on the UCS of bio-treated soil have been limited, in particular with bio-stabilized silty-sand soils. A few studies investigated the impact of F-T cycles on strength of MICP-treated sand soils. Azadi et al. (2017), Blauw and Harkes (2013), and Cheng et al. (2012) mentioned that the UCS of MICP-treated sand decreased less than 10 % after F-T cycles. However,  Chen et al. (2016) showed approximately 50 % reduction of MICP strength after 3 F-T cycles. Cheng et al.

(2017) concluded that the MICP-treated of either finer sand or well-graded sand performed high durability with F-T testing.

The F-T cycling affects the strength of fine-grained soils due to the redistribution of the moisture in the soil matrix which occurs during thawing process (Kok and McCool 1990; Rosa et al. 2016). While previous studies showed that F-T cycles could be very detrimental to the strength characteristics of MICP treated sand, this could become more crucial for the soils with high fine-grained fractions. It is very well known that soils with fine-grained particles tend to be relatively more sensitive to frost actions (Dayioglu et al. 2017; Holtz and Kovacs 1981; Rosa et al. 2016). Currently, there is a limited information about the impact of F-T cycles on soils with fine-grained content that are treated with bio-stabilization techniques. Furthermore, only a few studies compared the F-T performance of bio-stabilized soils to those stabilized with conventional additives such as cement, class C fly ash, and lime (Cheng et al. 2012; DeJong et al. 2006).

The purpose of this study is to investigate the impact of F-T cycles on UCS of BEICP-treated sand and silty-sand soils and these results were compared to those stabilized with cement and class F fly ash. In addition to the UCS of specimens, their moisture, porosity and permeability of were evaluated after F-T cycles. The microstructural feature of samples was examined via scanning electron microscope (SEM) images to understand the changes on the soil morphology during F-T process.

### 5.3 Materials and Methods

### 5.3.1 Sand and Silty-sand Soil Materials

This study used Ottawa #20/30 silica standard sand for a coarse-grained soil and loess (silty) soil as a fine-grained soil. The following specimens were tested in the current study: 1)

100 % sand and 2) 80 % sand 20 % loess. The properties and grain size distribution curves of materials and soil mixtures were shown previously in Chapter 3 – Section 3.3.2.

The biological solution used for BEICP treatment is urease enzyme extracted from viable *S. pasteurii*. The process of bacteria cultivation and enzyme extraction were described previously in Chapter 3 – Section 3.3.1. A mixed chemical solution of urea and calcium had concentrations of 0.3 M by 1:1 ratio which was used for a cementation solution of BEICP treatment. Portland cement and class C fly ash materials were used as conventional stabilizers due to their ability to resist against frost action (Davidson and Associates 1961; Rosa et al. 2016).

Standard Type I/II Portland cement was used. It contains 90 – 95 % of Portland cement and other chemicals as gypsum (4 – 8 %), magnesium oxide (0.5 – 7 %), limestone (<5 %), flue dust (<3 %), and quartz (< 0.3 %) (Worth 2014). The initial moisture content of cement was 0.7%. Class F fly ash was used as another stabilizer in this study. The initial water content of class F fly ash was 0.1 %. Sieve and hydrometer analyses showed that fly ash contains 0 % gravel, 13.4 % sand, 84.3 % silt, and 2.3 % clay-sized particles. The components of F-class fly ash were showed in the x-ray diffraction (XRD) analysis (i.e., see Figure 5.1). Specific gravity of cement and class F fly ash were 3.12 and 2.47, respectively.
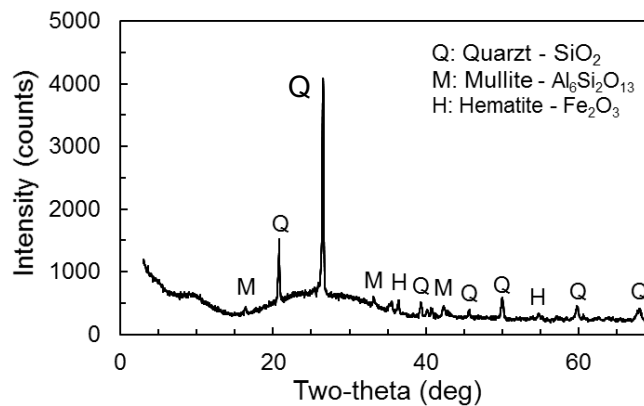


Figure 5.1 *XRD analysis of F class fly ash*

### 5.3.2 Soil Columns Preparation

Column specimens were packed in 10 cm of height and 5 cm of diameter PVC columns. A process of packing two soil mixtures was described previously in Chapter 3 – Section 3.3.3. The bio-stabilization circulation – percolation technique used in this study at variant cycles of treatment was shown in Table 5.1. The procedures for BEICP treatment were described in detail previously in Chapter 3 – Section 3.3.3. Soil-cement/fly ash specimens (column specimens) were packed to the same density as those packed for BEICP treatment to ensure that density of the specimens did not influence the F-T cycling performance comparison of each specimen.

Two separate soil mixtures were used to stabilize the sand and silty sand soils with cement and Class F fly ash. First, the oven sandy soil (100 % coarse grained – 0 % fine-grained) and silty sand soils (80 % coarse grained – 20 % fine-grained) were mixed uniformly with deionized (DI) water at approximately 5 % of moisture content (Choi et al. 2016a; Hoang et al. 2018). Then the cement/fly ash stabilizer was uniformly blended with soil. The proportion of stabilizers were 4 – 8 % and 5 – 15 % by weight for the Portland cement and fly ash, respectively. An additional water for Portland Cement/Fly Ash-soil mixtures was added to achieve approximately the final moisture content of 7 % to allow specimens to hydrate (Hansen 1986). The wet mixtures of soil-chemical stabilizers were poured and tamped gently into PVC molds (diameter: height – 5 : 10 cm) layer by layer. To ensure the uniformity and consistency with BEICP treated column preparation, each column had 10 layers with 10 mm of thickness per each layer. The weight of each layer of stabilized soil was adjusted to achieve approximately 0.6 of void ratio for the entire soil column. Finally, chemical stabilizer-soil columns were wrapped by plastic firms and cured at room temperature ($25 \pm 1$ ºC) for 7 days before performing other engineering tests. Detailed

information about all specimens were summarized in Table 5.1. It should be noted that the method of preparation for chemically stabilized soils used in this study was followed to form uniform and medium dense cemented specimens to compare biologically cemented soil specimens in the lab-scale experiments (DeJong et al. 2006). The other studies of cement/fly ash stabilized soil generally applied high compaction energy to pack very dense chemically stabilized soils.

### 5.3.3 Freeze and Thaw Cycling Process

Freezing and thawing tests were conducted in accordance with ASTM D560 and the reported procedure by Aldaood et al. (2016). Permeability tests were conducted on BEICP treated specimens before they are subjected to the F-T cycles. Permeability tests were not conducted on chemically stabilized soils. All specimens were fully saturated and placed on a pad that is soaked in water. Specimens were frozen at - $22 \pm 2$ °C during 24 hr and were thawed at room temperature ($25 \pm 1$°C) for 24 hr to complete a one-full F-T cycle. Specimens were subjected to 1, 3, 5, and 10 F-T cycles.

### 5.3.4 Testing Program

The testing program was summarized in Table 5.1 including treatment methods, types of soil mixtures, treatment levels, number of F-T cycles, number of specimens for engineering properties testing. Triplicates were conducted for each specimen for each test. For the BEICP treatment, soil specimens were treated with either 8- or 16- cycle for 100-0 soil mixture and either 12 – or 16-cycle for 80-20 soil mixture. Number of treatment cycles were selected based on Hoang et al. (2018). Specimens were mixed with 4 and 8 % Portland cement by weight. The sandy soil was mixed with 5 and 10 % fly ash while the silty sand soil was mixed with 10 and 15% fly ash by weight. The contents of chemical stabilizers selected herein were typically reported values in previous studies. All specimens were tested at

similar conditions and experiment routing to obtain comparable results. First, after treatments, the BEICP-treated samples were measured the permeability. Second, the PVC molds were removed to obtain the bio-soil columns for the porosity testing before they are subjected to UCS (for no F-T cycles) or F-T cycles. After curing period, the chemically stabilized soils were un-wrapped from the plastic molds, then subjected to compression strength tests (for 0 F-T cycles) and F-T experiments. Third, the UCS tests were performed with the stabilized samples after F-T cycling. Fourth, the broken parts of column after UCS test were conducted the moisture content test and $CaCO_3$ content test (for BEICP samples only). It should be noted that the specimens that were not subjected to 0 F-T cycles were sheared at dry condition.

The porosity of specimen is determined based on pore volume measurements in accordance with ASTM C830. A clean and oven dried sample was pre-weighted, saturated with a DI water of known density. The saturation process was applied a vacuum pressure at 207 kPa for 60 min. After saturation stage, the suspended weight and the saturated weight of sample were measured. The exterior volume and volume of open pores were calculated. The porosity expresses as a percentage the relationship of the volume of open pores in the test specimen to its exterior volume (ASTM C830). The porosity reduction was determined by subtraction of the initial porosity of the specimens from the final porosity (e.g. after treatment). Water content of each specimen was measured immediately after UCS test to prevent evaporation of moisture from samples. Test procedures for UCS and permeability tests, $CaCO_3$ content measurement technique, and SEM analyses were described in detail at Chapter 3 – Section 3.3.4.

Table 5.1 *Characteristics of testing specimens*

| Treatment method | Soil mixture | Treatment level | F-T cycle | | | | | Number of specimens for testing | | | | | |
|---|---|---|---|---|---|---|---|---|---|---|---|---|---|
| | | | 0 | 1 | 3 | 5 | 10 | UCS | Permeability | Porosity | Moisture | CaCO$_3$ | SEM |
| BEICP | 100- 0 | 8 cycles | x | | x | x | x | 12 | 12 | 12 | 9 | 12 | 3 |
| | | 16 cycles | x | | x | x | x | 12 | 12 | 12 | 9 | 12 | 3 |
| | 80 - 20 | 12 cycles | x | x | x | | | 9 | 9 | 9 | 6 | 9 | 3 |
| | | 16 cycles | x | x | x | | | 9 | 9 | 9 | 6 | 9 | 3 |
| Portland cement | 100 – 0 | 4 % | x | | x | x | x | 12 | N/A[a] | N/A | 9 | N/A | N/A |
| | | 8 % | x | | x | x | x | 12 | N/A | N/A | 9 | N/A | N/A |
| | 80 – 20 | 4 % | x | x | x | x | | 12 | N/A | N/A | 9 | N/A | N/A |
| | | 8 % | x | x | x | x | | 12 | N/A | N/A | 9 | N/A | N/A |
| Fly ash | 100 – 0 | 5 % | x | | x | x | x | 12 | N/A | N/A | 9 | N/A | N/A |
| | | 10 % | x | | x | x | x | 12 | N/A | N/A | 9 | N/A | N/A |
| | 80 – 20 | 10 % | x | x | x | x | | 12 | N/A | N/A | 9 | N/A | N/A |
| | | 15 % | x | x | x | x | | 12 | N/A | N/A | 9 | N/A | N/A |

Note: [a] not analyzed

## 5.4 Results and Discussion

### 5.4.1 UCS Reduction Due to F-T cycling

#### Sandy soil stabilization

The F-T cycling reduced the UCS and increased moisture content of sandy soil regardless of stabilization technique that was used (Figure 5.2). The UCS of BEICP-treated sandy soil lost its 21 – 24 % of original strength whereas those of cement-treated soil decreased 35 – 38 % after 3 F-T cycles for low and high level of treatment. The UCS reduction of bio-stabilized sandy soil remained nearly constant at 50 % loss after 5 F-T cycles for both level of treatment. On the other hand, while UCS of sandy soil stabilized with 8 % cement remained constant after 5 F-T cycles, an increase in UCS of the sandy soil stabilized with 4 % cement was observed after 5 F-T cycles. The average UCS of sand 4 % cement mixtures after 10 F-T cycles was 523 kPa which was higher than that of original treated specimen that was not subjected to any F-T cycles (e. g. 440 kPa). Although, the sandy soil stabilized with 8 % cement also experienced an increase in the UCS after being subjected to 10 F-T cycles than that of observed after 5 F-T cycles, the average UCS values were lower than that of original cement stabilized sand. In contrast to UCS reduction, the moisture content of specimens increased regardless of stabilization technique with an increase in the number of F-T cycles. The moisture content of each specimen leveled off almost after 5 F-T cycles. The variation trends of moisture content after F-T cycling were consistent with previous studies of chemically stabilization soil (Aldaood et al. 2014, 2016b; Solanki et al. 2013).

UCS reduction of BEICP-treated sand after F-T cycles was a result of formation of micro cracks inside of the soil specimens. During freezing, the water from below raised up to soil specimens due to capillary forces. Then, capillary water in soil expanded

during freezing and increased internal pressure within the soil specimen which resulted in breaking of bonding of grain – calcite – grain formation. However, the micro-cracks in this study could not be seen by naked eyes as reported by Aldaood et al. (2016), since the soil columns were gently tamped at high porosity (~37 %) while soil specimens in the past literature were compacted at high compaction energy to form very dense specimens. Therefore, the micro-cracks may have propagated in bonding of soil particles instead of on the surface of specimens. It is speculated that these micro-cracks may have affected the strength of treated soil specimens. Similar findings were also reported in Cheng et al. (2017).

The changing pattern of UCS correlated to moisture content at different F-T cycles. From 0 to 5 F-T cycles, the UCS of treated soil decreased steadily related to dramatically increasing of water content in soil samples. However, the data of UCS and moisture content were projected to have a constant trend from 5 to 10 cycles of F-T. The most likely causes of no UCS reduction after 5 and 10 F-T cycles were that the water content of specimens remained constant in treated soil samples during those F-T cycles. As expected, the change in water contents of specimens during F-T cycling affected the strength of stabilized sand soil.

This paper evaluated the effectiveness of frost action resistance of BEICP method compared to those traditional stabilizers (Portland cement and F class fly ash). The F fly ash-sand mixture columns provided very low average UCS at 0 F-T cycling and were broken apart after 1 F-T cycle for low and high level of treatment. On the contrary, other treatment methods (BEICP and Portland cement) provided higher strength and freeze-thaw durability. For comparison of strength improvement and F-T resistance capacity,

sandy soil samples were treated at low level, 8 cycles for BEICP and 4 % by weight for cement, and high level, 16 cycles of BEICP and 8 % of cement. As it is seen in low treatment levels (Figure 5.2a), the UCS and trend of strength reduction of sand soil were similar for both methods from 0 to 3 F-T cycles. From 3 to 10 F-T cycles, the UCS of BEICP-treated sand specimens had experienced a slight decrease and then stayed constant at 170 kPa, while that of cement-soil mixtures increased to 520 kPa. When the number of F-T cycles increased, it is speculated that an increase in UCS of cement stabilized specimens after certain F-T cycles may have been a result of cement hydration to be more dominant than the micro crack formation within the specimen. It should be noted that cement hydration continue during F-T process which were reported by Al-Assadi et al. (2010, 2015) Regarding the high treatment level (Figure 5.2b), the average UCS of BEICP-treated sand columns were approximately 50 % higher than those of cement-treated specimens. Figure 5.2b shows that similar UCS trends were observed for the sand soil specimens treated with higher treatment level to those treated with lower treatment level during same number of F-T cycles. The percentage of strength decrease of BEICP-treated sand after 5 and 10 F-T cycles in recent study were comparable to the results observed for MICP-treated sand after 4 and 10 F-T cycles reported by Cheng et al. (2017). Although the micro cracks may have reduced the strength of biostabilized sand, the calcite crystals formed at contact points which were able to maintain the strength of BEICP-treated sand after F-T cycling. A comparison of three soil stabilization method revealed the BEICP and the Portland cement methods could increase the F-T resistance of medium dense sand, while the F class fly ash treated sand was failed after 1 F-T cycle.

Figure 5.2 *Average of UCS versus moisture content of sandy soil stabilized at different cycles of F-T: (a) at low treatment level, (b) at high treatment level*

**Silty sand soil stabilization**

Cheng et al. (2017) found that the particle size distribution of sand influenced the F-T resistance of MICP-treated sand samples. The well-graded and finer sand were more durable against F-T cycles. However, the effects F-T cycling on bio-stabilized silty sand soil are still lacking in the ICP literature. The silty sand soil tested in the current study

contains silt and clay particles which could make any soil very sensitive to F-T cycling. This study conducted UCS tests on the silty sand samples treated by the BEICP, Portland, and F class fly ash materials that were subjected to different F-T cycles. The silty sand soil with 20 % silty loess soil was packed at medium dense condition (~ 37 % of porosity). Three stabilization methods were applied to solidify the soil columns at different treatment levels before applying F-T cycles.

Figure 5.3 shows that a correlation exists between the change in UCS and moisture content of stabilized specimens during F-T cycles. The BEICP-treated silty sand provided the highest UCS at 0 F-T cycling, approximately 1500 and 1800 kPa for 12 and 16 cycles of treatment, respectively. However, the specimens treated with 12- treatment cycle experienced a sharp drop in strength by losing 65 and 80 % of their initial UCS after 1 and 3 F-T cycles, respectively. The decline of UCS of these specimens after F-T cycles was a result micro-crack formation during F-T cycling. The specimens treated with 16-cycle experienced lower reduction rate with number of F-T cycles than those at 12-cycle. The UCS reduction of 16-cycle silty sand samples were 30 % after 1 F-T and 65 % after 3 F-T cycles. At high level of treatment, BEICP-treated silty sand soil was the least affected in terms of strength reduction from F-T cycling which is most probably due to the higher $CaCO_3$ content precipitated which provided more binding crystals in soil matrix (Hoang et al. 2018). The strength of bio-solidified silty sand had a steady fall after F-T cycling while the decrease in UCS of BEICP-treated sand was stable after 5 F-T cycles. A possible explanation for this could be that the BEICP-treated silty sand samples could have been suffered a large number of micro-cracks formed by expansion of free

water in void space and absorbed water on clay minerals. It can be seen in Figure 5.3 that the moisture content has been a gradually increased after each F-T cycle.

In addition, the BEICP-treated silty sand specimens had much higher UCS value than those stabilized with cement and fly ash. The F class fly ash soil mixture had the lowest strength after 0 and 1 F-T cycles and then were failed at the second cycle of F-T. Although the Portland cement samples had higher UCS than the F class fly ash soil mixtures, the F-T cycles caused significant reduction in UCS of specimens as expected. UCS of specimens decreased about 95 and 78 % after 5 F-T cycles for those stabilized with 4 and 8 % cement by weight, respectively. In addition, the average UCS of cement-silty sand specimens were much lower than those of the BEICP-treated specimens in both low and high level of treatments. The 7 days curing for cement stabilized specimens may not provide the adequate time hydration process for cement to be completed to achieve the maximum strength. For 1 and 3 F-T cycles, the water contents in the Portland cement soil samples were very high compared to the BEICP-treated silty sand which may have caused lower strength for cement stabilized specimens. Cheng et al (2012) found that the Portland cement sand was significantly affected by F-T cycles compared to the MICP-treated sand. Overall, it can be concluded that BEICP method was be able to increase the strength and durability of silty sand mixture against F-T cycling.

## 5.4.2 Observation of Failure Patterns of Stabilized Soil Columns Before and After F-T Durations

Figure 5.4 shows the failure modes of specimens before they are exposed to F-T cycling. Three unconfined compression tests were conducted sequentially in each treatment case in oven dried condition. Afterward, the broken specimens were

photographed at the end of the UCS test to observe the failure patterns. The side surface

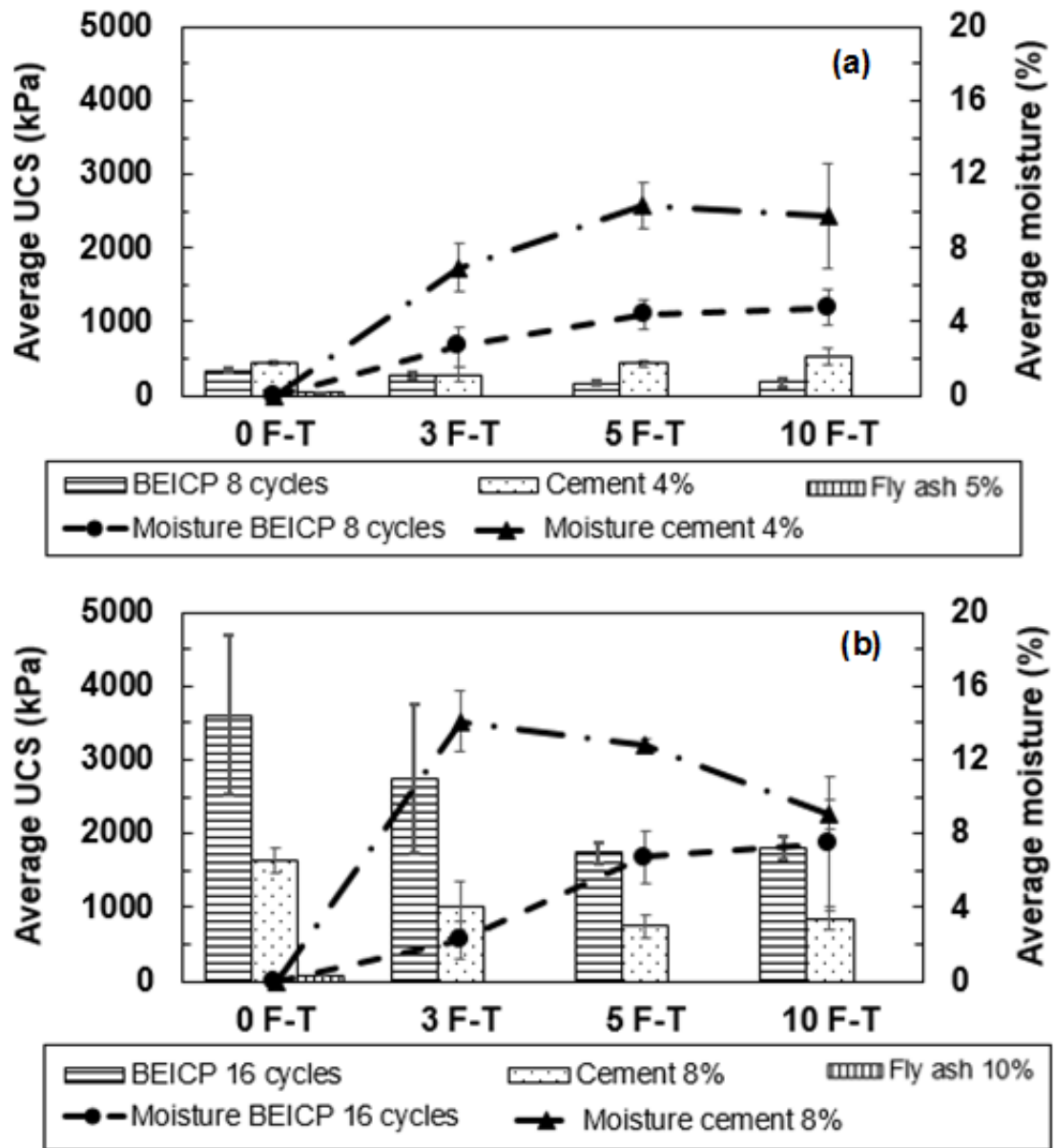of samples presented a uniform packing and treatment of soil columns.
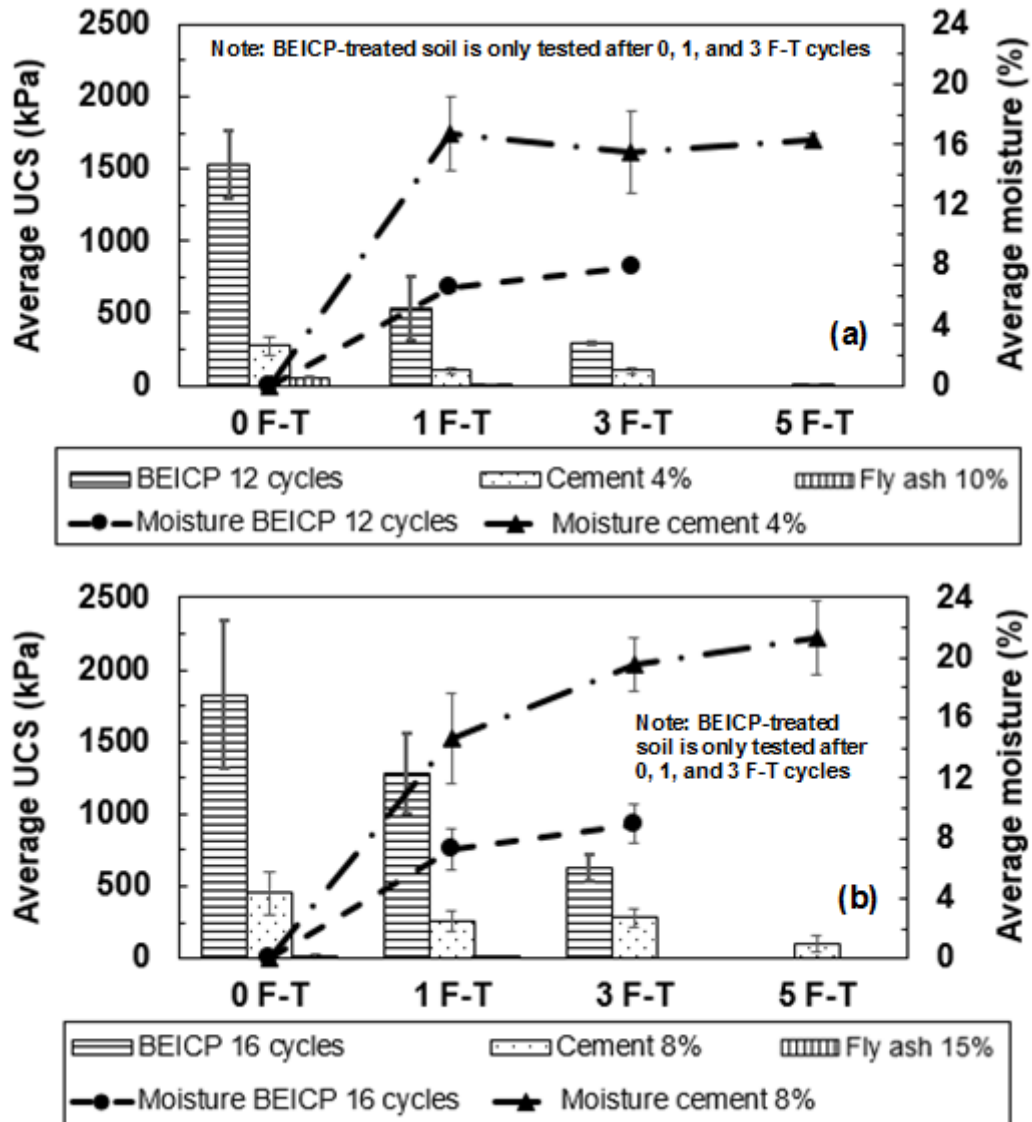


Figure 5.3 *Average of UCS versus moisture content of silty sand soil stabilized at different cycles of F-T: (a) at low treatment level, (b) at high treatment level*

Therefore, the cracks were formed from top to the bottom of compressed

specimens. This was a typical failure mode of solidified columns specimens under

uniaxial compression load. The top-bottom fractures of dry samples indicated that the

strength of specimens was improved uniformly from the top to the bottom part. It should

be noted that the BEICP-treated soil columns were solidified by gravity percolation method while the Portland cement and fly ash soil specimens formed strength by hydration of cement/fly ash materials during curing process.
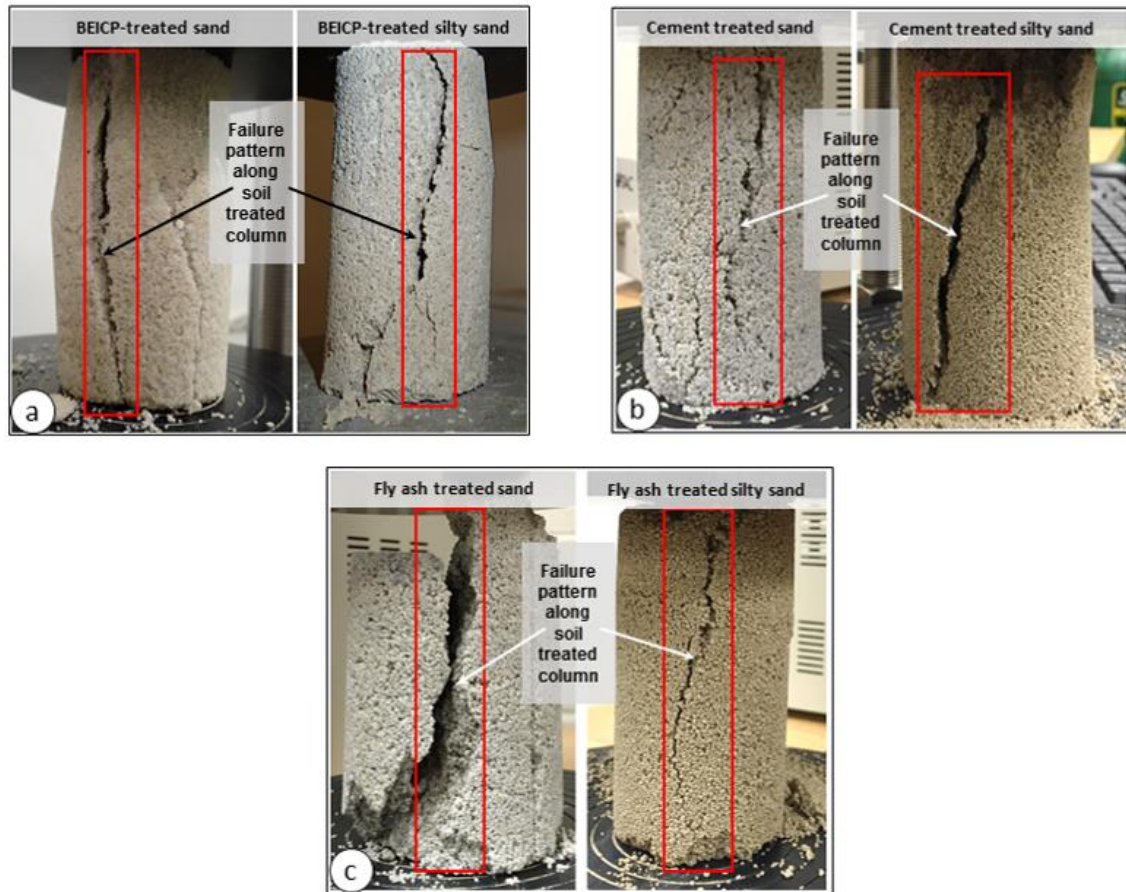


Figure 5.4 *Failure patterns of soil stabilization column under UCS test before F-T cycles (0 F-T): (a) BEICP-treated soil columns, (b) Portland cement treated soil columns, (c) F class fly ash treated soil columns*

Figure 5.5 shows the capillary water in treated soil columns and failure patterns of wet samples after different number F-T cycles. The water was sucked up into sandy soil and silty sand soil columns due to the capillary action. The height of water foot print in sandy soil was lower than those observed in silty sand soil. The reason for this was high silt/clay content of silty sand soil. It is very well known that finer grains (silt/clay particles) absorbs more water than sand grains (Sridharan and Nagaraj 1999). As

discussed in the previous sections, the higher water content in silty sand treated columns resulted in the steady decline of strength after F-T cycling. The capillary water mainly located at the lower part of soil specimen which affected strength of that portion of the specimens in particular. Figure 5.5 shows that the BEICP and cement treated soil columns split and failed at the bottom portion of the specimens after being subjected to F-T cycling. The fractures mainly accumulated at the location that contained high moisture footprint (dark color). The cracks were created at the bottom of the specimens due to low strength compared to the top portion of the specimen. The reduction of UCS in the bottom of the specimen was caused by micro-crack formation during F-T process. Additional picture of frozen water in Figure 5.5b confirmed that the lower portion of the specimen was damaged more than the upper portion of the soil specimen. However, there was no visible crack propagation and volume change in soil column after F-T cycling. It should be noted that the top and bottom portions of the specimens should have a similar strength in the dry condition as discussed previously. For the F class fly ash stabilizer, the soil fly ash mixture columns were broken apart after 1 F-T cycle for sandy soil and 2 F-T cycle for silty sand soil (Figure 5.5e). The existing of fines (silt/clay minerals) and water may have increased the strength of these mixtures to improve the durability of silty sand and fly ash mixture compared to sandy soil after the F-T cycling. However, the average UCS of fly ash soil columns were far lower than those of BEICP and cement treated soil (Figures 5.2 and 5.3). These results indicated that the BEICP treatment and the Portland cement material could solidify and improve the frost resistance of soils. However, the lower portion of the solidified soil columns experienced a significant damage during F-T cycling.
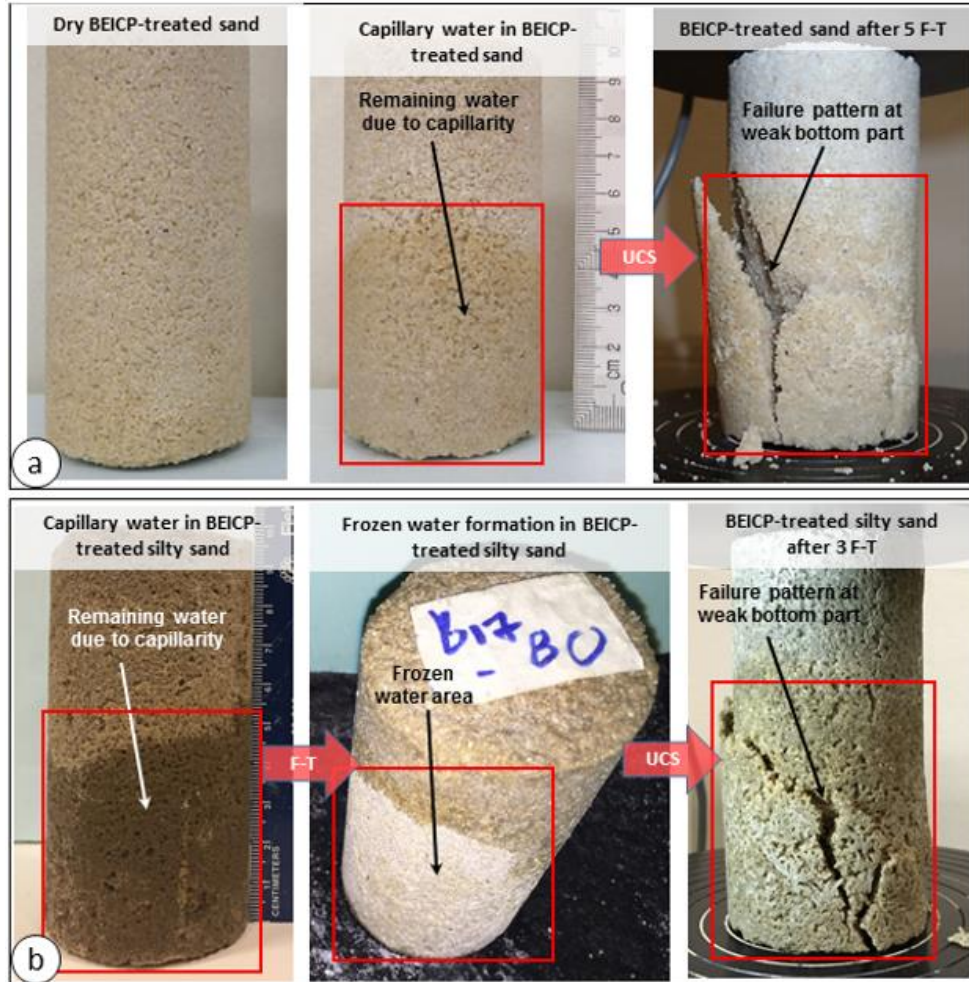
Figure 5.5 *Footprints of capillary water and failure patterns of soil stabilization column under UCS test after different F-T durations: (a) BEICP-treated sandy soil columns, (b) BEICP-treated silty sand soil columns*

### 5.4.3 Effect of $CaCO_3$ on Permeability and Porosity Reduction, and Relationship of $CaCO_3$ to UCS after F-T Cycling for BEICP-treated Soil

Cheng et al. (2012, 2017) mentioned that soil porosity, permeability and bonding

behavior ($CaCO_3$ precipitation) affected the F-T resistance of MICP-treated sand. In the

current study, the permeability and porosity of treated soil samples were measured by

using the constant head permeability test and fluid saturation with intact samples,

respectively. The acid rinse was used to determine the $CaCO_3$ content with small sub-

samples after unconfined compression test. Overall, the amount of calcium carbonate

precipitation affected the reduction of permeability, porosity and durability of BEICP-

treated sandy soils and silty sand soils.
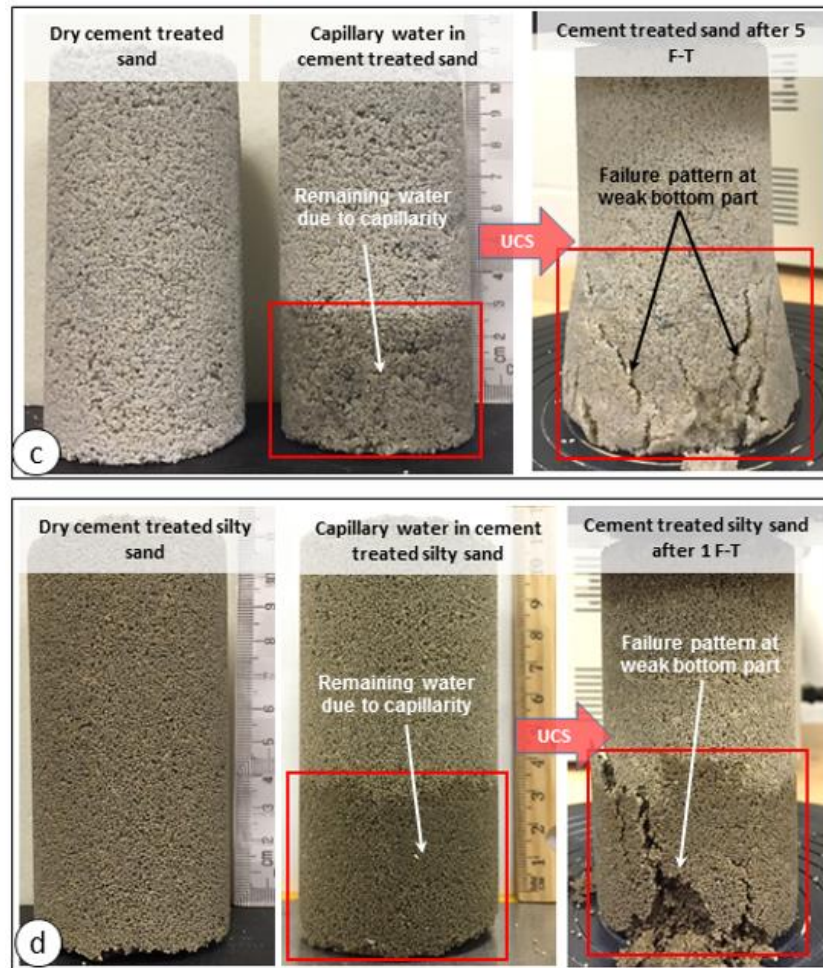


Figure 5.5 *(continued) (c) Portland cement treated sandy soil columns, (d) Portland cement treated silty sand soil columns*



Figure 5.5 *(continued) (e) F class fly ash treated silty sand soil columns*

**CaCO₃ precipitation *versus* permeability and porosity of bio-treated soil**

Figure 5.6 a and b shows the $CaCO_3$ effects on permeability and porosity of sandy soil and silty sand soil samples after BEICP treatment process, respectively. For sandy soil (Figure 5.6a), at low precipitation level of $CaCO_3$ (2 – 4 %) where those samples were solidified at 8 cycles of treatment, the permeability of the specimens reduced about 0.5-fold while the porosity reduction was approximately 4 %. At high precipitation level of $CaCO_3$ (8 – 12 %) where those samples were solidified at 16 cycles of treatment, the permeability decreased more than 1-fold while the average of porosity reduction was 7 – 8 %. The results of permeability correlated to $CaCO_3$ content were consistent with the data from previous study of Hoang et al. (2018) at 8 and 16 cycles of treatment. The results of porosity reduction in  this study were also in general agreement with previous data from Neupane et al. (2013) and Yasuhara et al. (2011) which investigated the reduction of porosity of EICP-treated sand. These studies mentioned that the porosity of EICP-treated sand matrix decreased approximately 1 and 4 % at 1 and 4 times of injection, respectively. The reduction of permeability and porosity in bio-stabilized sand sample was a consequence of accumulation of calcium carbonate precipitation at pore volume of sand matrix (Cheng et al. 2013; Hoang et al. 2018; Al Qabany and Soga 2013). Figure 5.6a presents a similar reduction rate of permeability and porosity in BEICP-treated sand. The high-level bio-treatment specimens had significantly lower permeability and porosity than those treated at low level treatment cycles. The lower porosity of the materials could result in higher capillarity water absorption potential. In addition, the lower permeability was able to remain more water during the thawing process which could result in higher water content as observed for the sand soil treated with 16-cycle.

The sand treated with 16-cycle had higher moisture content than that of treated with 8-cycle (Figure 5.2).

CaCO$_3$ contents of silty sand treated with 12 and 16 cycles were not significantly different from each other. The average of calcium carbonate contents of BEICP-treated silty sand at 12- and 16- cycle was 10.5 and 13.5 %, respectively. These values were higher than those reported in bio-treated sand literature. The permeability of BEICP treated silty sand specimens reduced more than 2-fold whereas the porosity decreased approximately 8 – 13 %. The relationship between CaCO$_3$ content and permeability were in line with the data from Hoang et al. (2018). A comparison of the two results of sandy soil and silty sand soil treated by BEICP, it can be concluded that the permeability and porosity of treated silty sand samples were significantly lower than that of treated sand. The result therefore indicated that a lower porosity and permeability plus higher fine content in bio-treated silty sand soil could have resulted in a higher water content compared to BEICP-treated sand (Figures 5.2 and 5.3).

**CaCO$_3$ *versus* UCS after F-T cycling**

Figure 5.7 shows the relationship between UCS and CaCO$_3$ precipitation for sandy soil and silty sand soil. For both treated soils, the UCS improvement resulted from an increase in the CaCO$_3$ content. It can be seen in Figure 5.7a, the results of treated sandy soil were distributed in two different zones in the plot which was a similar relationship between permeability and CaCO$_3$ content in Figure 5.7a. Results indicated that 16-cycle of treatment could significantly improve the strength of sandy soil by producing higher content of CaCO$_3$at contact points of sand grains (Cheng et al. 2012; Cui et al. 2017; Hoang et al. 2018). After F-T durations, although Figure 5.2 showed the

similar UCS reduction rates for both 8- and 16-cycle BEICP sands, Figure 5.7a presented

that the residual strength of 16-cycle treated samples were much higher than those treated

with 8-cycle treatment.
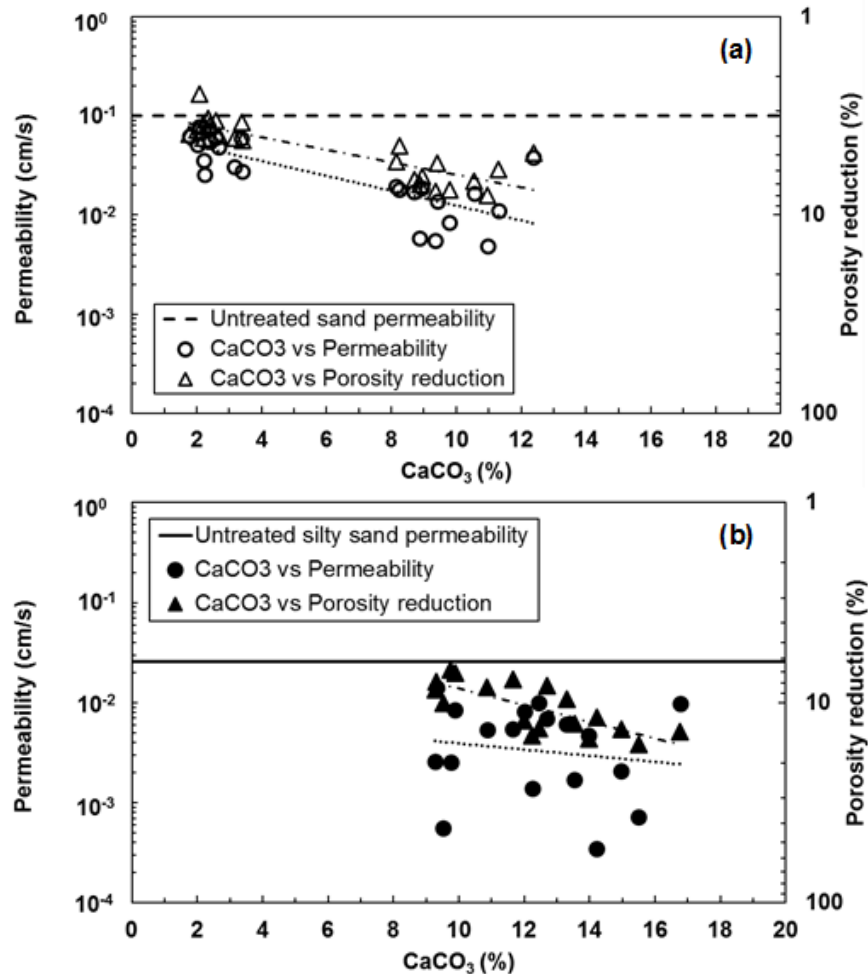


Figure 5.6 *Effect of CaCO₃ precipitation on permeability and porosity reduction of BEICP-treated soil: (a) BEICP-treated sandy soil, (b) BEICP-treated silty sand soil*

On the other hand, the BEICP-treated silty sand soil did not have a distinctive

UCS and CaCO₃ ranges between 12- and 16-cycle of treatment (Figure 5.7b). A similar

behavior was observed in the relationship between CaCO₃, permeability and porosity in

Figure 5.6b. To compare with sandy soil, although the calcium carbonate content was

higher in silty sand soil, the UCS data before and after F-T cycling were much lower than

those observed in BEICP-treated sandy soil. The BEICP-treated sand specimens

contained lower water content (Figures 5.2 and 5.3) and higher porosity (Figure 5.6)

which can be more effect of frost resistance. Therefore, the BEICP treatment method

could be better to increase the F-T resistance of sandy soil.
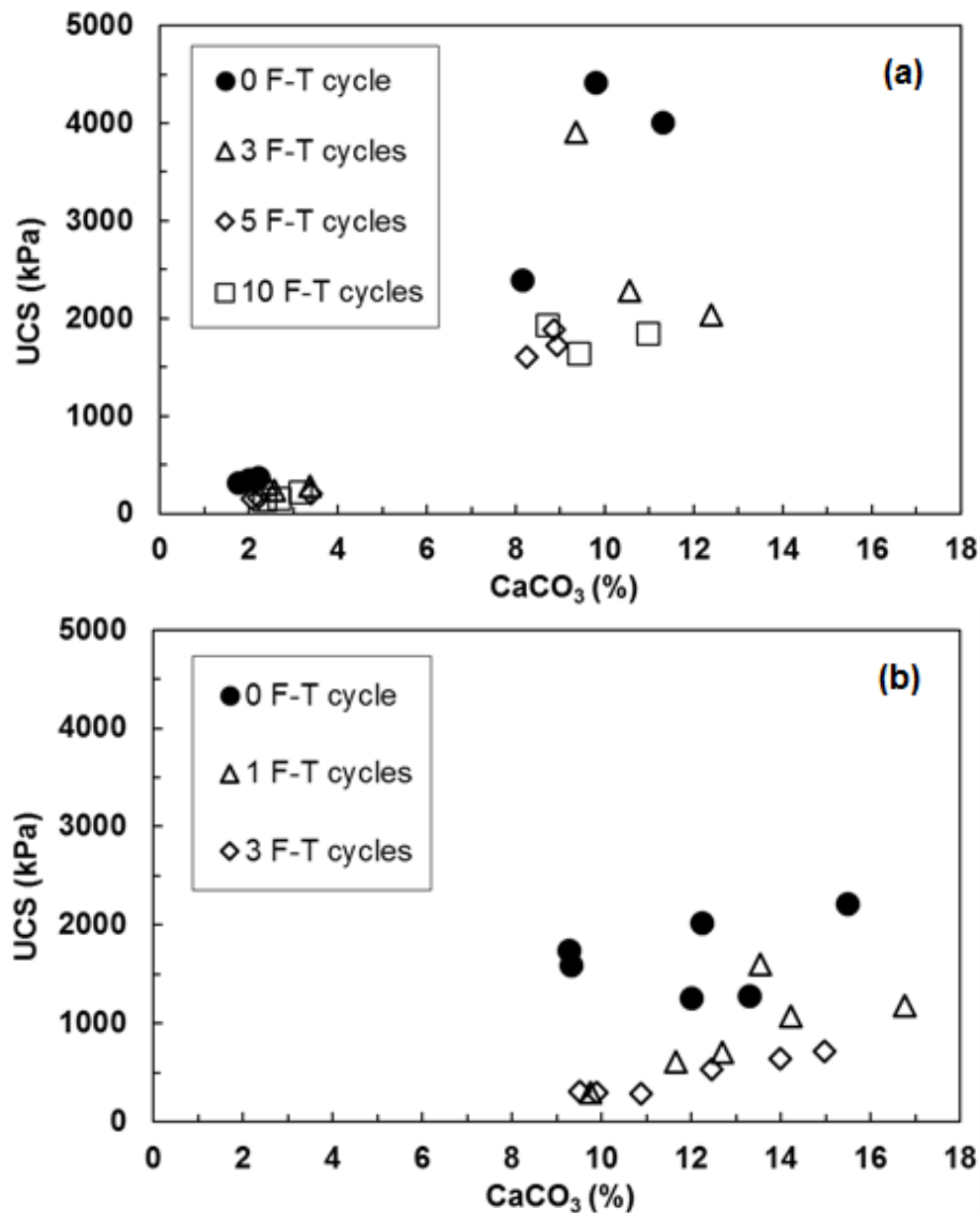


Figure 5.7 *Effect of F-T cycles on UCS of different soil mixture treated with different amounts of BEICP: (a) sandy soil, (b) silty sand soil*

**5.4.4 Micro-crack Analyses of BEICP-Treated Soil After F-T durations**

The main purpose of this work was to observe and evaluate the possible formation of micro-cracks which may have developed with biocemented samples following F-T cycling. Therefore, the BEICP-treated samples, both with and without F-T cycling, were examined at a microstructural-level using SEM imaging. All biocemented soil specimens were collected and prepared carefully under similar conditions to negate the possible formation any micro-cracking simply due to sample preparation procedures. Small pieces of samples were then collected immediately after UCS test. These samples were then tested in an 'as-is' mode, without subsequent surface refinement (e.g., using filing and coating steps). A vacuum pressure of 80 kPa was applied inside the SEM chamber for all specimens during images taking process, at which no prior cracking behavior would have been expected. Lastly, the SEM staff operator randomly chose points of observation and image scanning, in a fashion where these results were not biased towards desired observation outcomes.

**BEICP-treated sandy soil**

Figure 5.8 shows a series of SEM images for BEICP-treated sand after 8 and 16 cycles of treatment. These images presented the damage of sample at micro-scale after the F-T cycling which in turn led to the decrease in strength of BEICP-treated sands as discussed previously. The SEM images were taken after different cycles of F-T and at the outer diameter surface and at the fracture surface. These images were used to analyze and compare the propagation of micro cracks in solidified specimens. Figures 5.8 a & j showed the SEM images of fracture surface samples before F -T cycling  for BEICP 8- and 16-cycle of treatment, respectively. There was no micro-crack in calcite clusters or

broken bonding at contact points. However, comparing those two images and the other SEM images after F-T cycling showed that the formation of visible micro-cracks was propagated at the surfaces of outer diameter and fracture of samples. It should be noticed that no visible crack was observed on surfaces of samples after F-T cycling (Figure 5.5). As discussed previously, the SEM samples with and without F-T cycling were prepared under similar conditions. Therefore, a reasonable conclusion regarding the observed of micro-cracks being created during F-T cycling was that these changes are real and not the result of any sample preparation steps.

The formation of micro-cracks was caused by expansion pressure generated by increase in volume of capillary water. The expansion volume of capillary water may have followed sequential steps. First, the water was moved up from the saturated felt pad to the BEICP-treated sand specimens due to capillary action. Second, when the sand specimens were subjected to the frozen temperature ($-22\ ^{o}C$), the water within the voids froze. Third, the frozen water in pore spaces expanded the volume which applied pressure on the pore walls. If the required volume for expanded water was larger than the available void spaces in the treated sand matrix, the expansion pressure could break the calcite clusters and the bonding of sand and calcite. This resulted in the formation of micro-cracks in the calcite clusters or between sand grains and calcite crystals.

When the F-T cycling was repeated, the increase in water content caused more micro-cracks formation to lead more damage to the bio-stabilized sand. Figure 5.2 shows the steady UCS reduction correlated to the moisture content increasing from 3 to 5 F-T cycles. In addition, when the F-T durations were repeated, the water filled into newly formed micro-cracks at the thawing period which could have enlarged existing micro-

cracks. Comparing SEM images between 3 and 10 F-T cycles as shown in Figures 5.8 c –
f & 5.8 i – m indicate that the number and size of micro-cracks increase in specimens at
high numbers of F-T cycles. Thus, the micro-cracks and their quantity and size were
major factors in UCS reduction of BEICP-treated sand specimens. The strength of sand
treated specimens at the high number of F-T cycles with higher moisture content was
lower than that of sand columns at low number F-T cycles with lower water content.
However, when the water content was constant, the expansion pore spaces would no
longer be required which did not cause any new micro-cracks to be developed in sand
matrix. Therefore, the Figure 5.2 presents that the rate of UCS reduction becomes stable
as water content remains constant from 5 to 10 F-T cycles.

Another significant aspect of pore capillary water is the location of expansion
water. The study investigated the SEM images taken at two surfaces in samples. The first
SEM location was at the outer diameter surface where had one free space contacted to
atmosphere (see Figures 5.8 b & h). The second SEM location was at the fracture surface
inside the specimen where had a confined space during F-T cycling (see Figures 5.8 c – f
& 5.8 i – m). It should be noted that the fracture surface was obtained after the UCS test.
It can be seen in Figures 5.8 b & h, there were few micro-cracks formed at outer diameter
surfaces after 10 F-T cycles in BEICP-treated sand 8- and 16- cycles of treatment,
respectively. However, there were more and large size of micro-cracks generated at
fracture surfaces after 3 and 10 cycles of F-T. From previous discussion, the expansion
pressure caused by expanded water volume created micro-cracks in calcite clusters. The
pore water at outer diameter surface had one free space for expanding volume without
resistance while the water inside the core of specimen were confined by sand grains,

calcite clusters. When the specimen was subjected to freezing temperature, the frozen water at outer diameter surface can expand out to the free space which may have reduced the pressure on sand particles and calcite crystals. On the contrary, the sand grains and $CaCO_3$ around pore water must be sustained all expansion pressure from frozen water. Therefore, it was clear that, the fracture surfaces inside sand column were suffered more cracking, as expected. An observation during unconfined compression test showed that the fracture appeared at the center of bottom end first, then propagated to the upper side as a splitting failure pattern (Figure 5.5).

A comparison of the two series of SEM images as Figures 5.8 c – f & 5.8 i – m revealed that BEICP-treated 16-cycle specimens had high number of micro-cracks with larger width of than those observed in the ones treated with 8-cycle. In theory, higher porosity and permeability, better the F-T resistance. As can be seen in Figure 5.6a, sand treated with low level treatment cycles have higher porosity and permeability than those of treated with high level of treatment cycle. The 16-cycle BEICP-treated sand specimens had low porosity which caused higher capillarity force. In addition, the lower permeability of specimen treated with 16-cycle could slow down the water evaporation process during thawing process. Therefore, the specimens with lower porosity and permeability (i.e. 16-cycle treatment sand) could retain more capillary water after the F-T cycling. The high volume of capillarity water and low pore space sand may have caused high number and large sizes of micro-cracks in the specimens treated with 16-cycle treatment. Although the microstructural analysis revealed that the specimens treated with 16-cycle BEICP-treated sand had more micro-cracks failure, the UCS reduction rates between sand treated with low and high level of BEICP treatments were similar after F-T

cycles. Cheng et al. (2016) mentioned that more $CaCO_3$ precipitated at the contact points of sand grains which caused higher durability due to reduction of the acting tensile stress per particle contact. Figure 5.7a shows that the $CaCO_3$ content in the 16-cycle treatment sand columns was significantly higher than that of in the 8-cycle treated specimens. Therefore, the specimens treated with 16-cycle BEICP treatment had higher durability in spite of higher amount of micro-damage. These results showed that to obtain higher residual strength after F-T cycling, the sandy soil should be solidified at high level of BEICP treatment.

### BEICP-treated silty sand soil

Figure 5.9 presents a series of SEM images of silty sand soil solidified by BEICP method after different numbers of F-T cycles. Figures 9 a – c show SEM images of 12-cycle treatment specimens after 0 and 1 F-T cycle while the images of 16-cycle treatment columns after 0 and 3 F-T cycles are displayed in Figures 5.9 d – f. All these SEM images were taken at the fracture surfaces of soil columns. At before F-T cycling (i.e. 0 cycle) (Figure 5.9 a and d), there was no micro-cracks existed in both levels of BEICP treatment. However, after the first F-T cycle, many micro-crack appeared in calcite clusters of 12-cycle treatment specimens (Figures 9 b & c). The micro-cracks were continuously propagated and enlarged when the number F-T cycles increased. Figures 5.9 e & f show the larger size of micro-cracks after 3 F-T cycles compared to those after 1 F-T cycles as shown in Figures 5.9 b & c. In addition, a broken bonding between sand particle and calcite crystal is observed in Figure 5.9c.
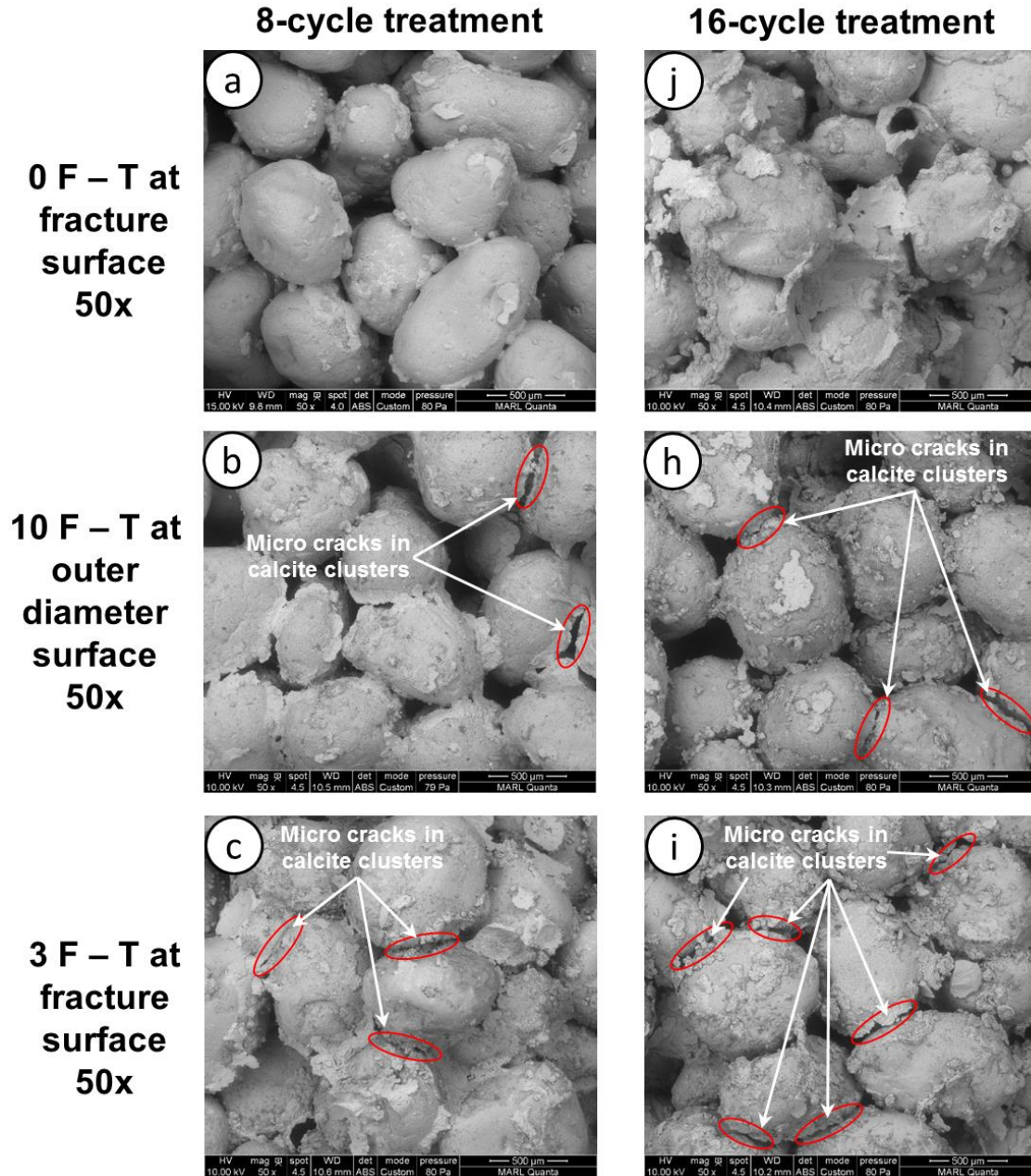
Figure 5.8 SEM images of BEICP-treated sand samples: (a – c) 8-cycle of treatment, (j – i) 16-cycle of treatment
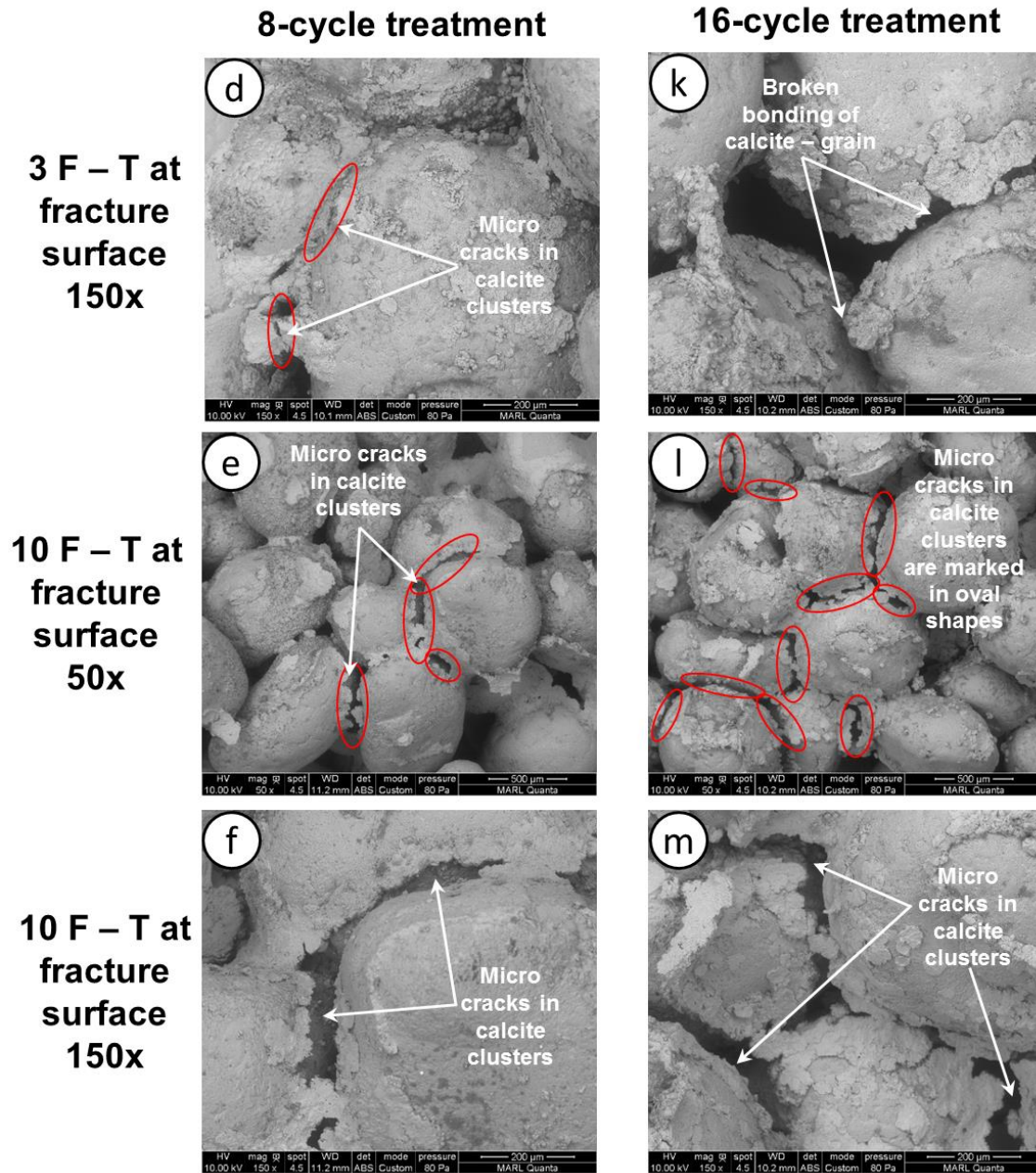
Figure 5.8 *(continue) SEM images of BEICP-treated sand samples: (d – f) 8-cycle of treatment, (k – m) 16-cycle of treatment*

The serious damage displayed in microstructural analysis correlated to a steady reduction of UCS in BEICP-treated silty sand specimen (Figure 5.3). The contribution of the water content on the durability of BEICP-treated silty sand specimens after F-T cycles may be attributed to the several phenomena:

1. Water expansion pressure: the pressure acted on the treated specimens could have been caused by two types of expanded water pressure. As discussed in the previous section, the water existed in the pores of soil matrix results from capillarity action. Another water retained in silty sand soil is absorbed water which wraps around fine particles contained clay minerals. The clay mineral is able to absorb an extremely high volume of water compared to their size. Those types of water expanded the volume due to freezing period which applied the pushing forces on the soil structure to create micro-cracks in the calcite clusters and between soil grains and calcite crystals. The repeated F-T process may cause more micro-crack damage to soil which ultimately decreased the strength.

2. Osmotic flow pressure: the osmotic flow occurs in soil matrix containing clay particles. When the soil samples were subjected to low temperature, the frozen water was formed in the void spaces. It can be assumed that the clay minerals will locate in the non-frozen water near to the pore walls. The clay minerals may have caused a process of re-establishing the equilibrium with the environment by moving non-frozen water towards pore spaces contained ice water, as the osmotic flow progress. The migration of osmotic flow is able to apply pressure on soil matrix to propagate the micro-cracks.

3. Calcite crystal formation pressure: during F-T cycling, the water content was a favored condition for a bio-chemical reaction between residual enzyme and cementation solution to form new calcite crystals. The growth of new calcite crystals could have increased the pressure on soil matrix. Because of lacking

evidences in the current study, the future work should therefore investigate the

growth of calcite crystals during F-T cycling process.
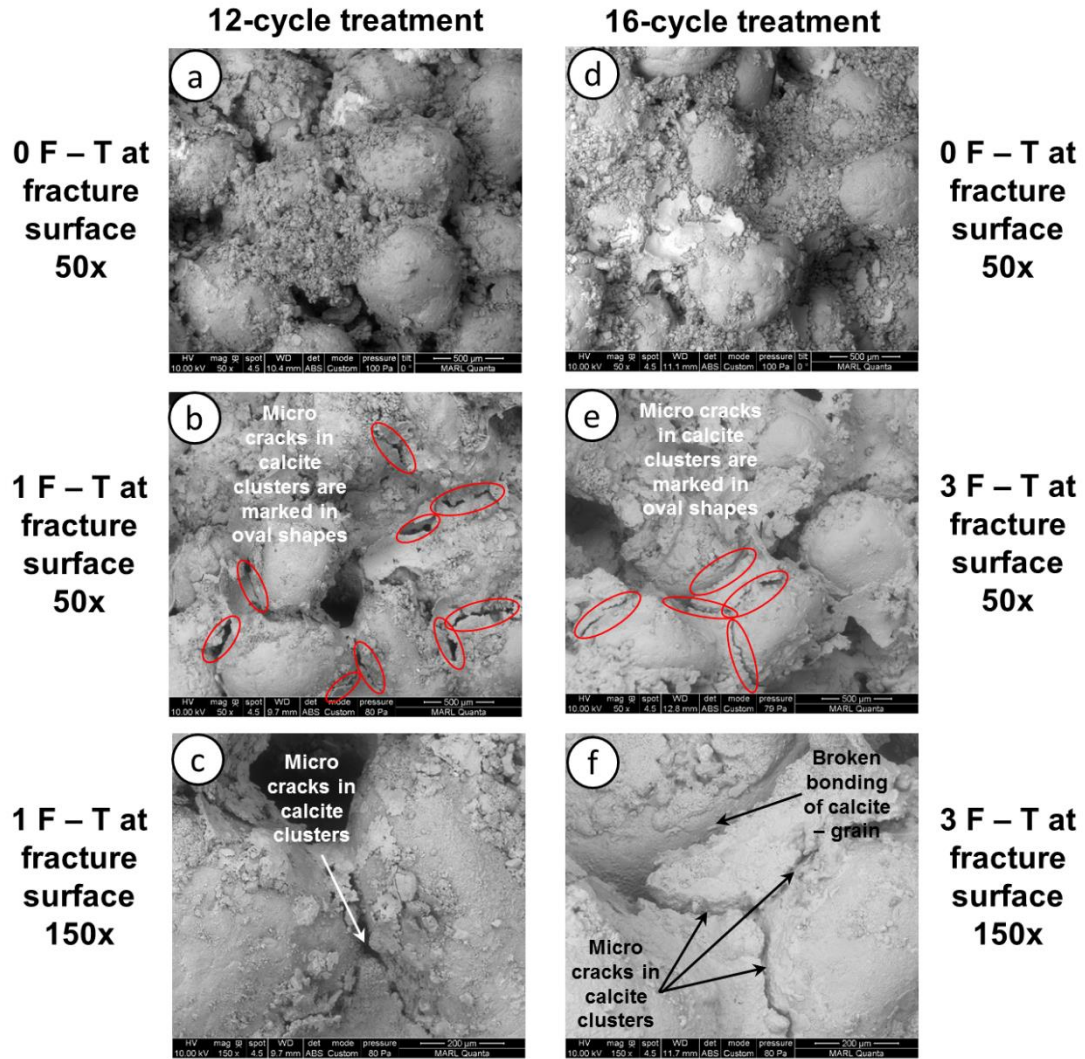


Figure 5.9 *SEM images of BEICP-treated silty sand samples (a – c) 12-cycle of treatment, (d – f) 16-cycle of treatment*

### 5.5 Conclusions

In this investigation the aim was to assess F-T durability of BEICP-treated

medium dense soil. The result of this study showed that BEICP method could improve

the F-T durability of soil. The UCS reduction of BEICP-treated sand remained constant

after 5 F-T durations while those of treated silty sand samples steadily reduced after 3 F-

T cycles. A comparison with other traditional stabilizers as the Portland cement and F class fly ash revealed that BEICP method and cement shared a similar F-T resistance for both types of soil. However, the F class fly ash could not have increased the F-T durability of medium dense soil.

The factors affected the F-T resistance of treated soil have been studied in the current study. The $CaCO_3$ content was a main factor to improve the strength and durability of bio-treated soil. The heavier treatment of the specimens with the high calcium carbonate content could have provided higher residual strength after the F-T cycling. However, the F-T resistance of the treated soil was contributed by other factor as well such as water content, porosity and permeability. The findings showed that the high volume of capillarity water significantly reduced the strength of soil due to the formation of micro-cracks. The higher porosity and permeability of soils resulted in low capillary force and allowed more rapid water drainage in the soil matrix, which could increase the F-T resistance.

SEM analysis showed that the micro cracks after F-T cycling process was located in calcite clusters and between sand grains and calcite crystals. The micro-damage in bio-treated soil specimens after F-T cycling has not been shown in the previous MICP or EICP studies. The micro-cracks observed in soil matrix supported the empirical results of the UCS reduction. It indicated that the expansion capillarity water caused micro-cracks which decreased the strength of stabilization soil after F-T cycles.

An implication of these findings was that BEICP method could improve the strength and F-T durability of soil, particular in sandy soil. Such engineering application

could be useful for soil improvement at cold regions where the F-T cycling significantly

impacts the soil engineering properties.

## 5.6 References

Al-Assadi, G., Casati, M. J., Fernandez, J., and Galvez, J. C. (2010). "Effect of the curing conditions of concrete on the behaviour under freeze – thaw cycles." *Fatigue & Fracture of Engineering Materials & Structures*, (34), 461–469.

Al-Assadi, G., Casati, M. J., Gálvez, J. C., Fernández, J., and Aparicio, S. (2015). "The influence of the curing conditions of concrete on durability after freeze-thaw accelerated testing." *Materiales de Construcción*, 65(320), 1–21.

Aldaood, A., Bouasker, M., and Al-mukhtar, M. (2014). "Impact of freeze – thaw cycles on mechanical behaviour of lime stabilized gypseous soils." *Cold Regions Science and Technology*, Elsevier B.V., 99, 38–45.

Aldaood, A., Bouasker, M., and Al-Mukhtar, M. (2016a). "Effect of water during freeze-thaw cycles on the performance and durability of lime-treated gypseous soil." *Cold Regions Science and Technology*, Elsevier B.V., 123, 155–163.

ASTM. (2015a). "Standard test methods for freezing and thawing compacted soil-cement mixtures." *ASTM D560-96*, i, 1–6.

ASTM. (2015b). "Standard test methods for apparent porosity, water absorption, apparent specific gravity, and bulk density of burned refractory brick and shapes by vacuum pressure." *ASTM C830 − 00*, 00(Reapproved 2015), 1–3.

Azadi, M., Ghayoomi, M., Shamskia, N., and Kalantari, H. (2017). "Physical and mechanical properties of reconstructed bio-cemented sand." *Soils and Foundations*, The Japanese Geotechnical Society, 57(5), 698–706.

Bang, S. S., Bang, S. S., Frutiger, S., Nehl, L. M., and Comes, B. L. (2009). "Application of novel biological technique in dust suppression." *Proc., Transportation Research Board 88th Annual Meeting*, Transportation Research Board (CD-ROM), Washington, DC, USA, DC, USA, 6–7.

Blauw, M., and Harkes, M. (2013). Biotechnological strengthening of flood embankments.

Chen, F., Deng, C., Song, W., Zhang, D., Al-, F. A., Mortuza, M. G., Gadd, G. M., and Pan, X. (2016). "Biostabilization of desert sands using bacterially induced calcite precipitation biostabilization of desert sands using bacterially induced calcite precipitation." *Geomicrobiology Journal*, 0451(February), 243–249.

Cheng, L., Cord-Ruwisch, R., and Shahin, M. A. (2012). "Cementation of sand soil by microbially induced calcite precipitation at various degrees of saturation." *Can. Geotech*. J., 50, 81.

Cheng, L., Shahin, M. A., and Mujah, D. (2017). "Influence of key environmental conditions on microbially induced cementation for soil stabilization." Journal of Geotechnical and Geoenvironmental Engineering, 143(1), 04016083.

Choi, S.-G., Wang, K., and Chu, J. (2016). "Properties of biocemented, fiber reinforced sand." *Construction and Building Materials*, Elsevier Ltd, 120, 623–629.

Choi, S. G., Chu, J., Brown, R. C., Wang, K., and Wen, Z. (2017). "Sustainable biocement production via microbially induced calcium carbonate precipitation: use of limestone and acetic acid derived from pyrolysis of lignocellulosic biomass." *ACS Sustainable Chemistry and Engineering*, 5(6), 5183–5190.

Chu, J., Stabnikov, V., Ivanov, V., and Li, B. (2013). "Microbial method for construction of an aquaculture pond in sand." *Géotechnique*, (10), 1–5.

Cui, M. J., Zheng, J. J., Zhang, R. J., Lai, H. J., and Zhang, J. (2017). "Influence of cementation level on the strength behaviour of bio-cemented sand." *Acta Geotechnica*, Springer Berlin Heidelberg, 12(5), 971–986.

Davidson, D. T., and Associates. (1961). Soil stabilization with cement. Ames, Iowa.

Dayioglu, M., Cetin, B., and Nam, S. (2017). "Stabilization of expansive Belle Fourche shale clay with different chemical additives." *Applied Clay Science*, Elsevier, 146(January), 56–69.

DeJong, J. T., Fritzges, M. B., and Nüsslein, K. (2006). "Microbially induced cementation to control sand response to undrained shear." *Journal of Geotechnical and Geoenvironmental Engineering*, 132(11), 1381–1392.

DeJong, J. T., Mortensen, B. M., Martinez, B. C., and Nelson, D. C. (2010). "Bio-mediated soil improvement." *Ecological Engineering*, 36, 197–210.

Dilrukshi, R. A. N., Nakashima, K., and Kawasaki, S. (2018). "Soil improvement using plant-derived urease-induced calcium carbonate precipitation." *Soils and Foundations*, The Japanese Geotechnical Society, 1–17.

Hamdan, N., and Kavazanjian, E. (2016a). "Enzyme-induced carbonate mineral precipitation for fugitive dust control." *Géotechnique*, 66(7), 546–555.

Hamed Khodadadi, T., Kavazanjian, E., Paassen, L. Van, and Dejong, J. (2017). "Bio-grout materials : A review." *Grouting 2017*, (January 2018), 1–12.

Hansen, T. C. (1986). "Physical structure of hardened cement paste. A classical approach." *Materiaux et Constructions*, 19(114), 423–436.

Hoang, T., Alleman, J., Cetin, B., Ikuma, K., and Choi, S.-G. (2018). "Sand and silty-sand soil stabilization using bacterial enzyme induced calcite precipitation (BEICP)." *Canadian Geotechnical Journal*, 1–66.

Holtz, R. D., and Kovacs, W. D. (1981). An introduction to geotechnical engineer. Prentice-Hall.

Ivanov, V., and Chu, J. (2008). "Applications of microorganisms to geotechnical engineering for bioclogging and biocementation of soil in situ." Reviews in *Environmental Science and Biotechnology*, 7(2), 139–153.

Javadi, N., Khodadadi, H., Hamdan, N., and Kavazanjian, E. J. (2018). "EICP treatment of soil by using urease enzyme extracted from watermelon seeds." *ASCE IFCEE 201*8, 115–124.

Kok, H., and McCool, D. K. (1990). "Quantifying freeze/thaw-induced variability of soil strength." *Int. Symposium on Frozen Soil Impacts on Agricultural, Range, and Frost Lands, Cold Regions Research and Engineering Laboratory*, Hanover, NH, 501–506.

Krajewska, B. (2018). "Urease-aided calcium carbonate mineralization for engineering applications: A review." *Journal of Advanced Research*, 13, 59–67.

Li, L., Liu, S., Wen, K., Engineering, J. S. U. D. of C. & E., and Arkansas, U. of. (2017). Innovative bio-mediated particulate materials for sustainable maritime transportation infrastructure. Fayetteville, AR.

Nam, I., Chon, C., Jung, K., and Choi, S. (2014). "Calcite precipitation by ureolytic plant (Canavalia ensiformis) extracts as effective biomaterials." *KSCE Journal of Civil Engineering*, 1–6.

Neupane, D., Yasuhara, H., Kinoshita, N., and Unno, T. (2013). "Applicability of enzymatic calcium carbonate precipitation as a soil-strengthening technique." *ASCE Journal of Geotechnical and Geoenvironmental Engineering*, 139(December), 2201–2211.

van Paassen, L. A. (2009). "Biogrout: Ground improvement by microbially induced carbonate precipitation." *Ph.D. dissertation, Delft University of Technology*, Delft, Netherlands.

van Paassen, L. A., Ghose, R., van der Linden, T. J. M., van der Star, W. R. L., and van Loosdrecht, M. C. M. (2010). "Quantifying biomediated ground improvement by ureolysis: large-scale biogrout experiment." *Journal of Geotechnical and Geoenvironmental Engineering*, 136(12), 1721–1728.

Phillips, A. J., Gerlach, R., Lauchnor, E., Mitchell, A. C., Cunningham, A. B., and Spangler, L. (2013). "Engineered applications of ureolytic biomineralization: A review." *Biofouling*, 29(6), 715–733.

Al Qabany, A., and Soga, K. (2013). "Effect of chemical treatment used in MICP on engineering properties of cemented soils." *Geotechnique*, 63(4), 331–339.

Ran, D., and Kawasaki, S. (2016). "Effective use of plant-derived urease in the field of geoenvironmental/geotechnical engineering." *Journal of Civil & Environmental Engineering*, 6(1), 207.

Rosa, M. G., Cetin, B., Asce, A. M., Edil, T. B., Asce, D. M., Benson, C. H., and Asce, F. (2016). "Freeze – thaw performance of fly ash – stabilized materials and recycled pavement materials." 29(2015), 1–13.

Safavizadeh, S., Montoya, B. M., and Gabr, M. A. (2018). "Microbial induced calcium carbonate precipitation in coal ash." *Géotechnique*, 1–14.

Solanki, P., Zaman, M., and Khalife, R. (2013). "Effect of freeze-thaw cycles on performance of stabilized subgrade." *Geo-Congress 2013*, San Diego, California, United States, 567–581.

Sridharan, A., and Nagaraj, H. B. (1999). "Absorption water content and liquid limit of soils." *Geotechnical Testing Journal*, 22(2), 121–127.

Terzis, D., and Laloui, L. (2018). "3-D micro-architecture and mechanical response of soil cemented via microbial-induced calcite precipitation." *Scientific Reports*, Springer US, 8(1), 1–11.

Whiffin, V. S., van Paassen, L. A., and Harkes, M. P. (2007). "Microbial carbonate precipitation as a soil improvement technique." *Geomicrobiology Journal*, 24(February), 417–423.

Worth, F. (2014). Portland cement data sheet. Kansas City, KS, USA.

Yasuhara, H., Hayashi, K., and Okamura, M. (2011). "Evolution in mechanical and hydraulic properties of calcite-cemented sand mediated mediated by biocatalyst." *Geo-Frontiers 2011* © ASCE 2011, Dallas, Texas, 3984–3992.

Yasuhara, H., Neupane, D., Hayashi, K., and Okamura, M. (2012). "Experiments and predictions of physical properties of sand cemented by enzymatically-induced carbonate precipitation." *Soils and Foundations*, Elsevier, 52(3), 539–549.

# CHAPTER 6.   CONCLUSIONS, RESEARCH CONTRIBUTIONS, LIMITTIONS, AND RECOMMENDATIONS

## 6.1 Summary Perspectives

This dissertation's research effort involved an investigation of bio-mediated soil stabilization, as well as a corresponding assessment of bio-stabilization soil properties at both a micro-structural-scale and at a macro-soil-scale under various application conditions. The main objectives of this research were as follows: (1) to explore a new bioimprovement method, known as 'bacterial enzyme induced carbonate precipitation' (BEICP), and (2) to evaluate the improvement of soil engineering properties plus frost-related resistance of BEICP-treated sand and silty sand soil.

This associated study consequently focuses on the following five research outcomes:

(1) to introduce a simple and efficient method of bacterial enzyme extraction by using sonication technique,

(2) to evaluate the geotechnical engineering properties of BEICP-treated soil and the impacted factors to their behaviors,

(3) to investigate the frost resistance of the BEICP-treated soil, and

(4) to analyse the microstructure of the bio-treated soil matrix including the framework to interpret the experimental results.

The following Section 6.2 'Conclusions' section (and its five sub-section portions) subsequently presents the main summaries and conclusions drawn from these latter research elements, and the following Chapter 6.3 'Recommendations' section offers a set of complementary for future topics which warrant additional research.

## 6.2 Conclusions

### 6.2.1 Bacterial Enzyme Extraction Process

Intracellular urease was effectively extracted from *S. pastuerii* bacteria by using the sonication technique developed during this dissertation effort. This expedient (approximately 120 min) cyclic run-cool sonication technique lysed viable bacterial cells to produce a level of urease enzyme activity which was unexpectedly higher than that of the original whole cell suspension. This extraction process was simple, expedient, and efficiency. One additional interrelated conclusion was that this enzyme solution could be stored at a temperature of 4 ℃ over a one-week period prior to its successful application. This extracted, soluble enzyme solution was, indeed, able to improve the engineering properties of sandy soil and silty sand soil by way of the induced calcite carbonate precipitation mechanism. As such, this dissertation effort confirms that the employed sonication technique was able to extract the urease enzyme from viable bacteria for the bio-mediated soil improvement.

### 6.2.2 BEICP Performance in Relation to Chemical Conversion Efficiency

This dissertation's investigation of chemical conversion efficiency when using BEICP soil stabilization demonstrated a reduction in the process precipitation ratio when applied at higher chemical substrate concentration levels. Although, the chemical conversion ratio when using whole-cell MICP processing was higher than that of BEICP's free-enzyme when comparatively evaluated at low urease activity (i.e. 2 – 4 mM urea per min) levels, this trend reversed when evaluated at a higher level of urease activity (i.e. 8 mM urea per min) (i.e., where BEICP treatment had a higher chemical conversion efficiency versus that of MICP).

### 6.2.3 BEICP Treatment Improves Engineering Properties of Sand and Silty Sand Soil

The BEICP method proved to be capable of improving soil strength when applied to non-plastic sands as well as two levels of low plasticity 90-10 and 80-20 (i. e., respective percentile fractions for coarse-fine grain) soil materials. When evaluating increased levels of soil bio-cementation, i.e., in relation to varying calcium carbonate precipitation content, the UC strength progressively increased and the permeability reduced with successive BEICP treatment cycles. Compare to the MICP-treated sandy soil, the UCS levels observed with BEICP-treated sand samples were slightly lower, while the permeability of BEICP samples remained far higher after similar numbers of treatment cycles. However, the $CaCO_3$ content of the BEICP-treated sand was much lower than that in the MICP-treated specimen. Therefore, the BEICP method provided a commensurately higher efficiency of UCS strength increase than MICP, while the MICP treatment reduced the permeability of sandy soils to a greater degree than that of BEICP processing, particularly with higher cycles of treatment. The properties of BEICP-treated sand were also affected by the sand particle size, where this impact resulted in changes of $CaCO_3$ content as well as the distribution pattern of crystal clusters. Furthermore, these experimental findings revealed noticeably high UC strengths and permeability in the BEICP-treated coarse sands as compared to that of soils bearing fine-grained sands at similar levels of $CaCO_3$ precipitation.

For BEICP-treated silty sand soil, the results with UCS testing were lower than those in bio-treated sandy soil, and this decline continued as the fine content increased. However, the calcium carbonate content increased when the fines content increased in BEICP-treated silty sand mixture. This outcome indicated that the level of $CaCO_3$

precipitation was not a sole factor influencing the strength of bio-treated soil. Furthermore, the stress-strain behavior of bio-treated silty sand was also affected by amount of fine content. The presence of fines wrapped around coarser grains reduced friction among the host sand particles, which increased the ductility of BEICP treated sands. Collectively, these research findings indicated that the BEICP method may be pragmatically suitable for full-scale applications with silty sand soils.

### 6.2.4 BEICP Treatment Improves Freeze-thaw Resistance of Soil

This dissertation findings indicated that frost action will negatively impact soils subjected to bio-stabilization within cold region areas. This disseration's investigation focused on the freeze-thaw (F-T) resistance of BEICP-treated medium dense soil. The UCS reduction ratio experienced by BEICP-treated sand was stable after 5 F-T durations, while those of treated silty sand samples steadily reduced after 3 F-T cycles. These BEICP findings were also comparatively evaluated relative to that obtained with two other commercial stabilizers, i.e., Portland cement and F-class fly ash. These testing results indicated that the F-T resistance of BEICP-treated soil was comparable to that secured with soil-cement treated samples. In contrast, though, the F-class fly ash material was unable to increase the F-T durability of medium dense soil.

Several additional processing factors (i.e., calcium carbonate content, water content, porosity and permeability) were studied during this dissertation effort. Several of these factors produced strong impacts on the frost resistance capacity of treated soil. When the $CaCO_3$ content increased, BEICP-treated soil samples showed higher residual strengths and a better F-T resistance capacity after repeated F-T cycling. The high capillarity water content significantly reduced the strength of soil due to the generation of

micro-cracks. For soils with higher levels of porosity and permeability, parallel increases in frost resistance given that there was a lower capillary force which allowed more rapid water to evaporate from within the soil specimen. In general, therefore, BIECP-mediated soil stabilization method was able to offer a successful technique for increasing the frost action resistance of both sand and silty-sand soils.

### 6.2.5 Microstructural Analysis of Bio-treated Soil

SEM images of bio-stabilized soil using both MICP and BEICP were carefully investigated to interpret and support the preceding findings during these bio-stabilization experiments. For sandy soil, the SEM observations showed that calcium cluster deposition predominantly occurred with BEICP at the contact points between sand grains, while the MICP method spread the $CaCO_3$ precipitation across the sand surface as well as within the pore space of the sand matrix. In contrast, the pattern of calcium carbonate formation in BEICP treated silty-sand materials revealed a far more wide-spread distribution of $CaCO_3$ precipitation than had been observed with the sandy soil processing, both on exterior particle surfaces and internal void spaces. The SEM images further revealed that the size of sand grains affected the pattern of $CaCO_3$ distribution. The BEICP-treated fine-grained sand specimens revealed a distinctly higher amount of non-effective calcium deposition clusters at the grains surfaces and within the void space, which resulted in lower UCS and lower hydraulic conductivity compared to the bio-treated coarse-grained sand.

The average size of calcium-rich crystals observed in BEICP-treated soils was smaller than those observed in MICP-treated samples. Notably, though, the smaller crystal size achieved with BEICP processing showed a higher UC strength as compared

to MICP's larger crystal size when compared at similar $CaCO_3$ deposition levels. However, the size of calcium crystals did not appear to affect to the levels of permeability reduction observed with either of these MICP- or BECIP-based processing methods.

Lastly, the experiment SEM findings pursuant to F-T cycling showed that frost action reduced the strength of BEICP-treated soil. SEM images analysis revealed the occurrence of micro-crack damage both within calcium deposition clusters and at the bridging points between sand grains and calcite crystals. These micro-cracks formations, caused by expanded capillary water within the soil matrix, correlated to the experimental findings of UCS reduction. This micro-crack behavior, and negative impact on UCS strength, within bio-treated soil samples following F-T exposure has not been previously shown within prior bio-geotechnical publications.

### 6.3 Research Contributions

This dissertation provides a comparative investigation of BEICP processing relative to that of MICP treatment, and an accompanying assessment of BEICP benefits relative to the use commercial- or plant-based EICP strategies. These BEICP finding also offer preliminary positive support for its future use as a practical geotechnical engineering strategy for full-scale ground improvement.

Although BEICP employs a similar urea hydrolysis mechanism as MICP and EICP methods to induced carbonate precipitation, the newer method features an innovative bacterial urease extraction process which appears to offer several advantages compared to the previous ICP techniques, including:

1) The demonstration of a robust & self-extraction process for producing cell-free urease from viable bacterial cells, which in turn helps ICP's researchers

to activity secure high-quality enzyme sources instead of relying on expensive, commercially purchased urease as has been reported by previous EICP studies.

2) BEICP's reliance on nano-scale solubilized urease enzyme reveals comprehensive advantages over the conventional use of whole-cell urease-producing microbes given that these cells are distinctly constrained in terms of their migration into very small, sub-micron pore spaces within silty sand soils. Therefore, the BEICP method has a much broader range of applicability with finer soils compared to the MICP method.

Overall, the BEICP process appears to offer an improved means of advancing soil strength and stability while at the same time this method uniquely retains a higher level of residual permeability within the treated soil samples which are potentially applicable in some geotechnical projects. For example, certain geotechnical applications require high strength of soil for bearing capacity and at the same time high permeability for water drainage, as might be the case with building foundations and back filling of retaining walls. The BEICP-treated soil subsequently provides a clear benefit in terms of retaining higher levels of porosity and permeability. One such particularly beneficial circumstance would be that of cold regions where freeze and thaw resistance is an acute challenge. Yet another engineering benefit of BEICP treatment is that the combined impacts of residual permeability and using soluble, nano-sized urease catalysts is that these features will enable the use of extended treatment cycles without far less vulnerability to a calcite-based clogging phenomenon as often occurs with the MICP method.

### 6.4 Limitations

The dissertation introduces a novel BEICP technique for soil stabilization. However, several scientific and engineering aspects with this process have not yet been fully elucidated and should subsequently be further investigated. The following list summarizes these needs for future research relative to three categories of investigation.

1) Two limitations with this dissertation research effort's mode of microbial analysis must be acknowledge, and both offer opportunities to upcoming future research. One such aspect is that this dissertation's approach to quantifying urease enzyme activity was based only substrate conversion per time (i.e., mM of urea converted per minute). This approach is commonplace within most biostabilization literature published within the biogeotechnical engineering realm. However, a more scientifically sophisticated approach to this analysis would take into account the actual level of protein mass involved in this reaction. A second limitation with this dissertation's breadth of analysis is that there are several additional factors in relation to enzyme storage conditions, inhibition factors, immobilization of enzymes, surficial sorption behavior, environmental impacts, etc. which will need to be further evaluated in order to optimize this BEICP method.

2) Yet another limitation with this dissertation research is that there were several geotechnical engineering aspects which were limited in terms of considering friction angles & cohesion, the behavior of stress-strain, the pore water pressure generation, and the critical state yield of loading samples. Those

factors are, of course, very important factors in relation to practical

geotechnics design.

Lastly, this study was mainly conducted at a lab-bench scale which does not show

the efficiency of the BEICP method in term of large-scale engineering applications,

potential cost saving, and environmental-friendly qualities compared to the standard

MICP method let alone conventional Portland cement and fly ash stabilizers.

### 6.5 Recommendations

The following future research topics are suggested in order to develop and

transition the BEICP process from its current lab-level status to that of a pragmatically-

applicable field-level method for successful full-scale soil bio-stabilization in the

geotechnical engineering.

1) Further investigation of the extracted enzyme properties, and continued efforts

   towards optimization of the applied lysing process, should be completed. For

   example, protein mass in relation to urease activity needs to be determined for the

   extracted enzyme solution. Additional evaluation factors include: original viable cell

   production and possible pre-sonication wash methods, enzyme storage conditions,

   inhibition factors, effects of environment, and sorption properties related to the

   enzyme should be investigated to evaluate the potential in-situ application of

   bacterial enzyme solution.

2) The shear strengths and stress-strain behavior of BEICP-treated soils should be

   evaluated in relation to the triaxial loading at both drained and un-drained

   conditions. The constitutive response of the bio-treated soil, and how it varies with

   the degree cementation and fines content, represents one such notably worth

investigation topic. Laboratory tests used to evaluate different stress paths and degree of consolidation should be performed in order to define yield surfaces of bio-cemented soils. Another key element of the laboratory experiments could be examined is the exhibition of a unique critical state line at large strains at different cementation levels. The behavior BEICP-treated soil under dynamic loading, resonant testing, and plane strain condition should be evaluated. And yet another related aspect would be that of developing numerical simulation models which are able to predict the response of BEICP-stabilized soils under real-world conditions.

3) The BEICP method appears to warrant future pragmatic evaluation at large-scale and field-scale test levels as applied to different types of soil. These tests could be applied for a variety of prospective bio-stabilization goals extending beyond basis soil improvement, including: soil liquefaction mitigation, and preventative measure to reduce internal erosion of levees, sea dikes, and sand dunes. For the industry to advance, these full-scale tests should also evaluate a full range of application outcomes, including: in-situ treatment process, application cost, and environmental issues.

# REFERENCES

Bang, S. S., Bang, S. S., Frutiger, S., Nehl, L. M., and Comes, B. L. (2009). "Application of novel biological technique in dust suppression." *Proc., Transportation Research Board 88th Annual Meeting*, Transportation Research Board (CD-ROM), Washington, DC, USA, DC, USA, 6–7.

Berggren, B. (2016). "Trends in ground improvement." Geotechnics for Sustainable Infrastructure Development - *Geotec Hanoi 2016*, Phung (edt)., 607–612.

Burbank, M. B., Weaver, T. J., Green, T. L., Williams, B. C., and Crawford, R. L. (2011). "Precipitation of calcite by indigenous microorganisms to strengthen liquefiable soils." *Geomicrobiology Journal*, 28(February), 301–312.

Christians, S., and Heinrich, K. (1986). "Nickel-content of urease from *Bacillus pasteurii*." *Arch Microbiol*, 6, 216–220.

Chu, J., Ivanov, V., Stabnikov, V., He, J., Li, B., and Naemi, M. (2011). "Biocement: Green building and energy saving material." *Advanced Materials Research*, 347–353, 4051–4054.

Chu, J., Varaksin, S., Klotz, U., and Menge, P. (2009). Construction processes. *Proceedings of the 17th International Conference on Soil Mechanics and Geotechnical Engineering: The Academia and Practice of Geotechnical Engineering*.

DeJong, J. T., Fritzges, M. B., and Nüsslein, K. (2006). "Microbially induced cementation to control sand response to undrained shear." *Journal of Geotechnical and Geoenvironmental Engineering*, 132(11), 1381–1392.

DeJong, J. T., Mortensen, B. M., Martinez, B. C., and Nelson, D. C. (2010). "Bio-mediated soil improvement." *Ecological Engineering*, Elsevier B.V., 36(2), 197–210.

DeJong, J. T., Soga, K., Banwart, S. a, Whalley, W. R., Ginn, T. R., Nelson, D. C., Mortensen, B. M., Martinez, B. C., and Barkouki, T. (2011). "Soil engineering in vivo: harnessing natural biogeochemical systems for sustainable, multi-functional engineering solutions." *Journal of the Royal Society*, Interface / the Royal Society, 8(54), 1–15.

Dilrukshi, R. A. N., Nakashima, K., and Kawasaki, S. (2018). "Soil improvement using plant-derived urease-induced calcium carbonate precipitation." *Soils and Foundations*, The Japanese Geotechnical Society, 1–17.

Erickson, H. P. (2009). "Size and shape of protein molecules at the nanometer level determined by sedimentation, gel filtration, and electron microscopy." *Biological Procedures Online*, 11(1), 32–51.

Gomez, M. G., Martinez, B. C., DeJong, J. T., Hunt, C. E., deVlaming, L. A., Major, D. W., and Dworatzek, S. M. (2015). "Field-scale bio-cementation tests to improve sands." *Proceedings of the Institution of Civil Engineers - Ground Improvement*, 168(3), 206–216.

Hamdan, N., and Kavazanjian, E. (2016). "Enzyme-induced carbonate mineral precipitation for fugitive dust control." *Géotechnique*, 66(7), 546–555.

Hamdan, N., Kavazanjian, J. E., and S., O. (2013). "Carbonate cementation via plant derived urease." *Proceedings of the 18th International Conference on Soil Mechanics and Geotechnical Engineering*, Paris 2013, 2489–2492.

Hamdan, N., Zhao, Z., Mujica, M., Kavazanjian, E. J., and He, X. (2016). "Hydrogel-assisted enzyme-induced carbonate mineral precipitation." *Journal of Materials in Civil Engineering*, 25(October), 864–870.

Harkes, M. P., van Paassen, L. A., Booster, J. L., Whiffin, V. S., and van Loosdrecht, M. C. M. (2010). "Fixation and distribution of bacterial activity in sand to induce carbonate precipitation for ground reinforcement." *Ecological Engineering*, 36(2), 112–117.

Ivanov, V., and Chu, J. (2008). "Applications of microorganisms to geotechnical engineering for bioclogging and biocementation of soil in situ." *Reviews in Environmental Science and Biotechnology*, 7(2), 139–153.

Javadi, N., Khodadadi, H., Hamdan, N., and Kavazanjian, E. J. (2018). "EICP treatment of soil by using urease enzyme extracted from watermelon seeds." *ASCE IFCEE 2018*, 115–124.

De Jong, J. T., Martinez, B. C., Mortensen, B. M., Nelson, D. C., Waller, J. T., Weil, M. H., Ginn, T. R., Weathers, T., Barkouki, T., Fujita, Y., Redden, G., Hunt, C., Major, D., and Tanyu, B. (2009). "Upscaling of bio-mediated soil improvement." *Proceedings of the 17th International Conference on Soil Mechanics and Geotechnical Engineering: The Academia and Practice of Geotechnical Engineering*, 3, 2300–2303.

Kavazanjian, E., and Hamdan, N. (2015). "Enzyme induced carbonate precipitation (EICP) columns for ground improvement." *Proc., ASCE IFCEE 2015*, M. Iskander, M. T. Suleiman, J. B. Anderson, and Debra F. Laefer, eds., ASCE, San Antonio, Texas, 2252–2261.

Kirsch, K., and Bell, A. (2013). Ground Improvement Third Edition. (K. Kirsch and A. Bell, eds.), CRC Press, Taylor & Francis Group.

Krajewska, B. (2009). "Ureases I. Functional, catalytic and kinetic properties: A review." *Journal of Molecular Catalysis B: Enzymatic*, 59(1–3), 9–21.

Krajewska, B. (2018). "Urease-aided calcium carbonate mineralization for engineering applications: *A review." Journal of Advanced Research*, 13, 59–67.

Larson, A., and Kallio, R. (1953). "Purification and properties of bacterial urease." Unknown, 68(1944), 67–73.

Long, J. C. S., Amadei, B., Bardet, J., Christian, J. T., Glaser, S. D., GOODINGS, D. J., Jr., E. K., Major, D. W., Mitchell, J. K., POULTON, M. M., and J. Carlos Santamarina. (2006). Geological and geotechnical engineering in the new millennium. *THE NATIONAL ACADEMIES PRESS*, WASHINGTON, D.C.

Meyer, F., Bang, S., Min, S., Stetler, L., and Bang, S. S. (2011). "Microbiologically-induced soil stabilization: application of Sporosarcina pasteurii for fugitive dust control." *Geo-Frontiers*, 4002–4011.

Mitchell, J. K., and Santamarina, J. C. (2005). "Biological considerations in geotechnical engineering." *Journal of Geotechnical and Geoenvironmental Engineering*, 131(10), 1222–1233.

Mobley, H. L. T., and Hausinger, R. P. (1989). "Microbial Ureases : Significance , Regulation , and Molecular Characterizationt." *Microbiological Reviews*, 53(1), 85–108.

Nakano, H., Takenishi, S., and Watanabe, Y. (1984). "Purification and properties of urease from Brevibacterium ammoniagenes." *Agric Biol Chem*, 48(June), 1495–1502.

Nam, I., Chon, C., Jung, K., and Choi, S. (2014). "Calcite precipitation by ureolytic plant (Canavalia ensiformis) extracts as effective biomaterials." *KSCE Journal of Civil Engineering*, 1–6.

Nassar, M. K., Gurung, D., Bastani, M., Ginn, T. R., Shafei, B., Gomez, M. G., Graddy, C. M. R., Nelson, D. C., and DeJong, J. T. (2018). "Large-scale experiments in microbially induced calcite precipitation (MICP): Reactive transport model development and prediction." *Water Resources Research*, 3, 1127–1145.

Nemati, M., Greene, E. A., and Voordouw, G. (2005). "Permeability profile modification using bacterially formed calcium carbonate: Comparison with enzymic option." *Process Biochemistry*, 40(2), 925–933.

Nemati, M., and Voordouw, G. (2003). "Modification of porous media permeability, using calcium carbonate produced enzymatically in situ." Enzyme and Microbial Technology, 33(5), 635–642.

Neupane, D., Yasuhara, H., Kinoshita, N., and Unno, T. (2013). "Applicability of enzymatic calcium carbonate precipitation as a soil-strengthening technique." *ASCE Journal of Geotechnical and Geoenvironmental Engineering*, 139(December), 2201–2211.

Oliveira, P. J. V., Freitas, L. D., and Carmona, J. P. S. F. (2016). "Effect of soil type on the enzymatic calcium carbonate precipitation process used for soil improvement." *Journal of Materials in Civil Engineering*, 29(4), 1–7.

van Paassen, L. A. (2009). "Biogrout: Ground improvement by microbially induced carbonate precipitation." *Ph.D. dissertation, Delft University of Technology*, Delft, Netherlands.

van Paassen, L. A. (2011). "Bio-mediated ground improvement: from laboratory experiment to pilot applications." *ASCE Geo-Frontiers*, 4099–4108.

van Paassen, L. A., Ghose, R., van der Linden, T. J. M., van der Star, W. R. L., and van Loosdrecht, M. C. M. (2010). "Quantifying biomediated ground improvement by ureolysis: large-scale biogrout experiment." *Journal of Geotechnical and Geoenvironmental Engineering*, 136(12), 1721–1728.

van Paassen, L. A., Harkes, M. P., Van Zwieten, G. A., Van Der Zon, W. H., Van Der Star, W. R. L., and Van Loosdrecht, M. C. M. (2009). "Scale up of BioGrout: A biological ground reinforcement method." *Proceedings of the 17th International Conference on Soil Mechanics and Geotechnical Engineering: The Academia and Practice of Geotechnical Engineering*, 3, 2328–2333.

Park, S.-S., Choi, S.-G., and Nam, I.-H. (2014). "Effect of microbially induced calcite precipitation on strength of cemented sand." *Journal of Materials in Civil Engineering*, 26(8), 47–56.

Phillips, A. J., Cunningham, A. B., Gerlach, R., Hiebert, R., Hwang, C., Lomans, B. P., Westrich, J., Mantilla, C., Kirksey, J., Esposito, R., and Spangler, L. (2016). "Fracture sealing with microbially-induced calcium carbonate precipitation: A field study." *Environmental Science and Technology*, 50(7), 4111–4117.

Al Qabany, A., and Soga, K. (2013). "Effect of chemical treatment used in MICP on engineering properties of cemented soils." *Geotechnique*, 63(4), 331–339.

Qin, Y. and J. M. S. C. (1994). "Kinetic studies of the Orease-Catalyzed Hydrolysis of Orea in a Buffer-Free System." *Applied Biochemistry and Biotechnology*, 49.

Ran, D., and Kawasaki, S. (2016). "Effective use of plant-derived urease in the field of geoenvironmental/geotechnical engineering." *Journal of Civil & Environmental Engineering*, 6(1), 207.

Riding, R. (2007). "The term stromatolite: towards an essential definition." Lethaia, 32(4), 321–330.

van der Star, W. R. L., van Wijngaarden-van Rossum, W. K., van Paassen, L. A., and van Baalen, L. R. (2011). "Stabilization of gravel deposits using microorganisms." *Proceedings of the 15th European conference on Soil mechanics and Geotechnical engineering*, A. Anagnostopoulos, ed., IOS Press, 85–90.

Sumner, J. B. (1926). "The isolation and crystallization of the enzyme Urease." *J. Biol. Chem.*, 69, 435–441.

Whiffin, V. S. (2004). "Microbial CaCO3 precipitation for the production of biocement." *Ph.D. dissertation, Murdoch University*, Australia.

Wikipedia. (2018). "Stromatolite." *<https://en.wikipedia.org/wiki/Stromatolite#cite_note-3>*.

Yasuhara, H., Neupane, D., Hayashi, K., and Okamura, M. (2012). "Experiments and predictions of physical properties of sand cemented by enzymatically-induced carbonate precipitation." *Soils and Foundations*, Elsevier, 52(3), 539–549.